

Physico-chemical Properties of Imidazolium-Based Ionic Liquids in Pure and Mixed Polar Solvents

A Dissertation Submitted to University of Dhaka for the Partial
Fulfillment of the Requirements of the Degree of
Master of Philosophy in Chemistry

Submitted by

Momana Afrosre

Registration No. 143

Session: 2012-2013



DEPARTMENT OF CHEMISTRY
PHYSICAL CHEMISTRY RESEARCH LABORATORY

University of Dhaka
Dhaka-1000, Bangladesh

February 2017

Dedicated

to

My Family and Supervisors

Acknowledgements

I am grateful to my respected supervisor **Professor Omar Ahmed**, Department of Chemistry, University of Dhaka for his valuable comments, advices and kind assistance for various problems in any situation during experiments. His patience and guidance were true inspiration for me.

I would like to express my sincere gratitude and appreciation to my supervisor **Professor Dr. Md. Abu Bin Hasan Susan**, Department of Chemistry, University of Dhaka, for his scholastic supervision, keen interest, constructive suggestions and continual guidance throughout the research work and his emendation of the manuscript without which the present research work might not have been completed. I sincerely owe to him for giving me an opportunity to work in close association with him.

I am indebted to **Professor Dr. M. Muhibur Rahman** and **Professor Dr. M. Yousuf Ali Mollah**, University grant Commission of Bangladesh, **Dr. M. Mominul Islam**, Associate Professor, Department of Chemistry, University of Dhaka, and **Dr. Muhammed Shah Miran** for their valuable comments and suggestions which helped me to resolve critical points related to this research work. I sincerely express my gratitude to **Dr. Saika Ahmed**, Lecturer, Department of Chemistry, University of Dhaka, for her friendly collaboration and encouragement during this work.

I am grateful to the authority of DU for providing financial support for this research work. I would like to extend my thanks to Dr. Ferdousi Begum, Gulshan Ara and other members of Material Chemistry Research Laboratory who shared with me to solve all the problems confronted in the whole thesis period.

I gratefully acknowledge support from the sub project (CP- 231) of the Higher Education Quality Enhancement Project of the University Grants Commission of Bangladesh financed by World Bank and Government of Bangladesh.

I gratefully express my sincere thank to the Bose Center for Advanced Study and Research in Natural Sciences for M. Phil. Fellowship.

I am grateful to my parents and all other family members and well-wisher for their encouragement. I am also thankful to my husband Serajul Islam for his continuous moral encouragement.

Above all, all thanks are due to almighty Allah for making things situation congenial and favorable for me for the task undertaken.

(Momana Afrose)

Abstract

Ionic liquids comprise entirely ions and are fluid at temperatures around 100 °C or below. The physico-chemical properties of IL change dramatically upon addition of one or more molecular solvent/s and therefore, binary and ternary mixtures of ILs with molecular solvents have received significant attention in recent years. They provide the means of accumulation of knowledge regarding the types of interaction and may exhibit the appearance of a new phenomenon, which is absent in the pure state of ILs. With a view to a proper understanding molecular level interactions of IL based systems, in this work, binary liquid mixtures of *N, N*-dimethylformamide (DMF) with acetonitrile (ACN), 1-ethyl 3-methylimidazolium bis(trifluoromethanesulfonylimide)([emim][TFSI]) with ACN and DMF in the whole composition range and 1-ethyl 3-methylimidazolium hexafluorophosphate([emim][PF₆]) with ACN and DMF have been prepared. The different interactions in these binary mixtures have been investigated by measuring physico-chemical properties with varying the compositions of different components. Effects of temperature and composition on some fundamental physico-chemical properties- density, viscosity, refractive index and conductivity of these binary mixtures also have been investigated. The excess molar volume (V^E), excess viscosity ($\Delta\eta$) and excess refractive index (Δn) were calculated and the results were fitted to Redlich-Kister polynomials. The values of V^E and $\Delta\eta$ were negative and Δn were positive over the whole composition range for these binary mixtures. The minima in V^E and $\Delta\eta$ were observed at mole fraction of IL, $X_{IL} \sim 0.2$ and 0.5 respectively for [emim][TFSI] and DMF mixtures, for [emim][TFSI]-ACN the minima in V^E and $\Delta\eta$ were observed at mole fraction of IL, $X_{IL} \sim 0.2$ and 0.6 , respectively. With increasing X_{IL} , the refractive index of these binary mixtures gradually increased. The conductivity of the binary mixtures have been measured by the impedance spectroscopy method and the data have been used to infer about the ionic characteristics of the binary systems. Finally, from the understanding of these three binary mixtures, ternary mixtures of [emim][TFSI], DMF and ACN have been prepared and physico-chemical properties of these ternary mixtures have been studied in the temperature range from 20 to 50 °C with change in the composition of different components. The changes in density, viscosity and refractive index as a function of compositions have been correlated with the variation of these properties with temperature. The excess molar volume, excess viscosity and excess refractive index of these ternary mixtures have been deduced from the results of physico-chemical

properties. The values of V^E and $\Delta\eta$ were negative over the whole composition range. Thus, the ultimate goal of this work has been to unveil inter-molecular interactions of different binary and ternary mixtures of ILs with different polar molecular solvents.

Title of the thesis:

Physico-chemical Properties of Imidazolium-Based Ionic Liquids in Pure and Mixed Polar Solvents

Submitted by:

Momana Afrose, M. Phil. Student, Department of Chemistry, University of Dhaka

Chapter 1: Background

Chapter 1 gives a brief account of the background research and reviews the available literature on ionic liquid (IL) based binary and ternary mixtures. This also addresses the rationale and objectives of the work and describes the strategy to accomplish those objectives.

Chapter 2: Molecular Interactions in Binary Mixtures of Acetonitrile with *N, N*-dimethylformamide

Chapter 2 describes the molecular interactions present in the DMF-ACN binary mixtures studied by measurements of physicochemical properties like density, viscosity and refractive index over the entire composition range at temperatures ranging from 20 to 45 °C. The density, viscosity and refractive index were found to increase with increasing mole fraction of DMF. Estimation of the binary coefficients and standard errors were possible by fitting various excess properties data to Redlich–Kister polynomial relation. The calculated excess properties such as excess molar volume and excess viscosity were found to be negative for all the mixtures at all temperatures indicating strong dipole-dipole interaction between DMF and ACN, while values of excess refractive index were positive over the whole composition range.

Chapter 3: Molecular Level Interactions in Binary Mixtures of Ionic Liquids and *N, N*-dimethylformamide

Chapter 3 presents the study on two binary systems; each consisting of an IL, [emim][PF₆] or [emim][TFSI], along with DMF. To understand the molecular interactions between DMF and [emim][TFSI] or [emim][PF₆], density, viscosity, refractive index and conductivity measurements were performed over the whole composition range. The excess molar volume, excess viscosity, and excess refractive index, calculated using the measured data, were fitted to Redlich-Kister polynomials

equation. The values of excess molar volume and excess viscosity were found negative, while those of excess refractive index were positive over the whole composition range for the binary mixtures. The intermolecular interactions and consequent structural variations were analyzed on the basis of the measured and derived properties.

Chapter 4: Molecular Level Interactions in Binary Mixtures of Ionic Liquids and Acetonitrile

Chapter 4 describes the physico-chemical properties of binary mixtures of an IL, [emim][TFSI] or [emim][PF₆], with highly polar solvent ACN, studied through precise measurements of density, viscosity, refractive index over a wide composition range and at a temperature range of 20-50 °C. The excess molar volume, excess viscosity, and excess refractive index were derived from these temperature dependent properties and their behavior was studied as function of concentration of ILs. The Redlich-Kister polynomial equation was used to correlate the results. The intermolecular interactions and their effect on the bonding structure were analyzed on the basis of measured and derived properties. A qualitative analysis of the results is discussed in terms of the ion-dipole, ion-ion, and hydrogen bonding interactions between ILs and DMF and their structural factors.

Chapter 5: Molecular Environment of Ternary Mixtures of Imidazolium-Based Ionic Liquid with Molecular Solvents

Chapter 5 discusses on the molecular environment inside the ternary mixtures of an IL, [emim][TFSI] with DMF and ACN predicted from their physico-chemical properties such as density and viscosity at temperatures ranging from 20 to 50 °C. These physico-chemical properties have been studied at a fixed X_{DMF} , X_{ACN} or $X_{[\text{emim}][\text{TFSI}]}$ (= 0.20) with variation of other two solvents accordingly in the ternary mixtures. For all the ternary mixtures, the density values were found to decrease with increasing both temperature and mole fraction of different solvents, DMF, ACN and [emim][TFSI]. On the contrary, viscosity values increased and decreased, respectively, while mole fraction of solvents and temperature were increased. The excess molar volume and excess viscosity of the ternary mixtures, evaluated from their density and viscosity measurements, were found negative over the entire range of mole fraction. The measured data of the ternary mixtures were also correlated with Redlich-Kister equation to calculate the ternary

adjustable parameters along with standard deviations. The results were interpreted to develop a fundamental understanding of the nature of interactions in IL-molecular solvent ternary mixtures.

Chapter 6: General Conclusions and Prospect

Chapter 6 summarizes the observations and analysis of the former chapters for a general conclusion and discusses the future prospects of IL based binary and ternary mixtures with polar solvents for achievement of tunable physico-chemical properties and exploring task specificity of hydrophobic ILs with controlled addition of molecular solvents under ambient condition.

CONTENTS

Chapter No.		Page No.
1	General Introduction	1-34
1.1	Background	2
1.1.1	Objective of the Work	4
1.1.2.	Outline of the Research	4
1.1.3.	Present Work	5
1.2	Ionic Liquids (ILs)	6
1.2.1.	History of ILs	8
1.2.2.	Structure of ILs	8
1.2.3.	Classification of ILs	9
1.2.4.	Properties of ILs	12
1.2.4.1.	Ionic liquids are liquids	13
1.2.4.2.	ILs as ‘Green Solvents’	13
1.2.4.3.	Designer Solvents	14
1.2.5.	Application of ILs	14
1.2.5.1.	ILs as Solvents	14
1.2.5.2.	Stoichiometric Organic Synthesis	15
1.2.5.3.	Catalyzed Reactions	15
1.2.5.4.	Extraction of Organic Compounds	15
1.2.5.5.	Gas Separations	16
1.2.5.6.	Carbon dioxide Extractions and Separations	16
1.2.5.7.	Metal Ion Extraction	16
1.2.5.8.	Membrane Separations	17
1.2.5.9.	Electrochemical Supercapacitors	17
1.2.5.10.	Dye-Sensitized Solar Cell	17
1.2.6.	Application of ILs Based Binary and Ternary Systems	18
1.3.	Review of literature	18
1.3.1.	Literature Review on Physico-chemical Properties of Pure IL	19
1.3.2.	Literature Review on Physico-chemical Properties of IL Binary Mixtures	21

1.3.3.	Literature Review on Physico-chemical Properties of IL Ternary Mixtures	25
	References	26
2.	Molecular Interactions in Binary Mixtures of Acetonitrile with <i>N, N</i>-dimethylformamide	35-50
	Abstract	36
2.1.	Introduction	36
2.2.	Experimental	37
2.2.1.	Materials	37
2.3.	Instruments	38
2.3.1.	Density Meter	38
2.3.2.	Microviscometer	38
2.3.3.	Refractometer	38
2.3.4.	Sonicator	38
2.3.5.	Water Purifier (Ultra Pure)	39
2.3.6.	Analytical Digital Microbalance	39
2.4.	Measurements	39
2.4.1.	Preparation of Binary Mixtures	39
2.4.2.	Measurement of Density	39
2.4.3.	Measurement of Viscosity	39
2.4.4.	Measurement of Refractive Index	40
2.5.	Results and Discussion	40
2.5.1.	Density of Binary Mixtures of DMF-ACN	40
2.5.2.	Viscosity of Binary Mixtures of DMF-ACN	44
2.5.3.	Refractive Index of Binary Mixtures of DMF-ACN	45
2.6.	Conclusions	47
	References	48
3	Molecular Level Interactions in Binary Mixtures of Ionic Liquids and <i>N, N</i>- dimethylformamide	51-70
	Abstract	52
3.1.	Introduction	52

3.2.	Experimental	55
3.2.1.	Materials	55
3.3.	Instruments	55
3.4.	Measurements	56
3.4.1.	Preparation of Binary Mixtures	56
3.4.2.	Measurement of Density, Viscosity and Refractive Index	56
3.5.	Results and Discussion	57
3.5.1.	Density of Binary Mixtures of [emim][TFSI]-DMF and [emim][PF ₆]-DMF	57
3.5.2.	Density as a Function of Temperature	58
3.5.3.	Excess Molar Volume of IL-DMF Binary Systems	59
3.5.4.	Viscosity of Binary Mixtures of [emim][TFSI]-DMF and [emim][PF ₆]-DMF	61
3.5.5.	Effect of Temperature on the Viscosity IL-DMF Systems	62
3.5.6.	Excess Viscosity of IL-DMF Binary Systems	63
3.5.7.	Refractive Index of IL Based Binary Systems	65
3.5.8.	Excess Refractive Index of IL-DMF Binary Systems	66
3.6.	Conclusions	67
	References	68
4	Molecular Level Interactions in Binary Mixtures of Ionic Liquids and Acetonitrile	71-86
	Abstract	72
4.1.	Introduction	72
4.2.	Experimental	73
4.2.1.	Materials	73
4.3.	Instruments	73
4.4.	Measurements	74
4.4.1.	Preparation of Binary Mixtures	74
4.4.2.	Measurement of Density, Viscosity, and Refractive Index	74
4.4.3.	Conductivity Measurement	74
4.5.	Results and discussion	75

4.5.1.	Density of Binary Mixtures of [emim][TFSI]-ACN and [emim][PF ₆]-ACN	75
4.5.3.	Density as Function of Temperature	76
4.5.3.	Excess Molar Volume of IL-ACN Binary Systems	76
4.5.4.	Viscosity of Binary Mixtures of [emim][TFSI]-ACN and [emim][PF ₆]-ACN	79
4.5.5	Effects of temperature on the viscosities of IL-CAN Systems	79
4.5.6.	Excess Viscosity of IL-ACN Binary Systems	80
4.5.7.	Refractive Index of [emim][TFSI]-ACN Binary System	81
4.5.8.	Excess Refractive Index of IL-ACN Binary Systems	82
4.5.9.	Conductivity of Binary Mixtures of [emim][TFSI] and ACN	82
4.6.	Conclusions	84
	References	84
5	Molecular Environment of Ternary Mixtures of Imidazolium-Based Ionic Liquid with Molecular Solvents	87-106
	Abstract	88
5.1.	Introduction	88
5.2.	Experimental	90
5.2.1.	Materials	90
5.3.	Instruments	90
5.4	Measurements	91
5.4.1	Preparation of Ternary Mixtures	91
5.5.	Results and Discussion	91
5.5.1.	Physico-chemical Properties of Ternary Mixtures of [emim][TFSI] with DMF and ACN	91
5.5.1.1.	Density as a Function of Mole Fraction and Temperature	91
5.5.1.1.1.	At a Fixed Mole Fraction of DMF is 0.20	92
5.5.1.1.2.	At a Fixed Mole fraction of ACN is 0.20	94
5.5.1.1.3.	At a Fixed Mole fraction of [emim][TFSI] is 0.20	95
5.5.1.2.	Viscosity as a Function of Mole Fraction and Temperature	97

5.5.1.2.1.	Viscosity of Ternary Mixtures of [emim][TFSI]-DMF-ACN at a Fixed X_{DMF} 0.20	97
5.5.1.2.2.	Viscosity of [emim][TFSI]-DMF-ACN at a Fixed X_{ACN} is 0.20	99
5.5.1.2.3.	Viscosity of Ternary Mixtures at a Fixed Mole fraction of IL is 0.20	101
5.6.	Conclusions	102
	References	103
6	General Conclusions	107-109
6.1	General Conclusions	108
6.2	Prospect	108
	Appendix	110-121
	List of Attended Seminars	122
	Abstracts Published as Contribution in the Scientific Meeting	122
	List of Workshops Attended	123

LIST OF FIGURES

Figure No.	Title	Page No.
1.1.3.1.	Structures of (a)[emim][TFSI], (b) [emim][PF ₆], (c) DMF and (d) CAN.	6
1.2.2.1	Some typical cations and anions of ionic liquids.	9
2.5.1.	Density of (a) DMF-ACN binary mixtures as a function X_{DMF} (b) as a function of temperature.	41
2.5.2.	The V^E for DMF-ACN system as a function of X_{DMF} at different temperatures. Solid lines are drawn by using calculated values according to Redlich- Kister equation.	42

2.5.3.	Viscosity of DMF-ACN binary mixtures (a) as a function of X_{DMF} and (b) as a function of temperature.	44
2.5.4.	$\Delta\eta$ of DMF-ACN system as a function of mole fraction of IL. Solid lines are drawn by using calculated values according to Redlich- Kister equation.	45
2.5.5.	Refractive index of DMF-ACN binary mixtures as a function of X_{DMF} .	46
2.5.6.	Excess refractive index of DMF-ACN system as a function of X_{DMF} . Solid lines are drawn by using calculated values according to Redlich- Kister equation.	47
3.1.1.	Resonance structure of DMF.	54
3.5.1.	Density of (a) [emim][TFSI]-DMF and (b) [emim][PF ₆] systems as a function of X_{IL} .	57
3.5.2.	Density of (a) [emim][TFSI] – DMF and (b)[emim][PF ₆]-DMF systems as a function of temperature.	58
3.5.3.	The V^{E} for [emim][TFSI]-DMF system as a function of X_{IL} at different temperatures. Solid lines are drawn by using calculated values according to Redlich- Kister equation.	60
3.5.4.	The η of (a) [emim][TFSI] – DMF and (b) [emim][PF ₆] binary systems as a function of X_{IL} .	62
3.5.5.	Viscosity of (a) [emim][TFSI]-DMF and (b) [emim][PF ₆]-DMF systems as a function of temperature.	63
3.5.6.1.	Excess viscosity of [emim][TFSI]-DMF system as a function of X_{IL} . Solid lines are drawn by using calculated values according to Redlich- Kister equation.	64
3.5.7.	Refractive index of (a) [emim][TFSI] – DMF and (b) [emim][PF ₆] binary systems as a function of X_{IL} .	65
3.5.7.1.	Refractive index of (a) [emim][TFSI]-DMF and (b)[emim][PF ₆]-DMF system as a function of temperature.	66
3.5.8.1.	Excess refractive indices for [emim][TFSI]-DMF systems as a function of X_{IL} at different temperature. Solid lines are drawn by using calculated values according to Redlich- Kister equation.	67

4.5.1.	Density of (a) [emim][TFSI]-ACN and (b) [emim][PF ₆]-ACN systems as a function of X_{IL} .	75
4.5.2.	Density of (a) [emim][TFSI] – ACN and (b)[emim][PF ₆]-ACN systems as a function of temperature.	76
4.5.3.	Excess molar volume V^E for [emim][TFSI]-ACN system as a function X_{IL} at different temperatures. Solid lines are drawn by using calculated values according to Redlich- Kister equation.	78
4.5.4.	Viscosity of (a) [emim][TFSI]-ACN and (b) [emim][PF ₆]-ACN binary systems as a function of X_{IL} .	79
4.5.5.	Viscosity of (a) [emim][TFSI]-ACN and (b) [emim][PF ₆] –ACN systems as a function of temperature.	80
4.5.6.	Excess viscosity of [emim][TFSI]-DMF system as a function of mole fraction of IL. Solid lines are drawn by using calculated values according to Redlich- Kister equation.	81
4.5.7.	Refractive index of (a) [emim][TFSI]-ACN and (b) [emim][PF ₆] –ACN systems as a function of temperature.	81
4.5.8.	Excess refractive indices for [emim][TFSI]-DMF systems as a function of mole fraction of IL at different temperatures. Solid lines are drawn by using calculated values according to Redlich- Kister equation.	82
4.5.9.1.	Conductivity of IL-ACN binary system at room temperature.	83
5.5.1.	Density for the [emim][TFSI]-DMF-ACN system as a function of IL mole fraction at different temperature where X_{DMF} is fixed.	92
5.5.2.	Excess molar volume for [emim][TFSI]-DMF-ACN system as a function of IL at different temperatures at a fixed X_{DMF} is 0.20.	93
5.5.3.	Density for the [emim][TFSI]-DMF-ACN system as a function of X_{IL} at different temperature where X_{ACN} is fixed.	94
5.5.4.	Excess molar volume for [emim][TFSI]-DMF-ACN system as a function of IL mole fraction at different temperatures at a fixed mole fraction(0.20) of ACN.	95
5.5.5.	Density for the [emim][TFSI]-DMF-ACN system as a function of X_{IL} at different temperature where the X_{IL} is fixed at 0.20.	96

5.5.6.	Excess molar volume for [emim][TFSI]-DMF-ACN system as a function of X_{IL} at different temperatures at a fixed X_{IL} is 0.20.	96
5.5.7.	Viscosity for the [emim][TFSI]-DMF-ACN system as a function of IL mole fraction at different temperatures where the X_{DMF} is fixed at 0.20.	98
5.5.8.	Excess viscosity for [emim][TFSI]-DMF-ACN system as a function of IL mole fraction at different temperatures at a fixed X_{DMF} is 0.20.	98
5.5.9.	Viscosity for the [emim][TFSI]-DMF-ACN system as a function of IL mole fraction at different temperature where the X_{ACN} is fixed at a 0.20.	100
5.5.10.	Excess viscosity for [emim][TFSI]-DMF-ACN system as a function of IL mole fraction at different temperatures at a fixed X_{ACN} is 0.20.	100
5.5.11.	Viscosity for the [emim][TFSI]-DMF-ACN system as a function of IL mole fraction at different temperature where the X_{IL} is fixed at 0.20.	101
5.5.12.	At fixed mole fraction of IL Excess viscosity for [emim][TFSI]-DMF-ACN system as a function of IL mole fraction at different temperatures at a fixed X_{IL} is 0.20.	102

LIST OF SCHEMES

Scheme No.	Caption	Page No.
1	Different molecular interaction between DMF-CAN with increasing X_{DMF} in the binary mixtures.	43
2	Interaction between [emim][TFSI] and DMF	61
3	Interaction between [emim][TFSI] and DMF	65

LIST OF TABLE

Table No.	Caption	Page No.
A1	Experimental density (ρ), viscosity (η), refractive index (n), excess molar volume (V^E), excess viscosity ($\Delta\eta$), and excess refractive index (Δn) of DMF-ACN binary mixtures at several temperatures.	110
A2	Coefficients, A_i , for $V^E/ \text{ cm}^3\text{mol}^{-1}$, $\Delta\eta/ \text{ mPa.s}$, Δn and standard deviation σ for DMF-ACN binary mixtures from equation 2.2: $V_m^E = x(1-x) \sum_{i=0}^4 A_i(1-2x)^i$	111
A3	Experimental ρ , η , n , V^E , $\Delta\eta$ and Δn of [emim][TFSI]-DMF binary mixtures at several temperatures.	112
A4	Coefficients, A_i , for $V^E/ \text{ cm}^3\text{mol}^{-1}$, $\Delta\eta/ \text{ mPa.s}$, Δn and standard deviation σ for [emim][TFSI]-DMF binary mixtures from equation 2.2: $V_m^E = x(1-x) \sum_{i=0}^4 A_i(1-2x)^i$	114
A5	Experimental ρ , η , n , V^E , $\Delta\eta$ and Δn of X_{ACN} at several temperatures for [emim][TFSI]-ACN binary mixtures.	115
A6	Coefficients, A_i , for $V^E/ \text{ cm}^3\text{mol}^{-1}$, $\Delta\eta/ \text{ mPa.s}$, Δn and standard deviation σ for [emim][TFSI]-ACN binary mixtures from equation 2.2: $V_m^E = x(1-x) \sum_{i=0}^4 A_i(1-2x)^i$	117
A7	ρ of [emim][TFSI]-DMF-ACN at a fixed X_{DMF} (0.20) at several temperatures.	117
A8	V^E [emim][TFSI]-DMF-ACN at fixed X_{DMF} (0.20) at several temperatures.	118
A9	ρ of [emim][TFSI]-DMF-ACN at several temperatures at a fixed X_{ACN} (0.20)	118
A10	V^E of [emim][TFSI]-DMF-ACN at a fixed X_{ACN} (0.20) at several temperatures.	118
A11	ρ of [emim][TFSI]-DMF-ACN at several temperatures at a fixed X_{IL} is 0.20.	119
A12	V^E of [emim][TFSI]-DMF-ACN at several temperatures at a fixed X_{IL} is 0.20.	119
A13	η of [emim][TFSI]-DMF-ACN at several temperatures at a fixed X_{DMF} is 0.20.	119

A14	η of [emim][TFSI]-DMF-ACN at several temperatures at a fixed X_{ACN} is 0.20	120
A15	η of [emim][TFSI]-DMF-ACN at several temperatures at a fixed X_{IL} is 0.20.	120
A16	$\Delta\eta$ of [emim][TFSI]-DMF-ACN at several temperatures at a fixed X_{DMF} is 0.20.	120
A17	$\Delta\eta$ of [emim][TFSI]-DMF-ACN at a fixed mole fraction of ACN (0.20) at several temperatures.	121
A18	$\Delta\eta$ of [emim][TFSI]-DMF-ACN at several temperatures at a fixed X_{IL} is 0.20.	121

1.1. Background

Ionic liquids (ILs) have burst into the scientific panorama providing new options in research and the development of further applications in different areas. They possess unique physico-chemical properties, which are related to the electrostatic interaction between their ionic components, to give these materials the chance of providing benefits over conventional molecular solvents.

The novel environmentally benign materials are suited as very potential media for diverse applications for their unusual properties. ILs serve as novel reaction media, as electrolytes in batteries, solar cells, and fuel cells and in nanoscience. The replacement of classical materials with ILs can have many benefits and has been shown to enhance catalytic reactions, simplify product or catalyst separation and reduce the risks associated with using volatile and highly flammable organic compounds. Through the choice of appropriate cations and anions there has been gain in interest to exploit the option of fine tuning the physico-chemical properties and many efforts are described toward a systematic characterization of pure ILs on the basis of the nature of their ions and their intermolecular interactions. It is in fact an essential requirement to encourage the use of ILs as solvents. However, systematic research on the ILs is needed to predict the fundamental properties of ILs, such as melting points, densities, viscosities, conductivities, dielectric constants etc. particularly for previously unknown salts.

Properties of ILs are specific to the cation-anion combination and their properties can differ considerably from one another as well as from molecular solvents. To expand the utility of ILs and improve their physico-chemical properties, much attention has recently been focused on IL-based mixed solvents systems. One of the fascinating tasks is to tailor the physico-chemical properties of a particular ILs in a favorable fashion by addition of suitable solvent. Studies of the physico-chemical properties of ILs in binary mixtures with water have recently been pursued to analyze the influence of solvent on structural and energetic properties. Some imidazolium and pyridinium based ILs can form aggregates in water at low concentrations. A specific arrangement of hydrophobic and hydrophilic domains similar to that of classical cationic surfactants can be observed in aqueous solutions due to the inherent amphiphilic nature of their cations, not only with

long hydrocarbon chains as alkyl groups but also with short chains. This capacity of ILs to aggregate, that is to show nano-heterogeneity in aqueous solution has further contributed to an increase in the importance of these compounds. Further research in this area using different polar solvents for series of ILs with similar structure is necessary to understand the solution behavior of ILs in polar solvents and to have a closer view of the mechanism of their action to provide useful knowledge concerning the interaction that take place in the mixture because of the organization resulting from a balance between interactions in pure ILs and those that can be established with the solvent.

Numerous studies have been made to explore the molecular interactions in mixtures of ILs with different molecular solvents by measuring physico-chemical properties [1-26]. Some physico-chemical properties such as density [1-17], viscosity [3-13,15-17], conductivity [3, 19-26], refractive index [6,8, 9, 14-18] of ILs based binary systems have been reported. Research to date reports molecular interaction of ILs based ternary systems with different molecular solvents by measuring physico-chemical properties [27-31]. A small number of physico-chemical data are presented in the literature, which mainly characterize ILs after synthesis work [32-36]. In this context, the aim is to study physico-chemical properties, of the molecular interactions between ILs and polar solvents. Till now there is no systematic documentation of studies of the imidazolium based ILs with organic molecular solvents. For these reasons, two binary mixtures of imidazolium based ILs are prepared and the physico-chemical properties of these binary mixtures are studied to know the molecular interaction. *N, N*-dimethylformamide (DMF) is an industrial solvent and a polar solvent used widely in a variety of industrial processes. Among them the manufacture of synthetic fibers, leathers, films and surface coating [37-39]. DMF is a stable compound with a strong electron-pair donating and accepting ability and is widely used in settings such as solvent reactive relationships [40-42]. The mixtures of ILs and DMF provide potential industrial applications for the utilization of both ILs and DMF. Further, the study intends to draw molecular level information from the macroscopic properties on the molecular interaction between ILs and DMF. Pankaj *et al.* [41] studied the excess molar volumes and deviations of isentropic compressibilities of 1-butyl-3-methylimidazoliumchloride [bmim][Cl] with DMF systems and reported that the packing efficiency between IL-DMF decreases at

higher concentration of IL leading to positive deviation and at lower concentrations the packing efficiency increases.

On the basis of well-known physical and electrochemical properties of ILs, the common nonaqueous electrochemical solvent acetonitrile (ACN) is one of the strongest candidates for electrochemical application. Conductivity of ILs in presence of ACN has been reported to undergo drastic increase. Based on the simulation studies, Chaban *et al.*[3] demonstrated that binary mixtures of five imidazolium-based ILs and ACN with a small content of IL allow to increase conductivity by more than 50 times. Such ability to significantly enhance ionic conductivity by varying exclusively the mole fractions of the mixture components favors the applications of IL and ACN systems as novel non-aqueous electrolytes [4].

1.1.1. Objective of the Work

Among the large variety of conceivable or already available ILs, probably those based on substituted imidazolium cations are the most intensively studied. This is reflected by a growing number of reviews dealing with the physico-chemical properties of such ILs in the pure state and of their mixtures with solvents.

ACN has been reported to boost up conductivity when it is mixed with IL [3]. It would be interesting to investigate the binary mixtures of IL with a molecular solvent of similar polarity with difference in structures and to prepare ternary mixtures by exploiting the advantageous features. The dielectric constant of ACN is 38.0 and that of DMF is 37.50. The physico-chemical properties associated with the mixtures may provide fundamental knowledge-base for molecular level interactions in such systems for further development.

The key objective of this work has therefore been to know the molecular interaction between imidazolium based ILs, [emim][TFSI] and [emim][PF₆] with molecular solvents, DMF and ACN in binary and ternary mixtures.

1.1.2. Outline of the Research

The research work reported in the present dissertation may be outlined as-

- Study of the physico-chemical properties of molecular solvents, DMF and ACN and their binary and ternary mixtures with [emim][TFSI] and [emim][PF₆].
- Investigation of the intermolecular interaction between these ILs with molecular solvents in binary and ternary mixtures.
- Exploration of the effect of temperature on the physico-chemical properties in binary and ternary mixtures.
- Correlation of the physico-chemical properties as a function of temperature with the change in these properties against the compositions.

1.1.3. Present Work

In this work, physico-chemical properties of imidazolium based ILs have been studied with different pure and mixed polar solvents and compared with those in the absence of any solvents. The choice of ILs has been made in order that, two of them contain the same cation but different anions. As a result, the structural effect of the anion and cation has been investigated and an attempt has been made to reveal the structure-property relationship in presence of molecular solvent. 1-ethyl-3-methylimidazoliumbis (trifluoromethanesulfonyl)-imide [emim][TFSI], 1-ethyl-3-methylimidazoliumtrifluoro phosphate [emim][PF₆] have been used for the preparation of binary and ternary mixtures with molecular solvents, *N,N*-dimethylformamide (DMF) and acetonitrile (ACN) which are polar aprotic solvents and their polarity are 36.71 and 37.08 respectively. The structures of the constituent ions in the ILs and molecular solvents are shown in the Figure 1.1.3.1. Here, the intensive properties: density, viscosity, refractive index and conductivity have been measured with varying compositions to analyze the internal molecular interaction between these ILs with DMF and ILs with ACN in binary mixtures

and ILs with DMF and ACN in ternary mixtures. The ultimate goal has been to understand the various molecular interactions between [emim][TFSI], DMF and ACN in their binary and ternary mixtures to tune properties of ILs for task specific applications.

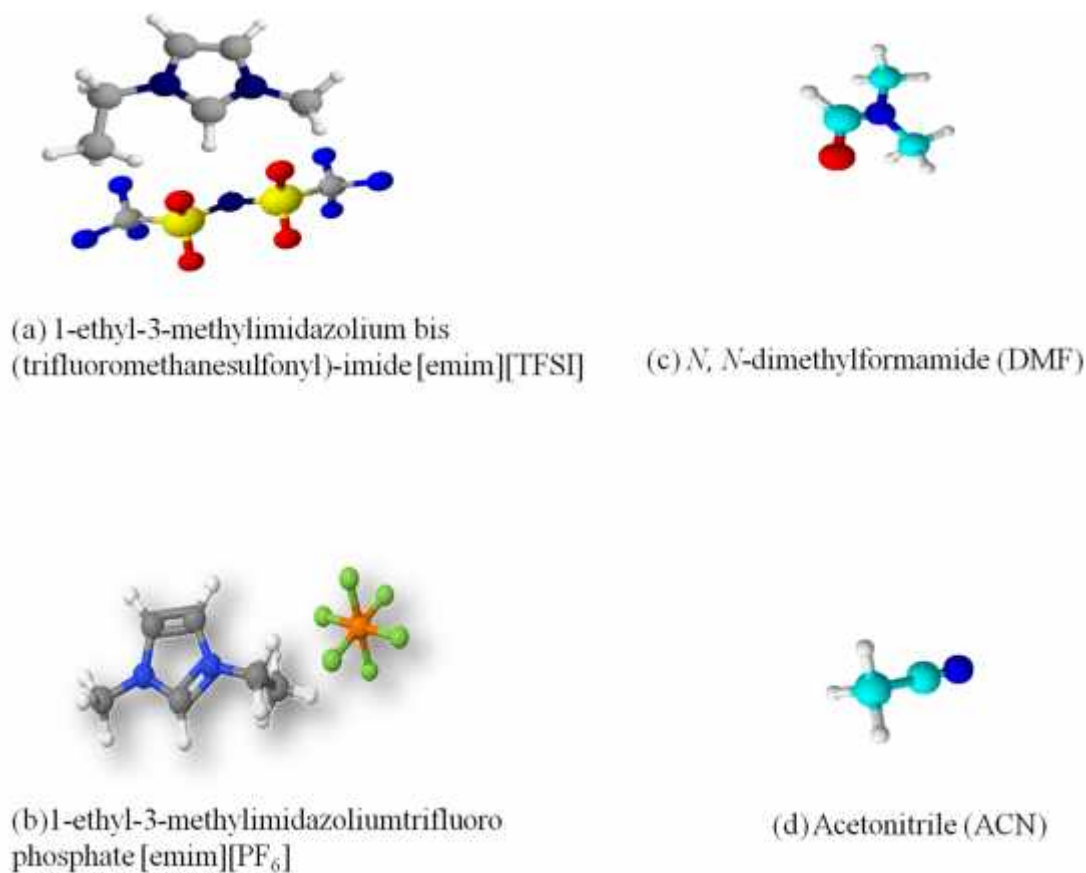


Figure 1.1.3.1 Structures of (a)[emim][TFSI], (b) [emim][PF₆], (c) DMF and (d) ACN.

Additionally, the excess molar volume (V^E), excess viscosity (η^E) and excess refractive index (n^E) have been calculated from the physico-chemical properties. The excess properties-mole fractions of different components profiles have been fitted to Redlich-Kister polynomial equation to further confirm the intermolecular interaction between these ILs and molecular solvents in binary and ternary mixtures.

1.2. Ionic Liquids (ILs)

ILs can be defined as a class of liquid salts which are composed entirely of bulky and asymmetrical cations in combination with a large variety of inorganic and organic anions with melting point below 100 °C. The unique set of physico-chemical properties of ILs such as negligible vapor pressure, non-flammability, high ionic conductivity, and high thermal, chemical and electrochemical stability [43-44] have rendered them as one of the most attractive materials in the field of modern science. The establishment and development of modern industries cannot be apart from creation and application of novel liquids. Featured by many advantageous properties including good tunability and solvation ability, organic solvents have been widely used in industrial activities. However, due to their organic nature, organic solvents are usually volatile, which greatly raises the risk of flammation and pollution [45]. To overcome these problems, inorganic molten salts working at high temperatures were once regarded as a “green” replacement to organic solvents in many applications [46]. Despite their many advantages, such as non-flammability, non-volatility, good stability, and conductivity, inorganic molten salts suffer from the high melting temperature owing to their strong ionic nature [47] allowing them to be promising “green” solvents utilized in many areas, such as chemical synthesis [43,49], catalysis [43,50], energy storage [43,51], lubricants [43, 52], materials [43,53], and biology [43,54]. Even though not all the ILs discovered so far are toxicity-free and biodegradable, their non-volatile and non-flammable features greatly reduce the risk of possible pollution and danger. Since different combinations of cation and anion produce at least millions of available ILs (much more than organic solvents) [43] with a large variety of physical and chemical properties, one can in principle always find a suitable candidate to meet the requirement of a designated application. On the other hand, also because of the vast number of candidates, determining the properties of all ILs one by one experiment is unfeasible. Therefore, selecting suitable candidates to meet specific requirements by computer-aided systematic design is essential for the efficient and smart utilization of ILs.

ILs are also called designer solvents, as their physico-chemical properties can be easily tuned simply by changing the structure of the component ions. They can also be used as electrolytes for energy devices such as lithium secondary batteries, electric double layer capacitors, supercapacitors, dye-sensitized solar cells (DSSC), fuel cells, actuators and as

a medium for electrodeposition [55-66]. Most interesting features of ILs can be attributed to remarkable interionic interactions and these can be an important key factor to study the characteristics of ILs at molecular level.

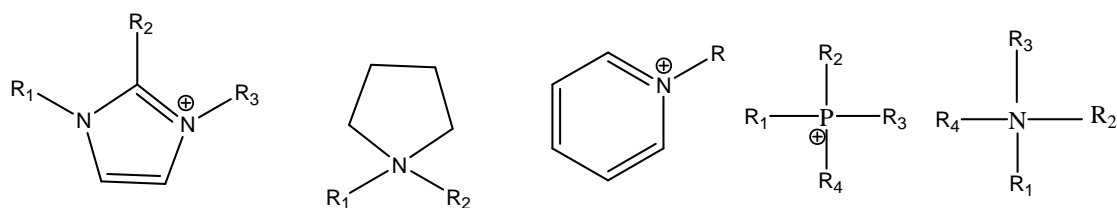
1.2.1. History of ILs

The origins of modern ILs, the chemistry of salts with low melting points, can be traced back to the second half of the nineteenth century when chemists noted that a liquid, known as “red oil”, often appeared as a separate phase during Friedel-Crafts reactions. Friedel and Crafts first described their alkylation reaction in a French scientific journal in 1877 [68]. They noted that when small quantities of anhydrous aluminium chloride were added to amyl chloride a reaction ensued that resulted in a liquid that divided into two layers. In Japanese it was later shown that the red oil consisted of an alkylated aromatic ring cation and a chloroaluminate anion and the oil is an IL. In 1888, Gabriel reported the discovery of the protic IL ethanalammonium nitrate (m.p. 52-53 °C), which was probably the first organic salt with melting point of less than 100 °C. One of the earlier known the first room temperature ILs was ethylammonium nitrate $[\text{C}_2\text{N}_5\text{NH}_3][\text{NO}_3]$ (m.p. 12 °C), which was first reported by P. Walden in 1914 [69]. But this IL did not attract further application-based research due to its explosive nature.

1.2.2. Structure of ILs

An IL consists of a cation, which is normally a bulk organic structure with low symmetry. The widely used cations in ILs are based on ammonium, sulfonium, phosphonium, imidazolium, pyridinium, picolinium, pyrrolinium, etc with different substitutions. The anion of IL may be organic or inorganic. For example, anions include $[\text{BF}_4]^-$, $[\text{PF}_6]^-$, $[\text{TFSI}]^-$, alkyl sulfates, etc. The forces operating between cation and anion of an IL are overwhelmingly columbic in nature. Figure 1.2.2.1 displays some typical cations and anions that are commonly employed in synthesizing ILs. The first generation ILs include a mixture of organic species with AlCl_3 . These ILs are known as chloroaluminates. In spite of their hygroscopic nature these IL have been used as electrolytes in batteries. ILs with $[\text{BF}_4]^-$, $[\text{PF}_6]^-$ anions etc are air stable and neutral. The ILs can react exothermically with Lewis acids and water. ILs containing $[\text{TFSI}]^-$ or $[\text{CF}_3\text{SO}_3]^-$ anions possess low melting points and are stable in water and the medium containing Lewis acids.

Cation



Anion

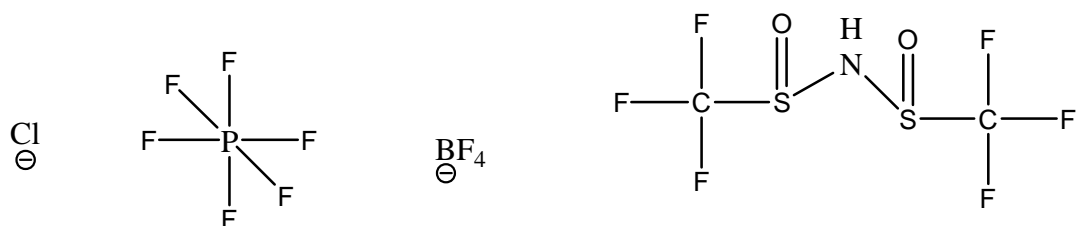


Figure 1.2.2.1. Some typical cations and anions of ionic liquids.

1.2.3. Classification of ILs

ILs are sometimes classified historically into three generations;

First Generation ILs

The haloaluminate ILs comprise the first generation. The earliest examples of room temperature ILs in this category are the eutectic mixtures of aluminium chloride and ethylpyridinium halides described by Hurley and Wier in 1951 [70]. Haloaluminate ILs have been studied extensively as solvents and catalysts for Friedel-Crafts and other reactions in organic chemistry. These ILs react with water and therefore have to be handled in a dry-box. Another example of this generation is dialkylimidazolium chloroaluminates that were first reported by Wilkes, Hussey and co-workers in 1982 [71].

Second Generation ILs

Second generation ILs are the non-haloaluminate ILs that can be used on the bench top. They have been used extensively as solvents in organic chemistry. The first examples

were described by Wilkes and Zaworotko in 1992 [72]. They included dialkylimidazolium ILs with weakly coordinating anions such as hexafluorophosphate [PF₆] and tetrafluoroborate [BF₄]. These ILs were originally thought to be stable in air and water but it was subsequently shown that they undergo hydrolysis under certain conditions, resulting in the formation of toxic and corrosive hydrogen fluoride [73]. Bonhote, Gratzel and co-workers in 1996 described the synthesis of hydrophobic ILs with [TFSI] anions [74]. These second-generation ILs are stable in the presence of air and water.

Third Generation ILs

The third generations are the task-specific ILs and chiral ILs. The third generations are broad categories and not exclusive. The generations generally refer to pyridinium and particularly imidazolium ILs as these are the families of ILs that have been studied most extensively in recent years.

Depending on the extent of water miscibility ILs are of two types. They are -

i) Hydrophilic IL

An IL, which is miscible with water in any proportion, is termed as a hydrophilic IL. The physical properties of this type of ILs are greatly influenced by the change in water content. In this type of ILs water molecules are stabilized in the bulk by favorable intermolecular interactions such as, hydrogen bond and dipole-dipole forces in such ILs [75-76]. Halide, ethanoate, trifluoro acetate, methyl sulphate based ILs are examples of this class.

ii) Hydrophobic IL

At room temperature some ILs show miscibility gap or phase split in water. These are commonly referred to as "hydrophobic". In hydrophobic ILs, water molecules in the bulk are less stable. Therefore, they are pulled out to surface to form a separate phase [26]. The common examples of hydrophobic ILs are alkylimidazolium bis(trifluoromethylsulfonyl)imide $[C_n\text{mim}][(\text{CF}_3\text{SO}_2)_2\text{N}]$ and hexafluorophosphate $[C_n\text{mim}][\text{PF}_6]$.

According to Angell *et al.* [77], ILs are classified into four types based on the constituent ions,

Aprotic ILs

If the cations and anions of IL are free from proton the IL is called aprotic IL. Example of aprotic ILs are 1-ethyl 3-methyl imidazolium bis trifluoromethan sulfonyl imide $[\text{emim}][\text{TFSI}]$ and 1-ethyl 3-methyl imidazolium bis trifluoro phosphate $[\text{emim}][\text{PF}_6]$ etc.

Protic ILs

When the IL is formed by the proton transfer from pure Br nsted acid to Br nsted, it is called protic IL. The classic example of a protic IL is ethylammonium nitrate, $[\text{C}_2\text{H}_5\text{NH}_3][\text{NO}_3]$, which is formed by the protonation of ethylamine. Another example is 1-methylimidazolium tetrafluoroborate $[\text{Hmim}][\text{BF}_4]$.

Inorganic ILs

Inorganic ILs consists entirely of inorganic entities. These are obtained, in both aprotic and protic forms. The aprotic example, lithium chlorate (melting point 115 °C). The protic example, hydrazinium nitrate, (melting temperature, $T_m = 80$ °C). The first IL were probably inorganic type, that was the eutectic mixtures of ammonium salts like the NH_4SCN and NH_4NO_3 [80]. A largely unexplored cases of salts with inorganic molecular cations, such as PBr_3Cl^+ , SCl_3^+ , $\text{ClSO}_2\text{NH}_3^+$ etc., with appropriate weak base anions is also present. A sharply melting compound $(\text{PNCI}_2)_3$. HTFSI, has been obtained from the equimolar melt of the components, [81] due to low "ionicity" [81-85] its conductivity is

too low to class it as an IL. The nitrogen atoms of PNCl_2 are known to be only weakly basic, so the salt, if formed with a stronger acid (e.g., HSbF_6), although of higher ionicity, also would be of high “acidity” [86] in fact, it would be a member of the class of *superacidic* ILs [87].

Solvate (Chelate) ILs

Solvate ILs contains nonionic entities. This is the liquid state of various ionic solvates. In these systems, molecules usually thought of as solvent molecules are bound tightly to high field cations and have no solvent function. These form a largely unstudied class of ILs that needs to be recognized because the class includes cases of multivalent cation salts that would not ordinarily be able to satisfy the criterion of $T_m < 100\text{ }^\circ\text{C}$. The first recognized members of this class were molten salt hydrates, like $\text{Ca}(\text{NO}_3)_2 \cdot 4\text{H}_2\text{O}$, whose mixtures with alkali metal salts were found to be almost ideal mixtures [88] The new class of molten salt mixtures, has concerns regarding the lifetime of the water molecules in the cation coordination shell. This should be long with respect to the diffusion time scale for the ILs classification to be unambiguous. In recent examples, long lifetime is guaranteed because the ligating groups all belong to the same molecule [89].

1.2.4. Properties of ILs

ILs have emerged as one of the most promising materials in the modern science due to their unique properties. Important properties are listed below.

- ILs have negligible vapor pressures, and therefore do not evaporate under normal conditions.
- ILs are generally non-flammable and many remain thermally stable at temperatures higher than conventional organic molecular solvents.
- ILs have wide liquid ranges than molecular solvents.
- ILs have a wide range of solubilities and miscibilities.

- ILs have wide electrochemical windows.
- ILs can be used as reaction media and / or catalysts for a wide variety of chemical reactions.
- ILs can be used for separations and extractions of chemicals from aqueous and molecular organic solvents.
- ILs can be readily recycled.

1.2.4.1. Ionic liquids are liquids

Ionic compounds are normally solid at standard temperature and pressure (STP) and have very high melting temperature. For example, melting points of sodium chloride and lithium chloride are 801 °C and 614 °C, respectively. Although ILs are comprised entirely of ions, they have relatively low melting points and exist in liquid state at ambient and far below ambient temperature. This difference in melting point arises due to the large size and asymmetry in the ions. The bulky and asymmetric ions interact weakly and are less likely to crystallize. So the ion size can be responsible behind the low melting temperature of ILs. The melting point of a compound is governed by the lattice energy which is a measure of the strength of the forces between the ions in an ionic compound. The lattice energy is dependent on the charge of the ion, distance between the ions and Madelung constant [91]. Generally, the cations of ILs are asymmetrical and large in size compared to those of molten salts and the anions have delocalized charge. The large size increases the distance between the ions and Madelung constants have lower values for ILs which results in lower binding energy of the ions. These cause reduction of melting points by lowering the Coulombic attractions between the ions. The asymmetric ions of ILs cause a distortion from the ideal close-packing of the ionic charges existing in the solid state lattice of molten salts. All these factors ultimately results in the lowering of lattice energy. Therefore, ILs have low melting points compared to molten salts. Researchers have inferred that besides pure Coulombic force other forces like hydrogen

bonds and van der Waals interactions play an important role on the properties of ILs which make them different from molten salts [91-93].

1.2.4.2. ILs as ‘Green Solvents’

ILs are good solvents for a wide range of organic inorganic and polymer materials. Because of their negligible vapor pressure they can serve as a green recyclable alternative to the volatile organic compounds that are traditionally used as industrial solvents [94-97]. Volatile organic solvents can escape into the atmosphere and pollute the environment where ILs are environmentally safe due to negligible vapor pressure, recycling possibility, biodegradability, nonflammability and non-combustibility.

1.2.4.3. Designer Solvents

ILs have been successfully used as solvents in many applications including organic and inorganic synthesis, chemical separations and electrochemistry. The physical, chemical and biological properties of ILs can be tuned or tailored by [98].

- a. switching anion or cation
- b. designing specific functionalities
- c. mixing two or more simple ILs
- d. changing the alkyl chain of cation

Since the properties of IL can be optimized to suit the requirement of a particular process, they are also designated as designer solvents.

1.2.5. Application of ILs

ILs have recently emerged as “green” and environment friendly solvents for their use in the industrial manufacture of chemicals. In the past decade, IL have been increasingly

used for diverse applications such as organic synthesis, catalysis, electrochemical devices and solvent extraction of a variety of compounds.

1.2.5.1. ILs as Solvents

Performing reactions in ILs is straightforward and practical when compared with similar reactions in conventional organic solvents due to their designable properties and broad variations of their solubility and miscibility. They can for example, dissolve both ionic and covalent compounds. ILs can also be selected or designed to dissolve a wide range of organic and inorganic gases, liquids and solids. Many organic reactions like Diels-Alder reaction, Friedel-Crafts alkylation and acylation, transition metal catalysis and photochemical reactions have been successfully carried out in IL media. [99]

1.2.5.2. Stoichiometric Organic Synthesis

Organic reactions in ILs have been studied widely, aiming to accelerate the formation of product or to tune the selectivity of the reaction. There have been a number of notable achievements reported [100]. One such example is the Diels–Alder reaction with the IL [EtNH₃][NO₃], reported by Jaeger and Tucker[104]. The selectivity of the cycloaddition of cyclopentadiene to methyl acrylate was comparable with those obtained when the same reaction was carried out in water [101-103], however the reaction rate was reported to be somewhat slower. Using chloroaluminate ILs, however, it was found to enhance the reaction rate as well as the selectivity [105].

1.2.5.3. Catalyzed Reactions

There is a plethora of catalysis reactions using ILs, most of which have been performed with varying degrees of success. Both Chauvin and Osteryoung incorporated transition metal complexes in organic chemistry using ILs in separate works. Chauvin catalyzed [106] the dimerization of alkenes using nickel complexes dissolved in acidic chloroaluminate ILs, while Osteryoung used Ziegler-Natta [107] catalysts in a similar solvent in the polymerization of ethylene. However, it was Zaworotko's water-stable IL

containing tetrafluoroborate, hexafluorophosphate, nitrate, sulfate and acetate anions which propelled the work forward [108,109], a key finding being the enhancement of reaction rates and selectivity of organic reactions using ILs.

1.2.5.4. Extraction of Organic Compounds

Unsaturated organic compounds, particularly aromatic compounds, tend to be soluble in ILs whereas saturated organic compounds are generally immiscible with ILs. As a result it should, in principle, be possible to separate the aromatic and aliphatic hydrocarbons produced by naphtha crackers. Dionysiou, Botsaris and co-workers have demonstrated that it is possible to extract organic contaminants such as chlorophenols from water using hydrophobic ILs [109].

1.2.5.5. Gas Separations

The widely variable solubilities of gases in ILs open up the possibility of using ILs as absorption liquids to separate one or more gases from mixtures of gases. The prospect is particularly attractive because ILs are non volatile and therefore do not evaporate and contaminate the gaseous mixture. ILs can absorb sulfur dioxide, (SO_2). SO_2 is used as a preservative and in the manufacture of sulfuric acid. However it is also emitted by volcanoes, by combustion of sulfur-containing fossil fuels and other industrial processes. When it escapes into the atmosphere it not only poses a human health problem but also can cause acid rain and smog. Industrial emissions are reduced by processes such as flue gas desulfurization, a process that employs lime (CaO) to react with the gas.

1.2.5.6. Carbon dioxide Extractions and Separations

The extraction of non-volatile organic compounds dissolved in ILs without the use of conventional organic solvents is one of the major technical challenges for the use of ILs in chemical manufacturing. Distillation or gas stripping cannot be used to remove non-volatile solute from ILs. The use of supercritical CO_2 could possibly overcome this problem. CO_2 dissolves in ILs to form a two-phase system. Super-critical CO_2 that is carbon dioxide that has been heated and pressurized above its critical temperature and

pressure is an environmentally-benign solvent. The fluid is not only abundant and inexpensive; it is also non-toxic and non-flammable.

1.2.5.7. Metal Ion Extraction

The use of hydrophobic ILs to replace hydrophobic volatile organic solvents as extracting phases to remove metal ion from aqueous solutions is an exciting prospect. Potential applications include the extraction of metal from ores, the removal of metal contaminants from water, and reprocessing of nuclear waste. However, the affinity of metal ions for hydrophobic ILs is generally low because the ions tend to be hydrated in aqueous solutions. The problem can be overcome by using conventional metal ion extractants, such as crown ethers. These extractants dehydrate the metal ions and form complexes with them. The metal-extractants complexes are more hydrophobic than the metal ions and therefore partition preferentially to the hydrophobic solvent.

1.2.5.8. Membrane Separations

The use of porous membranes impregnated with ILS to separate gases has attracted interest over recent years. Supported IL membranes (SILMS) operate on the same principle as supported liquid membranes (SLMS). A feed stream consisting of a mixture of gases under pressure is passed over one side of the membrane. Soluble gas molecules dissolve in the liquid inside the membrane pores. The molecules then permeate through the membrane by diffusion and desorb on the other side where they are swept out by a receiving gas in the so called permeate stream.

1.2.5.9. Electrochemical Supercapacitors

Electrochemical supercapacitors are simple energy storage devices with high rate charging discharging capabilities and high power density. It is based on the electrochemical double layer resulting from the electrostatic adsorption of ionic species at the electrode-solution interface, *i.e.*, no actual redox reaction is supposed to take place during the charging-discharging of these devices. To obtain the maximum possible capacitance, supercapacitor electrodes must have a high surface area; because these

devices are based on the electrosorption of ionic species, the region between the electrodes of the capacitor must contain an electrolyte with mobile ions. Because of the numerous favorable properties described above, ILs are considered to be promising electrolytes for electrochemical supercapacitors [110, 111].

1.2.5.10. Dye-Sensitized Solar Cell

The possibility of using ILs as electrolytes in dye-sensitized solar cells (DSSCs) has been an active area of research since the early 2000s. DSSCs are photovoltaic cells that mimic photosynthesis by using a photosensitive dye, typically a ruthenium bipyridyl complex. The dye has the same role as chlorophyll in plants.

1.2.6. Application of ILs Based Binary and Ternary Systems

In order to expand the utility of ILs and better tune their physico-chemical properties, IL-based mixed solvents appear to be very promising ones. Interesting ILs may be combined with another green solvent to tailor the physico-chemical properties of the IL of interest in a favorable fashion and controlled manner. From the combination of neat ILs with other solvents in binary mixtures the availability and diversity of the media can be strongly increased. Often in order to increase the efficiency of a process a solvent or solvent mixtures may be tuned by the addition of co-solvents. Mixing makes it easy to control the properties of solutions. Co-solvent modified ILs may alleviate the problem of limited solute solubility associated with many ILs as well as provide easily affordable solubilizing media with conveniently modified physico-chemical properties. This approach has the potential to increase the efficiency and applications of ILs. IL-molecular solvent mixed binary systems have found immense industrial, pharmaceutical and biomedical importance due to their environmentally compatible nature. For the presence of an array of interactions stemming from the individual molecular architectures of ILs and co-solvent, mixing an IL with a molecular solvent may result in medium that possesses desired, interesting and versatile physico-chemical properties. Reciprocally, properties of molecular solvent may also get modified in favorable manner by addition of an IL to it. Thus theoretically IL and co-solvent based binary system can be designed to deliver almost any application in the chemical science.

1.3. Review of literature

ILs have attracted extensive attention because of their extraordinary physico-chemical properties and applications in multidisciplinary fields. The history of ILs started with the development of aluminum chloride-based salts for electroplating in 1948. Since then the considerable basic research efforts have proved their potentials in various fields of application. A literature survey has been made on a number of articles that are based on experimental and computational works involving the structure and properties of IL and IL based binary systems.

1.3.1. Literature Review on Physico-chemical Properties of Pure IL

[EtNH₃][NO₃], $T_m = 12$ °C, was first reported in 1914 [69]. Research on ILs was renewed by discovery of alkyipyridinium or 1, 3-dialkylimidazolium haloaluminate salts. Aluminum halides were mixed with the corresponding imidazolium or pyridinium halides salts to obtain ILs [114], however, these haloaluminate ILs are highly sensitive to atmospheric moisture. A significant milestone in the development of ILs was achieved when a range of anions such as hexafluorophosphate, [PF₆] and tetrafluoroborate, [BF₄], were incorporated with imidazolium-based cations [113,114] to obtain air and water stable ILs.

Keneth R. Seddon holds a pioneering role in establishing IL as a convenient, environmentally benign, superior alternative to the conventional environmentally detrimental molecular solvents. Seddon and coworker reported the better catalytic activity of 1-butylpyridinium chloride and 1-ethyl-3-methylimidazolium chloride and their contribution to the reduction of hazardous byproduct formation in various chemical processes [115]. Later, in a review article, the incredibly expanding application of IL from the traditional industrial process to sophisticated space technology [116] was accounted.

An interesting overview of the field of low-melting ILs was presented by Austen Angell *et al.* They reported that ILs are classified as protic, aprotic, inorganic and solvate according to their structures [117].

Vyas *et al.* studied the electronic and structural properties of 1-ethyl-3-methylimidazolium bis(trifluoromethylsulfonyl)imide by using density functional theory (DFT) methods in addition to infrared and UV-vis spectroscopy. From DFT calculations three energetically similar conformers were obtained for each of the gas phase and solution phase [118].

A convenient and effective route to produce excellent ILs without any by-products was suggested by Ohno and Yoshizawa. A wide variety of ILs was prepared by neutralization of five kinds of imidazole derivatives with nine acids. Bulk physico-chemical properties of generated ILs revealed that these characteristics are quite effective to provide higher ionic conductivity [119].

Several ILs were found to decompose without significant contribution of evaporation. Hyem *et al.* determined the rate constant of thermal decomposition and the vapour pressure of four ILs: [emim] [MeSO₃], [emim] [CF₃SO₃], [bmim][NTf₂] and found that their vapour pressure is so low that it can be only detected by ultra sensitive magnetic suspension balance at high vacuum condition. Such a low volatility further reinforced the green credibility of ILs.

The potential of protic ILs (PILs) as fuel cell electrolytes was first explored by Susan *et al.* [120] The PILs were formed from the strong acid and a variety of different organic amine bases. They correlated the physico-chemical properties with the structure and properties of the constituent amines and the acids.

The presence of hydrogen bond in ILs was first proved by Fumino *et al.* from the far-IR spectroscopic measurement and illustrated the implications of H-bonding on melting point, enthalpy of vaporization and viscosities stating that despite the purely ionic structure and dominant coulombic force persisting in ILs, local and directional interaction

like H-bonding can destroy its charge symmetry to exert significant influence on the physico-chemical properties [121-124].

The diffusion behaviour of cations and anions was studied and compared for the room-temperature ILs [emim][BF₄], [emim][TFSI], [BP][BF₄], and [BP][TFSI]. Noda *et al.* [125] measured the thermal property, density, self-diffusion coefficient of the anions and cations, viscosity, and ionic conductivity for these ILs in wide temperature ranges and used pulsed-gradient spin-echo NMR method to independently determine self-diffusion coefficients of the anions (¹⁹F NMR) and the cations (¹H NMR). From the results they reported the trend, [MI][TFSI] > [emim][BF₄] > [BP][TFSI] > [BP][BF₄] for cationic and anionic diffusion coefficients summation of each IL under an isothermal condition and confirmed that the cations diffuse almost equally to the anion in [emim][BF₄], whereas they diffuse faster than the anion in [emim][TFSI] and [BP][TFSI].

Watanabe and co worker reported that protic ILs and salts (PILs/PSs) can be used as novel, low molecular weight organic precursors for the direct synthesis of carbon materials (CMs). In contrast to conventional precursors, PILs/PSs possess negligible volatility, comparable to that of aprotic ILs, but are easily obtained and widely available. The structural diversity of PILs/PSs also enables us to investigate the correlation between the precursor structures and the properties of the final CMs, which allows the synthesis of specific CMs with controlled structure and properties [126].

1.3.2. Literature Review on Physico-chemical Properties of IL Binary Mixtures

Pereiro and Rodriguez determined experimental densities, speeds of sound and refractive indices of the binary mixtures of ethanol with (1,3-dimethyl imidazolium methyl sulfate) [mmim]⁺[MeSO₄]⁻, 1-butyl-3-methyl imidazolium methyl sulfate [bmim]⁺[MeSO₄], 1-butyl-3-methylimidazonium hexafluorophosphate [bmim]⁺[PF₆]⁻, 1-hexyl-3-methylimidazonium hexafluorophosphate [bmim]⁺[PF₆]⁻ and 1-methyl-3-octylimidazonium hexafluorophosphate [omim]⁺[PF₆]⁻ at $T = (293.15 \text{ to } 303.15) \text{ K}$ and calculated excess molar volumes, changes of refractive index on mixing and deviation in isentropic compressibility for the above systems. They showed that the excess molar

volumes and deviations in isentropic compressibilities decrease when the temperature is increased for the systems studied [127].

The addition of an aprotic solvent to an IL greatly decreases the viscosity of the IL and, up to a certain mole fraction of solvent, increases the conductivity. Fox *et al.* [128] examined in detail the density, viscosity, thermal stability and ionic conductivity of mixtures of ILs with a variety of different aprotic solvents. Furthermore, the addition of solvent can greatly increase the temperature range over which the mixtures remain liquids.

The physico-chemical properties of various systems of binary mixtures involving ILs have been studied extensively. Singh and Kumar measured the densities and refractive indices for binary mixtures of 1-methyl-3-octylimidazolium tetrafluoroborate [omim]⁺[BF₄]⁻ with ethylene glycol monomethyl ether (EGMME, C₁E₁), diethylene glycol monomethyl ether (DEGMME, C₁E₂), and triethylene glycol monomethyl ether (TEGMME, C₁E₃), over the whole composition range and used experimental densities to estimate excess molar volumes, apparent molar volumes, partial molar volumes, excess partial molar volumes and their limiting values at infinite dilution [129].

Zafarani-Moattar and Shekaari reported the density, excess molar volumes, speed of sound data for 1-butyl-3-methylimidazolium hexafluorophosphate [BMIM]⁺[PF₆]⁻ + methanol and [BMIM]⁺[PF₆] + acetonitrile binary mixtures over the entire range of composition at $T = (298.15 \text{ to } 318.15) \text{ K}$ [130].

Gomez *et al.* determined the experimental densities, dynamic viscosities, excess molar volumes, speed of sound and isentropic compressibilities over the whole composition range for (1-ethyl-3-methylimidazolium ethylsulphate [EMIM]⁺[EtSO₄]⁻ + ethanol) and (1-ethyl-3-methylimidazolium ethyl sulphate [EMIM]⁺[EtSO₄] + water) binary systems at $T = (268.15, 313.15 \text{ and } 328.15) \text{ K}$ and atmospheric pressure and performed the fitting of the Redlich-Kister equation to the excess molar volume, viscosity deviation and the deviation in isentropic compressibility data for the binary systems [131].

Domanska *et al.* determined the solubility of 1-butyl-3-methylimidazolium octylsulphate $[\text{bmim}]^+[\text{OcSO}_4]^-$ in hydrocarbon (*n*-hexane, *n*-heptane, *n*-octane or *n*-decane) solutions and alcohols (methanol, 1-butanol, 1-hexanol, 1-octanol or 1-decanol) solutions. They also examined the densities and excess molar volumes for 1-methyl-3-methylimidazolium methyl sulphate $[\text{mimm}]^+[\text{MeSO}_4]^-$ with alcohols (methanol, ethanol or 1-butanol) and with water, for 1-butyl 3-methylimidazolium methyl sulphate $[\text{MMIM}]^+[\text{MeSO}_4]^-$ with an alcohol (methanol, ethanol, 1-butanol, 1-hexanol, 1-octanol or 1-decanol) and with water and for 1-butyl-3-methylimidazolium octylsulphate $[\text{MMIM}]^+[\text{OcSO}_4]^-$ with an alcohol (methanol, 1-butanol, 1-hexanol, 1-octanol or 1-decanol) at $T = 298.15$ K and atmospheric pressure [132].

Heintz *et al.* presented the experimental data of densities and viscosities for the system 4-methyl-N-butylpyridinium tetrafluoroborate and methanol at $T = 25, 40, 50$ and 323.15 K and ambient pressure and calculated the excess molar volumes and excess logarithm viscosities from the experimental data.

Lopes *et al.* reported, V_m^E , data of six binary mixtures composed of two different ILs with a common anion $[\text{Tf}_2\text{N}]^-$ $\{[\text{C}_m\text{MIM}]^- [\text{Tf}_2\text{N}]^- + \{[\text{C}_n\text{MIM}]^- [\text{Tf}_2\text{N}]^-$ with n and m ranging from 2 to 10 $\}$ at $T = (298.15$ and $333.15)$ K, as well, V_m^E , data of three binary systems containing $[\text{bmim}]$ as a common cation: $([\text{bmim}] [\text{Tf}_2\text{N}]^- + [\text{bmim}]^- [\text{PF}_6]^-)$, $([\text{bmim}]^+[\text{Tf}_2\text{N}]^- + [\text{bmim}]^- [\text{PF}_4]^-)$ and $([\text{bmim}]^+ [\text{BF}_4]^- + ([\text{bmim}]^- [\text{PF}_6]^-)$ [133].

ILs based on the imidazolium cation usually have low melting points, with many being liquids at room temperature. McEwen [134] in 1999 found that imidazolium based ILs have lower melting points and are thermally more stable than the lithium ion analogs.

The thermal stability of imidazolium-based ILs increase with increasing anion size, and heat capacities increase with temperature and increasing number of atoms in the IL, as found by Fredlake *et al.* [135] in their study of thermophysical properties of 13 imidazolium-based ILs.

Change in physico-chemical properties may be explained in terms of the effective ion contribution and the balancing level between multiple interacting forces, as shown by Tokuda *et al.* They also investigated the physico-chemical properties of imidazolium-based ILs depend on the structure [136-140] and may be tuned by controlling the structure of the constituent cation.

The toxicity of IL-ACN binary systems was studied by Chaban *et al.* [141] on the basis of an atomistic precision simulations of liquid/vapor interfaces over a wide composition range, of binary systems of ACN with [emim][BF₄] and with [bmim] [BF₄]. They evidenced that ILs are able to noticeably decrease the volatility of ACN, and hence, reduce a hazard.

By using high-pressure IR spectroscopy, Umebayashi *et al.* [142] investigated the microscopic structure of [emim][TFSI] and a molecular liquid ACN or methanol (MeOH). They observed the nature of local organization of imidazolium C-H in MeOH and ACN.

Chaban *et al.* [19] showed, for the first time, that conductivities of ILs only insignificantly depend on the cation size, shape, and mass. They demonstrated ability to enhance the ionic conductivity of IL by varying the mole fraction of solvent that favors oncoming applications of the IL-ACN mixtures.

In a study of the polarity of the binary mixtures of nine different ILs with dilute solutions of ACN, Garcia *et al.* [135] concluded that a slight (CN) wavenumber shift on changing [bmim][BF₄] to [bmim][TFSI] by using the Raman spectra.

The packing efficiency between IL-DMF was found to decrease at higher concentration of IL leading to positive deviation, and at lower concentrations, the packing efficiency increases, reported Pankaj *et al.*[2].

By solvatochromic method, using Reichardt's betaine dye K. Ahmed and co worker investigated the polarity behavior of a hydrophobic IL [emim][TFSI] and binary mixtures of [emim][TFSI]with ethanol, acetone and dichloromethane. Solvatochromic results

shows that the polarity of [emim][TFSI] is similar to that of ethanol. Irrespective of the polarity of the molecular solvent, addition of the IL in a solvent (polar, nonpolar or intermediate polar) brings about an apparent increase in the polarity of the system due to enhancement of HBD ability [141].

The density, refractive index, and viscosity for ILs [C_nmim]Cl (C_nmim = 1-alkyl-3-methylimidazolium; n = 2, 4, 6, 8 for ethyl, butyl, hexyl, and octyl) with DMF binary systems were measured by Yan *et al.* [42] and his results showed that the trend is [C₂mim]Cl > [C₄mim]Cl > [C₆mim]Cl > [C₈mim]Cl for the ILs with longer carbon chain cannot be close packed in the microscopic structure.

Yan *et al.*[137] showed that ILs with longer chains cannot be close packed in the microscopic structure. They measured the density, refractive index, and viscosity for [C_nmim]Cl (C_nmim = 1-alkyl-3-methylimidazolium; n = 2,4,6,8 for ethyl, butyl, hexyl, and octyl) with DMF binary systems over the entire range of composition at T= 288.15 K to 318.15, finding that the trend was [C₂mim]Cl > [C₄mim]Cl > [C₆mim]Cl > [C₈mim]Cl.

By using near-infrared (NIR) spectroscopy, Mayeesha *et al.* [142] described the structures of different water species present in binary mixtures of an IL, 1-ethyl 3-methylimidazolium tetrafluoroborate and water of varying compositions and for the first time they showed the aggregation behavior and interactions between different species in the system have been inferred from the analyses of combination bands of NIR spectra. The size of the aggregates has been found to increase with increasing amount of IL and decrease with increasing temperature. Finally, the properties of the IL-water binary mixtures have been found to be governed by the strength of IL-water bonds and population of IL-IL and water-water clusters.

1.3.3. Literature Review on Physico-chemical Properties of IL Ternary Mixtures

A range of studies have been done with binary mixtures of ILs. Xu *et al.*[137] studied the excess molar volumes of [bmim][PF₆] with ACN, and Ma and coworkers measured the densities of binary mixtures of [bmim][PF₆] and [bmim] [BF₄] with ACN, benzene and propanol, while Clavar *et al.*[29] measured densities, refractive index, speeds of sound

and isentropic compressibilities of binary mixtures of [C₄mim][Cl] and water and ethanol and also ternary mixture of [C₄mim][Cl] with water and ethanol at 298.15K.

Malyanah *et al.* [140] showed that density and refractive index values of [bmim] [BF₄] with MEA and water increase with increasing mole fraction of MEA. They also calculate the excess molar volume and excess refractive index and concluded that excess molar volume increased with increase in z and excess refractive index decrease with increase in z .

The density, speed of sound, heat capacity, of pure [emim] [BF₄], (NMP), (2-Py), pyridine were reported Sharma *et al.* [132]. They also measured these properties of binary mixtures of (NMP) and pyridine, and ternary mixtures of [emim][BF₄] and NMP and pyridine, as a function of temperatures. They observed thermodynamic properties of the binary as well as ternary mixtures have been calculated by utilizing the topology of the constituents of mixtures.

Miscibility often poses a setback in preparation and characterisation of ternary mixtures and their binary components. Navarro *et al.* [27] reported refractive indices and densities of the 2-propanol with water and [bmim][BF₄] at 298.15 K, where physical properties of 2-propanol and water and water and [bmim][BF₄] binary mixtures were measured at the same temperature, but the 2-propanol and [bmim][BF₄] mixture has been measured at 323.15 K, because the total miscibility for this mixture is achieved above this temperature.

References

- [1] P. Attri, P. Venkatesu, A. Kumar, *Journal of Physical Chemistry B*, **2010**, 114, 13415-13425.
- [2] P. Attri, M. Reddy, P. Venkatesu, A. Kumar, T. Hofman, *Journal of Physical Chemistry B*, **2010**, 114, 6126-6133.
- [3] E. T. Fox, E. Paillard, O. Borodin, W. A. Henderson, *Journal of Physical Chemistry C*, **2013**, 117, 78-84.
- [4] T. Kavitha, P. Attri, P. Venkatesu, R. S. Rama Devi, T. Hofman, *Journal*

- of Physical Chemistry B*, **2012**, 116, 4561-4574.
- [5] P. Attri, P. M. Reddy, P. Venkatesu, *Indian Journal of Chemistry A*, **2010**, 49, 736-742.
- [6] X. J. Yan, S. N. Li, Q. G. Zhai, Y. C. Jiang, M. C. Hu, *Journal of Chemical and Engineering Data*, **2014**, 59, 1411-1422.
- [7] D. Song, J. Chen, *Journal of Chemical and Engineering Data*, **2014**, 59, 257-262.
- [8] L. S. Andreia, Gouveia, C. Liliana, Tome, Isabel M. Marrucho, *Journal of Chemical and Engineering Data*, **2016**, 61, 2828-2843.
- [9] G. A. Dopazo, M. G. Temes, D. L. Lopez, J. C. Mejuto, *Mediterranean Journal of Chemistry*, **2014**, 3, 972-986.
- [10] M. Krlikowska, P. Lipinski, D. Maik, *Thermochimica Acta*, **2014**, 582, 1-9.
- [11] U. Domanska, M. Krolikowska, *Journal of Solution Chemistry*, **2012**, 41, 1422-1445.
- [12] L. Zhang, X. Lu, D. Ye, Y. Guo, W. Fang, *Journal of Chemical and Engineering Data*, **2016**, 61, 3834-3848.
- [13] S. Akhtar, A. N. M. O. Faruk, M. A. Saleh, *Journal of Physical Chemistry*, **2001**, 39, 383-399.
- [14] M. A. Iglesias-Otero, J. Troncoso, E. Carballo, L. Romani, *Journal of Solution Chemistry*, **2007**, 36, 1219-1230.
- [15] M. Anouti, A. Vigeant, J. Jacquemin, C. Brigouleix, D. Lemordant, *Journal of Chemical Thermodynamics*, **2010**, 42, 834-845.
- [16] Lu. Bai, Shu-Ni Li, Quan-Guo Zhai, Yu-Cheng Jiang, Man-Cheng Hu, *Chemical Papers*, **2015**, 69, 1378-1388.
- [17] A. N. Sonar, N. S. Pawar, Rasayan, *Journal of Chemistry*, **2010**, 3, 250-254.
- [18] D. S. Wankhede, *International Journal of Chemistry Research*, **2011**, 2, 24-26.
- [19] V. V. Chaban, I. Voroshylova, O. Kalugin, O. Prezdo, *Journal of Physical Chemistry B*, **2012**, 116, 7719-7723.
- [20] A. M. Rizzuto, R. L. Pennington, K. D. Sienerth, *Electrochimica Acta*,

- 2011**, 56, 5003-5008.
- [21] A. Stoppa, J. Hunger, R. Buchner, *Journal of Chemical and Engineering Data*, **2009**, 54, 468-472.
- [22] Y. Litaïem, M. Dhahbi, *Journal of Molecular Liquids*, **2012**, 169, 54-62.
- [23] O. Borodin, *Journal of Physical Chemistry B*, **2009**, 113, 11463-11467.
- [24] H. Tokuda, S. Suzuki, M. A. B. H. Susan, K. Hyamizu, M. Watanabe, *Journal of Physical Chemistry*, **2006**, 110, 19589-19593.
- [25] S. Tsuzuki, H. Tokuda, K. Hayamizu, M. Watanabe, *Journal of Physical Chemistry B*, **2005**, 34, 109-114.
- [26] A. Noda, K. Hayamizu, M. Watanabe, *Journal of Physical Chemistry B*, **2001**, 46, 105-109.
- [27] V. K. Sharma, S. Bhagour, S. Solanki, A. Rohilla, *Journal of Chemical and Engineering Data*, **2013**, 58, 1939-1954.
- [28] M. T. Malyanah, M. M. Akbar, T. Murugesan, *Journal of Molecular Liquids*, **2014**, 190, 23-29.
- [29] N. Calavar, B. Gonzalez, A. Dominguez, J. Tojo, *Journal of Solution Chemistry*, **2006**, 35, 1217-1225.
- [30] P. Navarro, M. Larriba, S. Garcia, J. Garcia, F. Rodriguez, *Journal of Chemical and Engineering Data*, **2012**, 57, 1165-1173.
- [31] X. J. Yan, N. L. Shu, Q. G. Zhai, Y. C. Jiang, M. C. Hu, *Journal of Chemical and Engineering Data*, **2014**, 59, 1411-1422.
- [32] Welton, *Chemical Reviews*, **1999**, 99, 2071-2084.
- [33] V. I. Parvulescu, C. Hardacre, *Chemical Reviews*, **2007**, 107, 2615-2665.
- [34] M. Armand, F. Endres, D. R. Macfarlane, H. Ohno, B. Scrosati, *Nature Materials*, **2009**, 8, 621-629 .
- [35] A. Somers, P. Howlett, D. MacFarlane, M. Forsyth, *Lubricants*, **2013**, 1, 3-21.
- [36] T. Torimoto, T. Tsuda, T. Okazaki, K. Kuwabata, *Advanced Materials*, **2010**, 22, 1196-1221.
- [37] P. Venkatesu, *Fluid Phase Equilibria*, **2010**, 289, 173-191.
- [38] E. Zagar, M. Zigon, *Polymer*, **2000**, 41, 3513-3521.

- [39] K. Y. Kang, J. S. H. Park, *Molecular Structure*, **2004**, 676, 171-176.
- [40] B. Garcia, R. Alcalde, M. J. Leal, S. J. Matos, *Journal of Chemical Society*, **1997**, 93, 1115-1118.
- [41] P. Venkatesu, J. M. Lee, M. H. Lin, *Journal of Chemical Thermodynamics*, **2005**, 53, 996-1002.
- [42] P. Venkatesu, P. V. M. Rao, *Journal of Chemical and Engineering Data*, **1997**, 42, 90-92.
- [43] V. N. Plechkova, K. R. Seddon, *Chemical Society Review*, **2008**, 37, 123-150.
- [44] P. Hapiot, Lagrost, *Chemical Reviews*, **2008**, 108, 2238-2264.
- [45] R. Rogers, K. R. Seddon, *Science*, **2003**, 302, 792-793.
- [46] M. Gaune-Escard, G. M. Haarberg, *Molten Salts Chemistry and Technology*. John Wiley and Sons, Ltd (2014).
- [47] Wilkes, *Green chemistry*, **2002**, 4, 73-80.
- [48] J. S. Wilkes, M. J. Zaworotko, *Journal of the Chemical Society*, **1992**, 965-967.
- [49] J. P. Dyson, C. M. Grossel, N. Srinivasan, T. Vine, T. Welton, J. D. Williams, P. J. A White, T. Zigras, *Journal of Chemical Society*, **1997**, 3465.
- [50] V. I. Parvulescu, Hardacre, *Chemical Reviews*, **2007**, 107, 2615-2665.
- [51] E. J. Martyn, S. S. M. Jose, G. A. Manuela, K. R. Seddon, J. A. Widegren, *Nature*, **2006**, 439, 831-834.
- [52] M. Palacio, B. Bhushan, *Tribology Letters*, **2010**, 40, 247-268.
- [53] K. R. Seddon, *Nature Materials*, **2003**, 2, 363-367.
- [54] V. Rantwijk, K. R. Sheldon, *Chemical Reviews*, **2007**, 107, 2757-2785.
- [55] T. Sato, G. Masuda, K. Takagi, *Electrochimica Acta*, **2004**, 49, 3603-3611
- [56] H. Sakaebe, H. Matsumoto, *Electrochemistry Communications*, **2003**, 5, 594-618.
- [57] C. Nanjundiah, S. F. Mcdevitt, V. R. Koch, *Journal of Electrochemical Society*, **1997**, 144, 3392-3409.

- [58] M. Ue, M. Takeda, A. Kominato, R. Hagiwara, Y. Ito, *Journal of Electrochemical Society*, **2003**, 150,499-504.
- [59] N. Papageorgiou, Y. Athanassov, M. Armand, P. Bonhote, H. Pettersson, A. Azam, M. Gratzel, *Journal of Electrochemical Society*, **1996**, 143, 3099-3108.
- [60] M. Doyle, S. K. Choi, G. Proulx, *Journal of The Electrochemical Society*, **2000**, 147, 3044-3049.
- [61] A. Noda, M. A. B. H. Susan, K.Kudo, S. Mitsushima, K. Hayamizu, M. Watanabe, *Journal of Physical Chemistry B*, **2003**, 107, 4024-4033.
- [62] M. A. B. H. Susan, A. Noda, S. Mitsushima, M. Watanabe, *Chemical Communications*, **2003**, 327, 938-939.
- [63] W. Lu, A. G. Fadeev, B. Qi, E. Smela, B. R. Mattes, J. Ding, G. M. Spinks, J. Mazurkiewicz, D. Zhou, G.G. Wallace, D. R. MacFarlane, S. A. Forsyth, M. Forsyth, *Science*, **2002**, 97, 983-997.
- [64] M. A. B. H. Susan, T. Kaneko, A. Noda, M. Watanabe, *Journal of American Chemical Society*, **2005**, 127, 4976-4983.
- [65] M. S. Miran, H. Kinsohita, T. Yasuda, M. A. B. H. Susan, M. Watanabe, *Physical Chemistry Chemical Physics*, **2012**, 14, 5178-5186.
- [66] M. S. Miran, T. Yasuda, K. Dokko, M. A. B. H. Susan *RSC Adv*, **2013**, 3, 4141-4144.
- [67] P. Venkatesu, P. V. M. Rao, *Journal of Chemical Thermodynamics*, **1998**, 30, 207-213.
- [68] C. Friedel, J. M. Crafts, *Journal Comptes Rendus*, **1877**, 84, 1392-1450.
- [69] P. Walden, *Bulletin Academic Imperial Science*, **1914**, 8, 405-422.
- [70] F. H. Hurely, T. P. Wier, *Journal of the Electrochemical Society*, **1951**, 98, 203-207.
- [71] J. S. Wilkes, J. A. Levisky, R. A. Wilson, C. L. Hussey, *Inorganic Chemistry Communications*, **1982**, 21,1263-1264.
- [72] J. S. Wilkes, G. Mamantov and R. Marassi, *Mathematical and Physical Sciences*, **1987**, 202, 405-416.
- [73] R. P. Swatloski, J. D. Holbrey, R. D. Rogers, *Green Chemistry*, **2003**, 5, 358-361.

- [74] P. Bonhote, A. P. Dias, N. Papageorgiou, K. Kalyanasundaram, M. Gratzel, *Inorganic Chemistry Communications*, **1996**, 35, 1168-1178.
- [75] R. M. L. Bell, *Molecular Physics*, **2003**, 101, 2625-2627.
- [76] C. D. Tran, S. H. D. P. Lacerda, D. Oliveira, *Applied Spectroscopy*, **2003**, 57, 148-152.
- [77] C. A. Angell, W. Xu, F. M. Yoshizawa, A. Hayashi, J. P. Belieres, P. Lucas, M. Videa, Z. F. Zhao, K. Ueno, Y. Ansari, J. Thomson, D. Gervasio, *Electrochemical Aspects of Ionic Liquids*, 2^{ed}. John Wiley and Sons, **2011**.
- [78] J. P. Belieres, D. Gervasio, C. A. Angell, *Chemical Communications*, **2006**, 4798-4799.
- [79] Z. Zhao, K. Ueno, C. A. Angell, *Journal of Physical Chemistry B*, **2011**, 115, 13467-13469.
- [80] K. Hayamizu, Y. Aihara, S. Arai, G. C. Martinez, *Journal of Physical Chemistry B*, **1999**, 103, 519-521.
- [81] M. Yoshizawa, W. Xu, C. A. Angell, *Journal of American Chemical Society*, **2003**, 125, 15411-15412.
- [82] C. A. Angell, N. Byrne, J. P. Belieres, *Accounts of Chemical Research*, **2007**, 40, 1228-1230.
- [83] D. R. MacFarlane, S. A. Forsyth, E. I. Izgorodina, A. P. Abbott, G. Annat, K. Frazer, *Physical Chemistry Chemical Physics*, **2009**, 11, 4960-4962.
- [84] K. Ueno, H. Tokuda, M. Watanabe, *Physical Chemistry Chemical Physics*, **2010**, 8, 1649.
- [85] J. P. Belieres, C. A. Angell, *Journal of Physical Chemistry B*, **2007**, 111, 4926-4928.
- [86] C. A. Angell, W. Xu, J. P. Belieres, M. Yoshizawa, **2010**, 132, 3078-3091.
- [87] C. A. Angell, *Journal of Electrochemical Society*, **1965**, 112, 1224-1226.
- [88] T. Tamura, T. Hachida, K. Yoshida, N. Tachikawa, K. Dokko, M. Watanabe, *Journal of Power Sources*, **2010**, 195, 6095-6097.

- [89] H. M. Evjen, *Physical Review*, **1932**, 39, 675-678.
- [90] K. Fumino, A. Wulf, R. Ludwig, *Angewandte Chemical International Edition*, **2009**, 48, 3184-3185.
- [91] W. Zhao, F. Leroy, B. Heggen, S. Zahn, B. Kirchner, S. Balasubramanian, F. Muller-Plathe, *Journal of American Chemical Society*, **2009**, 131, 15823-15825.
- [92] K. Dong, S. Zhang, D. Wang, X. Yao, *Journal of Physical Chemistry A*, **2006**, 110, 9775-9778.
- [93] J. S. Wilkes, M. J. Zworotko, *Chemical Communications*, **1992**, 58, 962-965.
- [94] T. Welton, *Chemical Reviews*, **1999**, 99, 2071-2074.
- [95] A. E. Visser, R. P. Swatloski, R. D. Rogers, *Green Chemistry*, **2000**, 21, 111-114.
- [96] J. G. Huddleston, H. D. Willauer, R. P. Swatloski, R. D. Rogers, *Chemical Communications*, **1998**, 98, 1762-1765.
- [97] H. Tokuda, S. Suzuki, M. A. B. H. Susan, K. Hyamizu, M. Watanabe, *Journal of Physical Chemistry B*, **2006**, 110, 19593.
- [98] C. Chiappe, D. Pieraccini, *Journal of Physical Organic Chemistry*, **2005**, 18, 275-279.
- [99] C. Catiuela, J. I. Garcia, J. A. Mayoral, A. J. Royo, L. Salvatella, X. Assfeld, M. F. Ruiz-Lopez, *Journal of Physical Organic Chemistry*, **1992**, 5, 230-234.
- [100] W. Blokzijl, M. Blandammer, J. Engberts, *Journal of American Chemical Society*, 1999, 113, 4241-4245.
- [101] R. Breslow, *Accounts of Chemical Research*, **1999**, 24, 159-162.
- [102] D. A. Jaeger, C. E. Tucker, *Tetrahedron Letters*, **1989**, 30, 1785-1788.
- [103] C. Lee, *Tetrahedron Letters*, **1999**, 40, 2461-2464.
- [104] Y. Chauvin, B. Gilbert, I. Guibard, *Chemical Communications*, **1990**, 23, 1715-1718.
- [105] R. T. Carlin, R. A. Osteryoung, *Journal of Molecular Catalysis*, **1990**, 63, 125-128.
- [106] P. A. Z. Suarez, J. E. L. Dullius, S. Einloft, R. F. de Souza, J. Dupont,

- Polyhedron*, **1996**, 15, 1217-1221.
- [107] T. J. Geldbach, P. J. Dyson, *Springer*, **2005**, 55, 245-248.
- [108] E. Bekou, D. D. Dionysiou, R. Y. Qian, G. D. Botsaris, R. D. Rogers, K. R. Seddon, *American Chemical Society*, **2003**, 544, 856-860.
- [109] A. B. McEwen, S. F. McDevitt, V. R. Koch, *Journal of Electrochemical Society*, **1997**, 502, 144-148.
- [110] A. B. McEwen, S. F. McDevitt, V. R. Koch, *Journal of Electrochemical Society*, **1997**, 144, 184-187.
- [111] P. Wasserscheid, W. Keim, *Angewandte Chemical International Edition*, **2000**, 39, 3773-3789.
- [112] H. Li Chum, V. R. Koch, L. L. Miller, *Journal of American Chemical Society*, **1975**, 97, 3264-3268.
- [113] J. Fuller, R. T. Carlin, C. De Long, D. Haworth, **1994**, 11, 299-300.
- [114] J. S. Wilkes, M. J. Zworotko, *Chemical Communications*, **1992**, 965-967.
- [115] K. R. Seddon, *Kinetics and Catalysis*, **1996**, 37, 693-697.
- [116] N. V. Plechkova, K. R. Seddon, *Chemical Society Reviews*, **2008**, 37, 123-127.
- [117] C. A. Angell, Y. Ansari, Z. Zhao, *Royal Society of Chemistry*, **2012**, 154, 9-27.
- [118] S. Vyas, C. Dreyer, J. Slingsby, D. Bicknase, J. M. Porter, C. M. Maupin, *Journal of Physical Chemistry*, 2014, 118, 6873-6882.
- [119] Y. W. H. Li, S. Han, *Journal of Physical Chemistry B*, **2006**, 110, 24646-24651.
- [120] M. A. B. H. Susan, A. Noda, S. Mitsushima, M. Watanabe, *Chemical Communications*, **2003**, 327, 938-939.
- [121] K. Fumino, A. Wulf, R. Ludwig, *Angewandte Chemical International*, **2009**, 48, 3184-3186.
- [122] K. Fumino, A. Wulf, R. Ludwig, *Physical Chemistry Chemical Physics*, **2009**, 11, 8790-8794.
- [123] A. Wulf, K. Hayamizu, R. Ludwig, *Angewandte Chemical International*, **2010**, 47, 12676-12679.
- [124] C. Roth, T. Peppel, K. Fumino, M. Kockerling, R. Ludwig, *Angewandte*

- Chemical International*, **2010**, 49, 10218-10221.
- [125] A. Noda, K. Hayamizu, M. Watanabe, *Journal of Physical Chemistry B*, **2001**, 105, 4603-4606.
- [126] S. Zhang, M. S. Miran, A. Ikoma, K. Dokko, M. Watanabe, *Journal of American Chemical Society*, **2014**, 136, 1690-1693.
- [127] B. A. Pereiro, A. Rodriguez, P. Verdia, E. Tojo, *Journal of Chemical and Engineering Data*, **2007**, 52, 337-340.
- [128] E. T. Fox, E. Paillard, O. Borodin, W. A. Henderson, *Journal of Physical Chemistry C*, **2013**, 78, 117-121.
- [129] A. B. McEwen, H. L. Ngo, K. LeCompte, J. L. Goldman, *Journal of Electrochemical Society*, **1999**, 46, 1682-1687.
- [130] C. P. Fredlake, J. M. Crosthwaite, D. G. Hert, S. N. V. K. Aki, J. F. Brennecke, *Journal of Chemical and Engineering Data*, **2004**, 49, 954-958.
- [131] H. Tokuda, K. Hayamizu, K. Ishii, M. A. B. H Susan, M. Watanabe, *Journal of Physical Chemistry B*, **2005**, 109, 6103-6107.
- [132] H. Tokuda, K. Hayamizu, K. Ishii, M. A. B. H Susan, M. Watanabe, *Journal of Physical Chemistry B*, **2006**, 110, 2833-2836.
- [133] V. V. Chaban, O. V. Prezhdo, *Journal of Physical Chemistry Letters*, **2011**, 2, 1496-2499.
- [134] Y. Umebayashi, J. Jiang, K. Lin, Y. Shan, K. Fujii, S. Seki, S. Ishiguro, S. H. Lin, H. Chang, *Chemical Physics*, **2009**, 131, 234-238.
- [135] A. Stoppa, J. Hunger, R. Buchner, *Journal of Chemical and Engineering Data*, **2009**, 54, 472-476.
- [136] Y. J. Xu, J. f. Shen, Q.w. Wang, H. Lin, H. Shiji, **2009**, 32, 661-665.
- [137] H. C. Garcia, L. F. C. Oliveira, B. G. Nicolau, M. C. C. Ribeiro, *Journal of Raman Spectroscopy*, **2010**, 4, 1720-1724.
- [138] V. K. Sharma, S. Bhagour, S. Solanki, A. Rohilla, *Journal of Chemical and Engineering Data*, **2013**, 58, 1939-1954.
- [139] T. M. Malyanah, M. M. Akbar, T. Murugesan, *Journal of Molecular Liquids*, **2014**, 190, 23-29.

- [140] P. Wasserscheid, T. Welton, *Ionic Liquid in Synthesis*, Wiley- VCH, Weinheim, **2003**, 242, 115-124.
- [141] K. Ahmed, A. Auni, G. Ara, M. M. Rahman, M. Y. A. Mollah, M. A. B. H. Susan, *Journal of Bangladesh Chemical Society*, **2012**, 25, 146-158.
- [142] M. Marium, M. M. Rahman, M. Y. A. Mollah, M. A. B. H. Susan, *RSC Advances*, **2015**, 5, 19907-19913.

Abstract

The density, viscosity and refractive index of binary mixtures of DMF with ACN over the entire composition range were measured in the temperature range of 20-45 °C. From the experimental results, the excess molar volume, (V^E), excess viscosity, (η^E) and excess refractive index (n^E) were calculated over the whole composition range. The variation of these parameters with composition and temperature of the mixtures has been discussed in terms of molecular interaction in these mixtures. The V^E and η^E were found negative and n^E were positive for all mixtures at all temperatures indicating the presence of specific interactions between ACN and DMF.

2.1. Introduction

The studies of physico-chemical properties of binary mixtures are of considerable importance in the fundamental understanding of the nature of the interactions between unlike molecules. There have been numerous attempts on several binary liquid systems to investigate and interpret the medium effects in chemical reactions and molecular interactions [1, 2]. The physico-chemical properties of non-aqueous binary liquid mixtures have relevance in theoretical and applied areas of research, and the information is frequently used in design process such as; flow, mass transfer or heat transfer calculation in many chemical and industrial processes. Mixed solvents are frequently used as media for many chemical, industrial, and biological [3-6] processes as they provide a wide range of desired new properties. Moreover, amides are convenient model systems for the investigation of peptide and protein interaction in biological systems [7]. In earlier study [8-15] many researcher reported the studies on volumetric, acoustic and transport properties of binary mixtures containing amides. Among other amides DMF is a polar solvent used widely in a variety of industrial processes, including manufacture of synthetic fibers, leathers, films, and surface coatings [16-18]. DMF is a stable compound with a strong electron pair donating and accepting ability and is widely used in studies on solvent reactivity relationships [19-21]. DMF is of particular interest since any significant structural effects are absent due to the lack of hydrogen bonds. Therefore, it may be used as an aprotic protophilic solvent with a large dipole moment ($\mu = 36.71$), and high dielectric constant ($\epsilon = 3.24$ D at 25 °C) [18] and in view of this, dipole-dipole

interactions are expected to play an important role in molecular interactions present in the liquid mixtures. In addition, DMF can serve as a model compound for peptides to obtain information on protein systems. The structure of DMF is shown in Figure 1.1.3.1(c) in Section 1. The present work is focused on the study of molecular interactions in binary mixtures of ACN, DMF over the entire composition range at various temperatures. ACN are aprotic but highly polar ($\mu = 3.7\text{D}$ at $25\text{ }^\circ\text{C}$) [23] with their dipoles oriented anti-parallel to each other and the strongly ordered structure in ACN is due to dipole–dipole interactions [23, 24], the structure of ACN is shown in Figure 1.1.3.1.(d) while the DMF is highly polar (3.24 D at $25\text{ }^\circ\text{C}$) [23], some amide such as formamide (FA) and *N*-methylacetamide (NMA) are strongly associated through hydrogen bonding in the pure state [24] and this association decreases with increase in the number of methyl groups in the molecule. Whereas, DMF and *N, N*-dimethylacetamide (DMA) are practically unassociated [25, 26]. The aim of the work is to understand the molecular interaction in ACN with DMF binary mixtures. To understand the molecular interaction, the present work reports the ρ , η , and n of the binary mixtures of ACN with DMF, including the pure liquids at $20\text{--}45\text{ }^\circ\text{C}$, covering the entire composition range expressed by X_{DMF} . The experimental values of ρ , η and n were used to calculate the deviations in V^E , ρ^E , and n^E of DMF- ACN binary mixtures and fitted to the Redlich–Kister polynomial equation [27]. The changes in these parameters with composition and temperature of the binary mixtures have been discussed in terms of molecular interactions.

2.2. Experimental

2.2.1. Materials

ACN and DMF, used in the study were the products from E. Merck and Fisher Scientific respectively with having purity of 99.9% for both the solvents. The mixtures were prepared by mass and were kept in special air-tight stopper glass bottles to avoid evaporation. The weighing were done an electronic balance with a precision of $\pm 0.1\text{ mg}$. The probable error in the mole fraction was estimated to be less than $\pm 1.10^{-4}$.

2.3. Instruments

2.3.1. Density Meter

The densities of the binary mixtures were measured with *Anton Paar* (Model DMA 4500 M) vibrating tube density meter. The density meter was calibrated with ultra pure water, and with dry air at atmospheric pressure. The repeatability of density measurement was $0.00001 \text{ g cm}^{-3}$ and accuracy of measurement was $0.000005 \text{ g cm}^{-3}$.

2.3.2. Microviscometer

The viscosities of the binary mixtures were measured with Lovis 2000ME Microviscometer with accuracy of $\pm 10^{-6} \text{ mPa s}$. Capillaries with diameters of 1.59 mm and 1.8 mm and a steel ball with maximum deviation of 0.2% was used for measurements. The capillaries with diameter 1.59 mm and 1.8 mm were calibrated with suitable standards.

2.3.3. Refractometer

Refractive indices were directly measured using *Anton Paar* Abbemat-350 automated refractometer having high resolution optical sensor. The refractometer was calibrated with deionized water before each run. The accuracy of the refractive index measurement was 0.00005. Pure ethanol was used to clean the surface of the refractometer prism. The measurements were performed at atmospheric pressure and temperatures from 20.0 to 45.0 °C. The mean data was derived from the repetitions (two times) of each measurement with a repeatability of 0.02%.

2.3.4. Sonicator

Homogeneous mixing of the components of the binary mixtures was ensured by using a sonicator, LU-2 Ultrasonic cleaner, Labnics Equipments, USA.

2.3.5. Water Purifier (Ultra Pure)

During experiments de-ionized water was obtained from HPLC grade water purifications system from BOECO, Germany. The conductivity of this de-ionized water is 0.0550~Scm^{-1} at $20\text{ }^{\circ}\text{C}$.

2.3.6. Analytical Digital Microbalance

For weighing the components for preparing binary solutions digital microbalance UBT-110 from UNILAB, USA was used.

2.4. Measurements

2.4.1. Preparation of Binary Mixtures

DMF was completely miscible in ACN at room temperature. All the binary mixtures of DMF-ACN were prepared gravimetrically in the whole range of composition. After preparation, all samples were sonicated for 20 min to ensure homogeneous mixing.

2.4.2. Measurement of Density

Less than 2.0 mL amount of sample was introduced into the inlet of the density meter. Density of each solution was measured from 20.0 to $50.0\text{ }^{\circ}\text{C}$. After raising the temperature to $50.0\text{ }^{\circ}\text{C}$ the sample was again cooled down to $25.0\text{ }^{\circ}\text{C}$. The density value obtained was found to be same as the initial value at $25.0\text{ }^{\circ}\text{C}$ before the temperature was raised. After each measurement the U-shaped tube was cleaned with ethanol and ultrapure water. Air and water check were performed before measuring the density of samples.

2.4.3. Measurement of Viscosity

A small amount of sample (<1.0 mL) was filled using a syringe into glass capillary which was introduced into a temperature controlled capillary block. This block was inclined at variable predefined angle. Angle of measurement and the diameter of the ball and capillary for sampling have been selected depending on the approximate viscosity of the mixture. For pure IL and binary systems with high IL mole fraction the measuring angle was 60° and the capillary used was of 1.8 mm diameter. For pure DMF and mixtures with lower X_{IL} , the measuring angle was 25° and 1.59 mm diameter capillary was used.

2.4.4. Measurement of Refractive Index

Refractive index of pure IL and their binary mixtures with DMF was directly obtained from 20.0 to 50.0 °C by placing the sample on the refractometer cell in the same amount (70 μ L) for each composition. Reproducibility of the results was confirmed by performing at least two experiments for each sample.

2.5. Results and Discussion

2.5.1. Density of Binary Mixtures of DMF-ACN

The variation of density with mole fraction of DMF is shown in Figure 2.5.1 and the results of density are listed in Table A1 (Appendix). Density increased non-linearly for all the binary systems with increase in mole fraction of DMF. This non-linear variation, is a deviation from ideal behavior, suggests interactions between molecules of component liquids of the mixtures. Figure 2.5.1(a) shows the change in density of DMF-ACN binary mixtures as a function of mole fraction of DMF (X_{DMF}) and 2.5.1(b) as a function of temperature.

In DMF-ACN binary mixtures (Figure 2.5.1(b)), the density increases with increasing temperature. The increase in temperature brings about increased thermal motion in molecules. These energetic molecules cause the expansion of volume which may lower density.

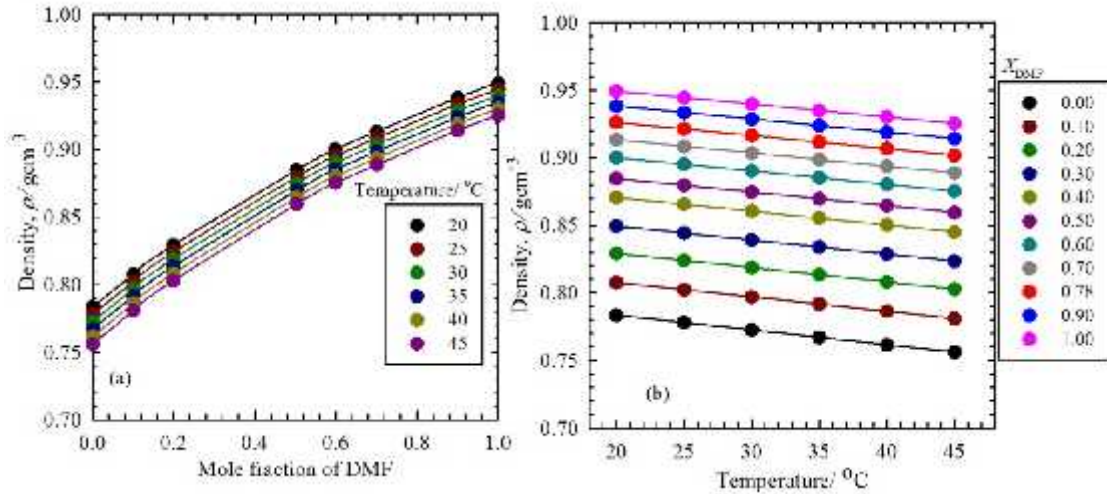


Figure 2.5.1. Density of (a) DMF- ACN binary mixtures as a function X_{DMF} (b) as a function of temperature.

From the density results excess molar volume V^E were calculated by using the following equation:

$$V^E = xM_1 \left(\frac{1}{\rho} - \frac{1}{\rho_1} \right) + (1 - x)M_2 \left(\frac{1}{\rho} - \frac{1}{\rho_2} \right) \quad (2.1)$$

Where M is the molar mass; subscripts 1 and 2 stand for pure components, ACN and DMF, respectively. The uncertainty in V^E is estimated to be within $\pm 2.10^{-3} \text{ cm}^3 \cdot \text{mol}^{-1}$. The values of V^E were fitted to a Redlich–Kister type polynomial equation:

$$V_m^E = x(1 - x) \sum_{i=0}^4 A_i (1 - 2x)^i \quad (2.2)$$

The values of coefficients, A_i , were evaluated by using the method of least squares, with all points weighted equally. The coefficients A_0 , A_1 , A_2 , A_3 , and A_4 for all the mixtures are listed in Table A2 (Appendix), along with standard deviation, σ , calculated by using the relation:

$$\sigma / (\text{cm}^3 \text{mol}^{-1}) = \left[\sum (V_{m,\text{calc.}}^E - V_{m,\text{Expt.}}^E)^2 / (n - j) \right]^{1/2} \quad (2.3)$$

where n is the number of experimental data points and j is the number of A_i coefficients considered. The values of $V_{m,Calc}^E$ were obtained from equation (2. 3) by using the best-fit values of A_i coefficients. The variations of V^E with mole fraction X of DMF at various temperatures, along with the V^E values by using equation (2. 3), are presented graphically in Figure 2.5.2.

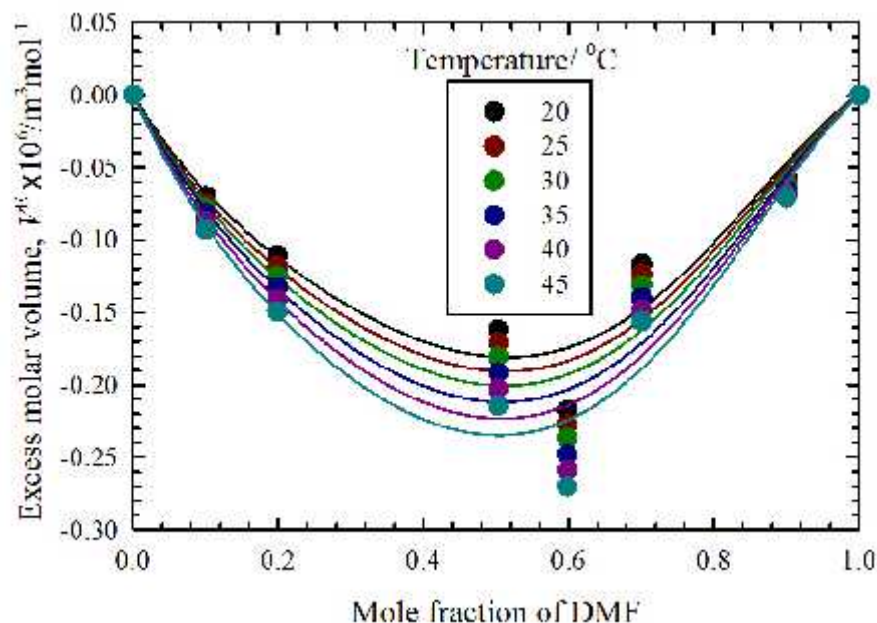
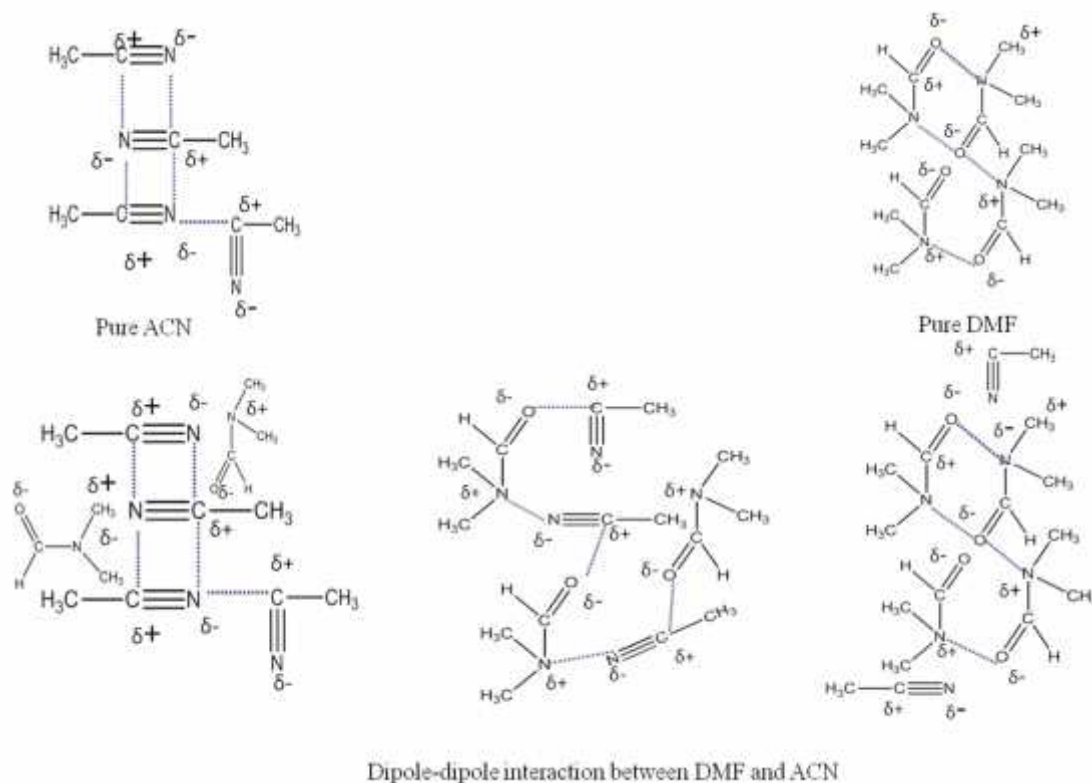


Figure 2.5.2. The V^E for DMF-ACN system as a function of X_{DMF} at different temperatures. Solid lines are drawn by using calculated values according to Redlich-Kister equation.

The V^E vs mole fraction of DMF is the resultant of several effects such as chemical, physical and structural. Physical contributions, which are non-specific interactions between the liquids of the mixture [28, 29] contribute to positive V^E values. The negative values to V^E are contributed by the chemical or specific intermolecular interactions [30] that result decrease in excess molar volume. The structural contributions are mostly negative and arise from interstitial accommodation of the mixing components corresponding to the difference in molar volumes [31]. In the present investigation the values of V^E are negative in DMF-ACN binary mixtures to support strong interactions existing between the liquids. The results presented in Table A1(Appendix), Figure 2.5.2

indicate that V^E s are negative over entire mole fraction range and at all temperatures for the binary mixtures of DMF-ACN.

The observed negative values of the V^E for ACN- DMF mixtures indicate the presence of specific interaction between ACN and DMF. A plausible qualitative interpretation of the behavior of these mixtures with composition has been suggested. As stated earlier, the ACN molecules have strong dipole-dipole interactions and DMF molecules are practically unassociated due to their inability to form hydrogen bond with them. The negative V^E results can be attributed to strong dipole-dipole interactions between the unlike molecules in the mixtures. Another contribution to negative results of the V^E comes from the fitting of small ACN (molar volume = $52.845 \text{ cm}^3\text{mol}^{-1}$ at 25°C) [32,33] into the voids present in bigger DMF molecules (molar volume = $77.3767 \text{ cm}^3\text{mol}^{-1}$ at 25°C) [32,33] Contributions arising from the fitting of smaller molecules into the voids available in the structure of bigger molecules were also considered by others [8, 34-36] for interpreting negative V^E values for binary mixtures that contains molecules of different molecular size. Scheme 2 shows the different molecular interaction between DMF- ACN with increasing mole fraction of DMF in the binary mixtures.



Scheme 1 Different molecular interaction between DMF-ACN with increasing X_{DMF} in the binary mixtures.

2.5.2. Viscosity of Binary Mixtures of DMF-ACN

At 25 °C, the viscosity of pure DMF and ACN is 0.8173 mPa.s and 0.3573 mPa.s respectively. The experimental results of viscosity, of binary mixtures of ACN with DMF, over the whole composition range, expressed in mole fraction X of DMF, the different temperatures are listed in Table A1(Appendix). For the binary mixtures of DMF-ACN increases with increasing X of DMF and increasing temperature decrease. Figure 2.5.3. shows the change in with mole fraction of DMF and temperature respectively.

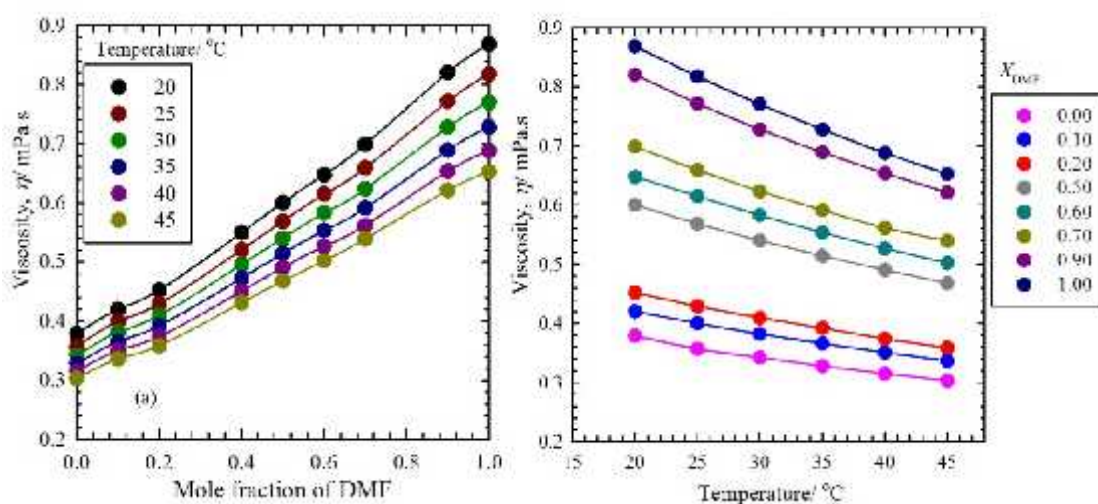


Figure 2.5.3. Viscosity of DMF-ACN binary mixtures (a) as a function of X_{DMF} and (b) as a function of temperature.

The excess viscosity were calculated from viscosity by the equation

$$\Delta\eta = \eta - (x_1\eta_1 + x_2\eta_2) \quad (2.4)$$

of DMF-ACN mixtures are listed in Table A1 (Appendix). The results were correlated by the Redlich–Kister equation. The coefficients A_0 , A_1 , A_2 , A_3 , and A_4 for all the mixtures are listed in A2 (Appendix), along with standard deviation, .

The deviations in viscosity may be generally explained by two factors [37]. One is difference in size and shape of the components that produces negative excess viscosity and the other is loss of dipolar association to a decrease in viscosity; specific interactions between unlike molecules such as H-bond formation and charge transfer complexes may cause increase in viscosity in mixtures rather than in pure component as a result produces positive deviation on η . Positive values of $\Delta\eta$ indicate strong interactions whereas negative values indicate weaker interactions [38]. The variations of $\Delta\eta$ with X of DMF at various temperatures, along with the $\Delta\eta$ values by using equation (2.4), are presented graphically in Figures 2.5.4.

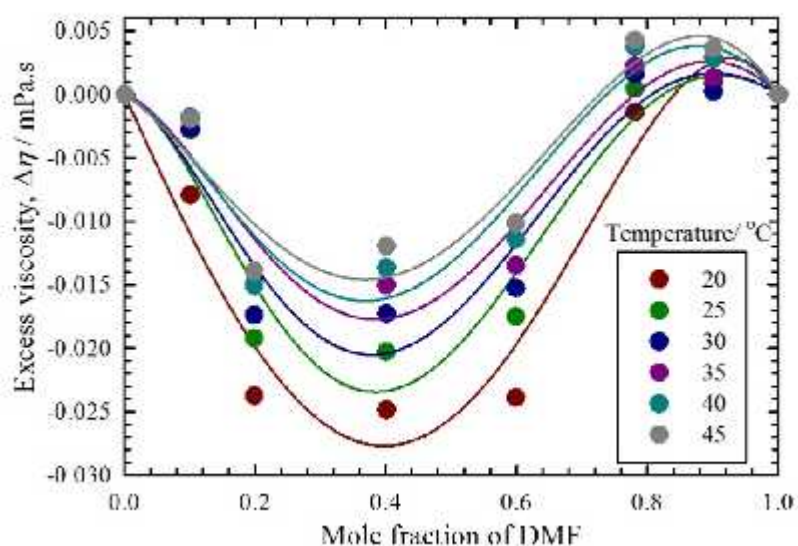


Figure 2.5.4. $\Delta\eta$ of DMF-ACN system as a function of mole fraction of IL. Solid lines are drawn by using calculated values according to Redlich- Kister equation.

Figure 2.5.4 indicates that $\Delta\eta$ results are negative for DMF-ACN binary mixtures over the entire range of X_{DMF} at each temperature. The negative $\Delta\eta$ results for DMF- ACN mixtures suggest the presence of dipole-dipole interaction between unlike molecules [39, 40]. Also negative values are observed for the mixtures having component molecules that are greatly different in sizes [40] as in DMF-ACN mixtures.

2.5.3. Refractive Index of Binary Mixtures of DMF-ACN

The refractive index is an important additive property of molecular structure of liquid. When a light of beam passes from one substance to another, the beam is bent so that it travels in different direction. If it is passed from less dense to denser medium it is refracted toward normal to form angle of refraction which is less than angle of incident. The refractive index is the ratio of angle of incident to the angle of refraction and it depends on the temperature and wavelength of light. The extent of refraction depends on: i) the relative concentration of atom or molecule and ii) The structure of atom or molecule. So refractive index gives idea about geometry and structure of molecule. Refraction of light is additive property, but also depends on the structural arrangement of atom in molecule. This can sometime be used to determine the structure of an unknown compound whose molecular formula is known.

Figure 2.5.5 shows the change in refractive index of DMF-ACN with mole fraction of DMF at different temperatures. Refractive index of DMF-ACN binary mixture gradually increases with increasing X of DMF.

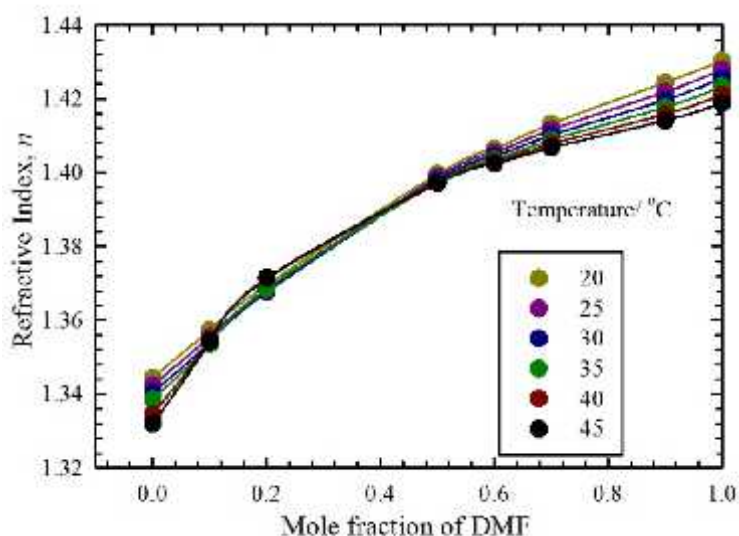


Figure 2.5.5. Refractive index of DMF-ACN binary mixtures as a function of X_{DMF} .

From the experimental data of refractive index, excess refractive index were calculated and correlated using Redlich–Kister polynomial equation with parameter given in Table A2 (Appendix).

$$\Delta n = n - (x_1 n_1 + x_2 n_2) \quad (2.5)$$

The variations of n with X of DMF at various temperatures, along with the n values by using equation 2.5, are presented graphically in Figure 2.5.6. The excess refractive index indicate that for the DMF-ACN binary mixtures exhibit positive values of the excess refractive index over the entire composition range at each temperature.

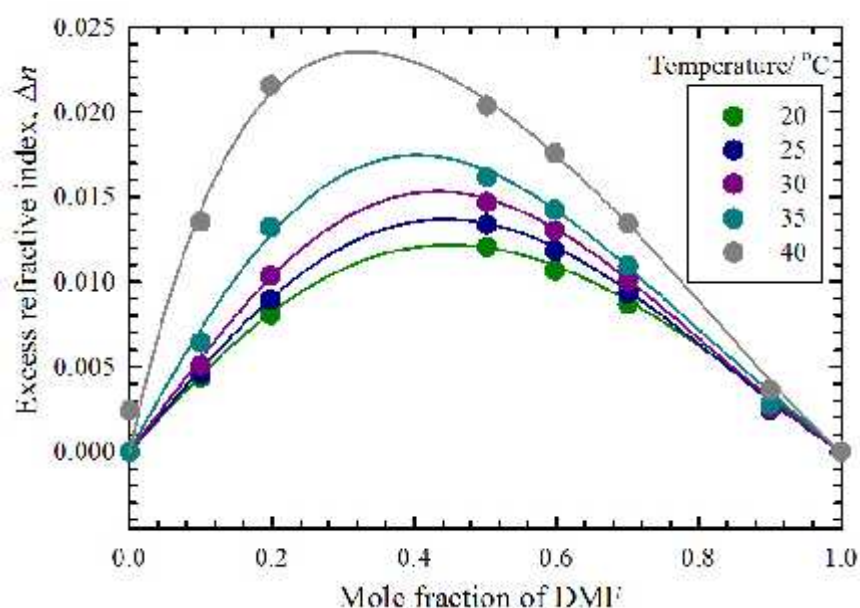


Figure 2.5.6. Excess refractive index of DMF-ACN system as a function of X_{DMF} . Solid lines are drawn by using calculated values according to Redlich- Kister equation.

The V^E was negative in the entire composition range, so the free volume will not be available hence photons will be more likely to interact with the molecules, as a result light will be bent at lower velocity in the medium concerned, and its refractive index will be higher.

2.6. Conclusions

The physico-chemical properties of DMF-ACN binary mixtures change with mole fraction of these mixtures. The density, viscosity and refractive index increase with increasing mole fraction of DMF. From the excess properties such as excess molar volume and excess viscosity results were found negative for all the mixtures at all

temperatures resulting strong dipole-dipole interaction between DMF and ACN, while excess refractive index results were positive over the whole composition range. These would help establishing a fundamental knowledge-base on prediction of molecular interaction between ACN and DMF and understanding of the molecular interaction and underpin further development for other binary and ternary mixtures comprising designer solvents, such as ionic liquids.

References

- [1] P. B. Undre, S. N. Helambe, S.B. Jagdale, P.W. Khirade, S. C. Mehrotra, *Journal of Physical Chemistry*, **2007**, 68, 851-861.
- [2] S.M. Puranik, A. C. Kumbharkhane, S. C. Mehrotra, *Journal of Chemical Society, Faraday Transactions*, **1992**, 88, 433-435.
- [3] S. Sharma, P. B. Patel, R. S. Patel and J. J. Vora, *European Journal of Chemistry*, **2007**, 4, 343-349.
- [4] H. Watanabe, Y. Tanji, H. Unno, K. Hori, J. Biosci. Bioeng, *Journal of Biotechnology*, **2008**, 106, 226-230.
- [5] F. Dai, Y. Xu and X. Chen, *Optics Letters*, **2010**, 8, 14-20.
- [6] Y. Xu, X. Chen and Y. Zhu, *Sensors*, **2008**, 8, 1872-1870.
- [7] G. T. Fraser, R. D. Suenram, F. J. Lovas, *Journal of Molecular Liquids*, **1988**, 189, 165-172.
- [8] A. Ali, A. K. Nain, *Bulletin of the Chemical Society of Japan*, **2002**, 75, 681-687.
- [9] A. K. Nain, A. Ali, M. Alam, *Journal of Chemical Thermodynamics*, **1998**, 30, 1275-1278.
- [10] A. Ali, A. K. Nain, B. Lal, D. Chand, *International Journal of Thermophysics*, **2004**, 25, 1835-1847.
- [11] A. Ali, A. K. Nain, D. Chand, R. Ahmad, *Physics and Chemistry of Liquids*, **2005**, 43205–43224.
- [12] A. Ali, Abida, A. K. Nain, S. Hyder, *Journal of Solution Chemistry*, **2003**, 32, 865–877.
- [13] A. Pal, R. Kumar Bhardwaj, *Journal of Chemical Engineering*

- Data*, **2002**, 47, 1128-1134.
- [14] K. L. Pattebahadura, S. D. Deshmukh, P. B. Undreb, S. S. Patil, P. W. Khirade, *Bionano Frontier*, **2015**, 8.
- [15] J. Zielkiewicz, *Physical Chemistry Chemical Physics*, **2003**, 5, 1619-1630.
- [16] A. Ali, A. K. Nain, B. Lal, D. Chand, *Indian Journal of Chemistry A*, **2005**, 44, 511-515.
- [17] K. Y. Kang, S. H. Park, *Journal of Molecular Structure*, **2004**, 676, 171-176.
- [18] H. Borrmann, I. Persson, M. Sandstrom, *Journal of Chemical Society Perkin Trans*, **2000**, 2, 393-402.
- [19] Y. Umebayashi, Y. K. Matsumoto, M. Watanabe, *Physical Chemistry Chemical Physics*, **2001**, 3, 5475-5481.
- [20] B. Garcia, R. Alcalde, J. M. Leal, J. S. Matos, *Journal of Chemical Society, Faraday Trans*, **1997**, 93, 1115-1118.
- [21] P. Venkatesu, M. J. Lee, H. M. Lin, *Journal of Chemical Thermodynamic*, **2005**, 53, 996-1002.
- [22] J. A. Riddick, W. B. Bunger, T. K. Sakano, *Organic solvents*, 4th ed.; Wiley-Interscience: New York, **1986**.
- [23] A. Ali, A. K. Nain, B. Lal, D. Chand, *Chinese Journal of Chemistry*, **2005**, 23, 377-385.
- [24] Y. Marcus, *Introduction to Liquid State Chemistry*, Wiley-Interscience, New York, **1977**.
- [25] H. Ohtaki, S. Itoh, T. Yamaguchi, S. Bratos, *Bulletin of the Chemical Society of Japan*, **1983**, 56, 3406-3412.
- [26] R. Gopal, S. Aggarwal, D. K. Aggarwal, *Journal of Chemical Thermodynamics*, **1976**, 8, 1205-1208.
- [27] O. Redlich, A. T. Kister, *Journal of Industrial and Engineering Chemistry*, **1948**, 40, 345-348.
- [28] M. N. Roy, A. Sinha, B. Sinha, *Journal of Solution Chemistry*, **2005**, 34, 1311-1325.
- [29] K. Hsu-Chen, T. Chein-Hsiun, *Journal of Chemical and Engineering*

- Data*, **2005**, 50, 608-615.
- [30] P. S. Nikam, S. J. Kharat, *Journal of Chemical and Engineering Data*, **2005**, 50, 455-459.
- [31] S. J. Kharat, P. S. Nikam, *Journal of Molecular Liquids*, **2007**, 82, 131-132.
- [32] A. Ali, A. K. Nain, *Bulletin of the Chemical Society of Japan*, **2002**, 75, 681-687.
- [33] N. K. Kim, H. J. Lee, K. H. Choi, J. A. Yu, C. J. Yoon, J. Park, Y. S. Choi, *Journal of Physical Chemistry B*, **2000**, 104, 5572-5578.
- [34] P. Assarson, F.R. Eirich, *Journal of Physical Chemistry*, **1968**, 72, 2710-2719.
- [35] A. Ali, A. K. Nain, M. Kamil, *Thermochimica Acta*, **1996**, 274, 209-221.
- [36] L. Pikkarainan, *Journal of Chemical and Engineering Data*, **1983**, 28 381-383.
- [37] R. Mehra, M. Pancholi, *Indian Journal of Physics*, **2006**, 80, 253-263.
- [38] C. Yang, W. Xu, P. Ma, *Journal of Chemical and Engineering Data*, **2004**, 49, 1794-1801.
- [39] H. N. Solimo, D. Riggio, F. Davolio, M. Katz, *Canadian Journal of Chemistry*, **1973**, 57, 1258-1265.
- [40] S. Oswal, M. V. Rathnam, *Canadian Journal of Chemistry*, **1984**, 62, 2851-2853.

Abstract

The physico-chemical properties of ILs, [emim][TFSI] and [emim][PF₆] with highly polar solvent DMF was studied through precise measurements of densities (ρ), viscosities (η), refractive index (n) over the whole composition range at atmospheric pressure and over a temperature range of 20-50 °C. The excess molar volume (V^E), excess viscosity (η^E) and excess refractive index (n^E) were predicted using these temperature dependence properties as a function of concentration of ILs. The Redlich-Kister polynomial equation was used to correlate the results. The intermolecular interactions and structural effects were analyzed on the basis of measured and derived properties. A qualitative analysis of the results is discussed in terms of the ion-dipole, ion-ion interactions, and hydrogen bonding between ILs and DMF molecules and their structural factors.

3.1. Introduction

ILs have emerged as one of the most promising materials in the field of modern science due to their unique properties such as negligible vapour pressure, non-flammability, high ionic conductivity and high thermal, chemical and electrochemical stability [1]. These remarkable properties have allowed ILs for performing more promising perspectives in the various fields such as organic synthesis [2], catalysis or biocatalysis [3-5], materials science [6], electrochemistry [7], separation technology [8, 9] and preserving the protein stability [10, 11] at laboratory level and even at industrial scale [12-18].

The significant attention in past decade the scientific community has shown toward ILs is mainly due to the greater versatility in cation-anion combinations and favorable unique properties. For these reasons, they rapidly gained interest as greener replacements for traditional volatile organic solvents. Moreover, ILs have become much popular because of their unique properties.

Several room-temperature ILs such as, [emim][BF₄], [emim][TFSI], [BP][BF₄], and [BP][TFSI] were prepared and characterized by Noda *et al.* [23]. They measured the thermal property, density, self-diffusion coefficient of the anions and cations, viscosity,

and ionic conductivity for these ILs in wide temperature ranges and used pulsed-gradient spin-echo NMR method to independently determine self-diffusion coefficients of the anions by ^{19}F NMR and the cations by ^1H NMR. They confirmed that the diffuse of cations almost equally to the anion in [emim][BF₄], but for [emim][TFSI] and [BP][TFSI] diffuse faster than the anion.

The ionic nature of the ILs as the molar conductivity ratio was defined Tokuda *et al.* [25], by using electrochemical impedance method. They calculated the molar conductivity and that estimated by use of pulse-field-gradient spin-echo NMR ionic self-diffusion coefficients and the Nernst-Einstein relation (Λ_{NMR}). And this result is compared with solvatochromic polarity scales.

The density, viscosity, thermal stability and ionic conductivity of mixtures of ILs with a variety of different aprotic solvents was examined by Fox *et al.*[26]. They concluded that the addition of an aprotic solvent to an IL greatly decreases the viscosity of the IL and, up to a certain mole fraction of solvent, increases the conductivity. Furthermore, the addition of solvent can greatly increase the temperature range over which the mixtures remain liquids.

For task specific applications in multidisciplinary areas, IL-based mixed solvent systems have the potential to offer a novel route for tuning the properties of these designer solvents. Optimization of the properties to desirable chemistry can be achieved by varying the composition of the binary mixtures. However, the high viscosity and considerable low conductivity of pure IL make them inadequate for use as electrolytes in commercial electrochemical devices. These can be overcome by the addition of polar solvents which lowers the viscosity and increase conductivity significantly [28-30]. An useful example of polar solvent can be DMF with high boiling point which is used widely in a variety of industrial processes, including manufacturing of synthetic fibers, leathers, films and surface coating [31-33]. It also used in manufacturing of solvent dyes which is an important raw material as well as a solvent in peptide coupling for pharmaceuticals, in the development and production of pesticides. DMF is a stable compound with strong electron pair donating and accepting ability and can widely be used for studies on solvent reactivity relationships [34-37].

DMF has particular interest since any significant structural effects are absent due to the lack of hydrogen bonds. Therefore, it may be used as an aprotic protophilic solvent with large dipole moment ($\mu = 3.24$ D), a high dielectric constant ($\epsilon = 36.71$ at 25°C) [38], and good donor-acceptor properties, which enable it to dissolve a wide range of both organic and inorganic substances. In addition, DMF can serve as a model compound for peptides to obtain information on protein systems. The resonance structure of DMF is shown in Figure 3.1.1

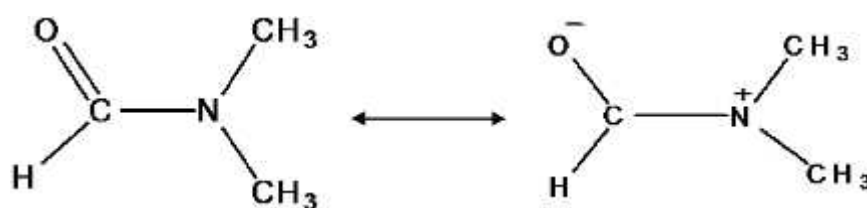


Figure 3.1.1. Resonance structure of DMF.

In DMF, the presence of two electron repelling, $-\text{CH}_3$ groups make the lone pair at nitrogen more perceptible toward donation [39, 40]. Thus it may be argued that the DMF is actually the donor of nitrogen electron pairs. The chemical structures of the ILs as well as DMF have been shown in Figure 1.1.3.1 in Section 1.

With view of wide scope of molecular interactions between DMF with imidazolium based ILs, it is essential to study physico-chemical properties to obtain deeper insight into the knowledge of molecular interactions of binary mixtures. Therefore, the present work mainly pursues to bring in molecular and structural information from a cation features based on the temperature dependence properties of ρ and η as well as derived properties of excess molar volume (V^E) and deviation of viscosity ($\Delta\eta$).

Numerous attempts have been made to explore the molecular interaction of the ILs-DMF binary systems. Pankaj *et al.* [41] studied the excess molar volumes and deviations of isentropic compressibilities of [bmim][Cl] with DMF systems and reported that the

packing efficiency between IL-DMF decrease at higher concentration of IL leading to positive deviation and at lower concentrations the packing efficiency increases.

The density, viscosity, and refractive index for ILs [C_nmim]Cl (C_nmim = 1-alkyl-3-methylimidazolium; n = 2, 4, 6, 8 for ethyl, butyl, hexyl, and octyl) with DMF binary systems were measured by Yan *et al.*[42] and results showed that the trend is [C₂mim]Cl > [C₄mim]Cl > [C₆mim]Cl > [C₈mim]Cl for the ILs with longer carbon chain cannot be close packed in the microscopic structure.

In spite of numerous studies, there have been no report on the binary mixtures on DMF with [emim][TFSI], and [emim][PF₆]. In this work, binary liquid mixture of DMF with [emim][TFSI] and [emim][PF₆] have been prepared considering whole composition range. The physico-chemical properties of these binary mixtures were studied by measuring ρ , η , and n in the temperature range of 20 to 50 °C. Additionally, the excess molar volume (V^E), excess viscosity (η^E) and excess refractive index (n^E) were calculated and the results were fitted to Redlich-Kister polynomial equation. The effect of temperatures on these properties also has been monitored in this work.

3.2. Experimental

3.2.1. Materials

The ILs, [emim][TFSI], and [emim][PF₆], were obtained from Sigma-Aldrich and were used without any further purification. HPLC grade DMF for preparation of binary mixtures was purchased from Fisher Scientific with purity of 99.9%. Water used for purposes like washing glassware was ultrapure water (specific conductivity, $\kappa = 0.0550 \mu\text{S cm}^{-1}$), BOECO pure, model- BOE 8082060, Germany.

3.3. Instruments

The density, viscosity, and refractive index of the binary mixtures were measured with *Anton Paar* (Model DMA 4500 M) vibrating tube densitometer, *Lovis 2000ME* Microviscometer with accuracy of $\pm 10^{-6}$ mPas, and *Anton Paar* Abbemat-350 automated

refractometer having high resolution optical sensor, respectively. Weighing the components for preparing binary liquid mixtures was done by using digital microbalance UBT-110 from UNILAB, USA and the mixtures were sonicated using a LU-2 Ultrasonic cleaner, Labnics Equipments, USA.

3.4. Measurements

3.4.1. Preparation of Binary Mixtures

In general ILs are immiscible with low-dielectric liquids and miscible with medium to high dielectric liquids [42]. Since DMF is high dielectric liquid [43] so [emim][TFSI] was completely miscible in DMF, whereas for the solid [emim][PF₆] with very low solubility in DMF binary mixtures of very low mole fraction (up to $X_{IL}=0.01$) of IL could be prepared.

All the binary mixtures of [emim][TFSI]-DMF were prepared gravimetrically in the whole range of composition. After preparation, all samples were sonicated for 20 min to ensure homogeneous mixing.

3.4.2. Measurement of Density, Viscosity and Refractive Index

Density was measured simultaneously with an Anton Paar (Model DMA 5000) vibrating-tube density meter. The density meter was calibrated with ultra pure water, and with dry air at atmospheric pressure. The temperature of the apparatus was controlled automatically within ± 0.01 K by a built-in Peltier device that corresponds to an uncertainty in density of ± 0.0002 %. The final uncertainty of density can be estimated in $\pm 10^{-6}$ gcm⁻³.

Measurement of viscosity was carried out using an Anton-Paar Lovis-2000 falling ball automated viscosimeter. Diameter of the capillary of sampling and the ball were calibrated prior to measurements. The temperature was controlled within 0.05 K by means of a built-in Peltier thermostat in the temperature range of 20-50 °C at 5 °C intervals. The accuracy of the measurements was $<0.2\%$.

Refractive index of binary mixtures was directly measured with Abbemat 300 refractometer having high resolution optical sensor. Measurements were made with a resolution and limit error $\pm 10^{-5}$. The temperature of the apparatus was controlled automatically within ± 0.01 K by built-in Peltier device.

3.5. Results and Discussion

3.5.1. Density of Binary Mixtures of [emim][TFSI]-DMF and [emim][PF₆]-DMF

The density of pure DMF, pure IL and those of binary mixtures of IL-DMF with different mole fractions were measured at 5 °C temperature intervals from 20 to 50 °C and the results of density are listed in Table A3 (Appendix). No bubbles were observed and no significant variation was noted at any temperatures during the density measurements. Variation of density against the mole fraction of IL for [emim][TFSI]-DMF and [emim][PF₆]-DMF system has been illustrated in Figures 3.5.1 (a) and 3.5.1 (b), respectively.

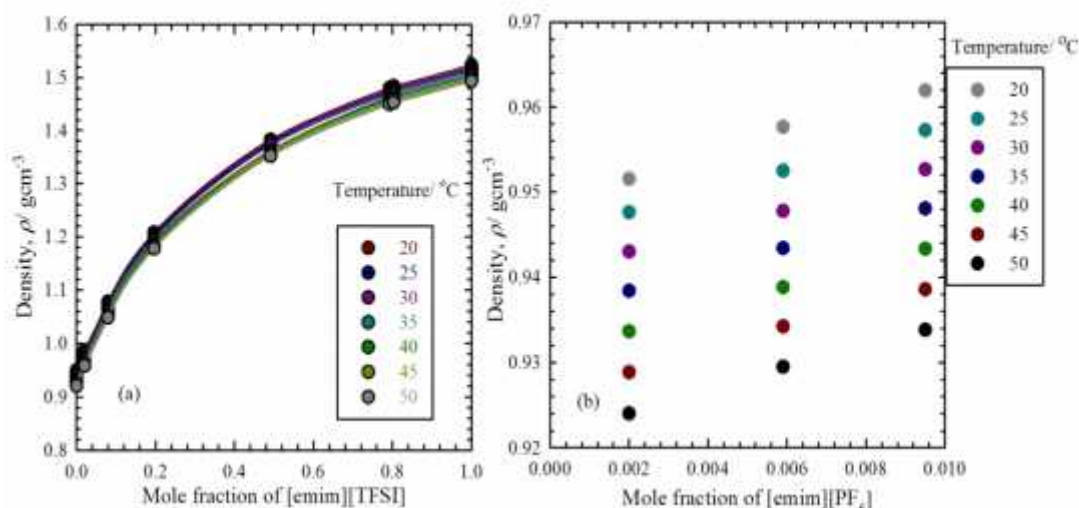


Figure 3.5.1. Density of (a) [emim][TFSI]-DMF and (b) [emim][PF₆] systems as a function of X_{IL} .

At all temperatures, the densities of [emim][TFSI]-DMF and [emim][PF₆]-DMF binary mixtures increase with increasing the mole fraction of IL. The decrease in density is

more pronounced in the DMF rich mixtures than the IL rich mixtures. This is due to the fact that the hydrogen bond is formed between the fluorine atoms of the [TFSI] anion and the hydrogen atoms of the imidazolium rings. This local quasi network of hydrogen bonds is responsible for the high densities of ILs [44]. Due to larger volume and poor symmetry of the anion, [TFSI], it has been found that anion is structurally favorable to the position near the C2-H group in the imidazolium- based ion-pairs. The most possible point of interaction in the cation for the formation of H-bonding with anion is the C2-H atoms. When DMF is added to IL, the DMF molecules may either interact with the cation or anion which weakens the existing bonding between the cation and anion. Thus, expansion of volume occurs and decreases in the density. This is consistent with literature. The density, viscosity, and refractive index for ILs $[C_n\text{mim}]\text{Cl}$ with DMF binary systems were measured by Yan *et al.* [42] and results showed that the ILs with longer carbon chain cannot be close packed in the microscopic structure. The excess molar volume and deviations of isentropic compressibilities of $[\text{bmim}][\text{Cl}]$ with DMF systems was explored by Pankaj *et al.* [41]. They reported that the packing efficiency between IL-DMF decrease at higher concentration of IL leading to positive deviation and at lower concentrations the packing efficiency increases.

The pattern of change in the density of $[\text{emim}][\text{PF}_6]$ as observed from Figure 3.5.1(b) indicate that density increases to a smaller extent. However, the small values of mole fraction of the IL due to solubility limit may be recalled at this point.

3.5.2. Density as a Function of Temperature

Experimental density as a function of mole fraction of IL X_{IL} at different temperatures are presented in Figure 3.5.2 and Table A3 (Appendix).

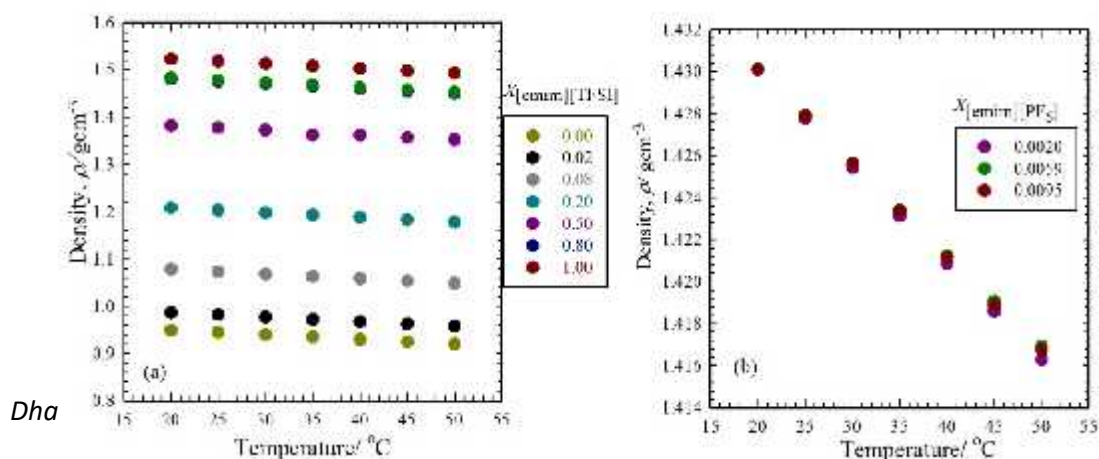


Figure 3.5.2. Density of (a) [emim][TFSI] – DMF and (b)[emim][PF₆]-DMF systems as function of temperature.

It is evident from Figures 3.5.2(a) that the effect of temperature is more pronounced at higher DMF mole fraction region. The increase in temperature brings about increased thermal motion in molecules. These energetic molecules cause the expansion of volume which may lower density. The densities of the [emim][PF₆]-DMF system was found to be dependent on the temperature as well. The effect of temperature is typical. Increase in temperature reduces the density of the system in a linear fashion. This effect can be observed in the Figure 3.5.2 (b).

3.5.3. Excess Molar Volume of IL-DMF Binary Systems

Excess molar volumes (V^E) are known to provide useful insights into structural effects of solutions and the intermolecular interactions between components molecules. The extent of deviation of liquid mixtures from ideal behavior is best expressed by excess functions. The V^E can be interpreted in the three areas, namely physical, chemical, and structural effects [45-47]. The physical effects involve dispersion forces and nonspecific interactions in the mixture, adding positive contributions to the V^E . The chemical and specific interactions result in a decrease in volume, which includes charge transfer type forces and other complex forming interactions between the two species, there by these chemical effects contribute negative values to the V^E . The structural effects that arise from the geometrical fitting of one component into the other are due to the different molar volumes and free volumes of pure components and add negative contributions to the V^E . The excess molar volumes were calculated from the composition dependence of density using the following equation

$$V^E = \frac{X_I M_I + X_D M_D}{\rho} - \left(\frac{X_I M_I}{\rho_I} + \frac{X_D M_D}{\rho_D} \right) \quad (3.1)$$

where X_{IL} and X_{DMF} are mole fractions of IL and DMF, ρ_{IL} , ρ_{DMF} and ρ are the densities of pure IL, DMF and their binary mixtures. The M_{IL} and M_{DMF} are the molar mass of IL and DMF. Furthermore these properties were mathematically fitted by variable degree functions using the Redlich- Kister expression:

$$Y = X_1 X_2 \sum_{i=0}^n A_i (X_1 - X_2)^i \quad (3.2)$$

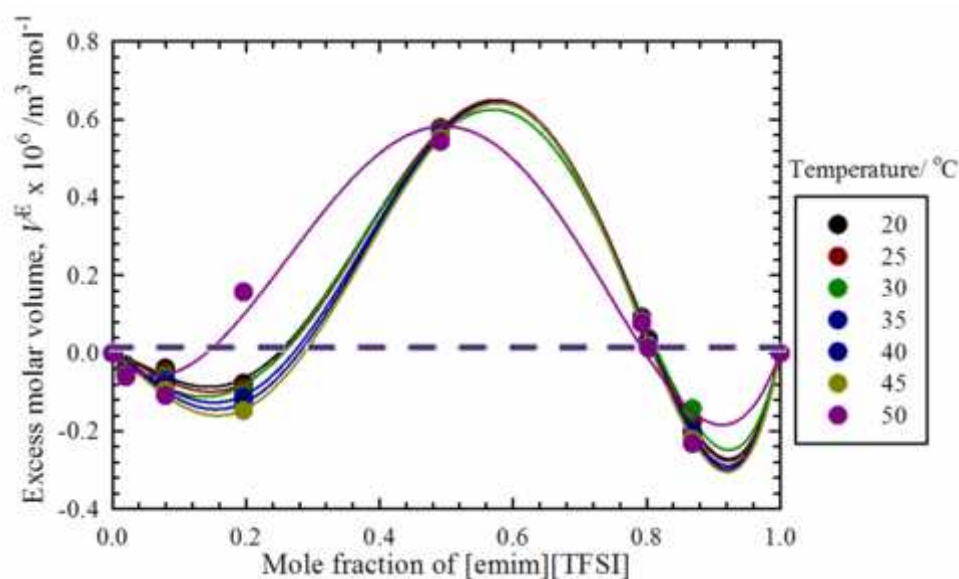
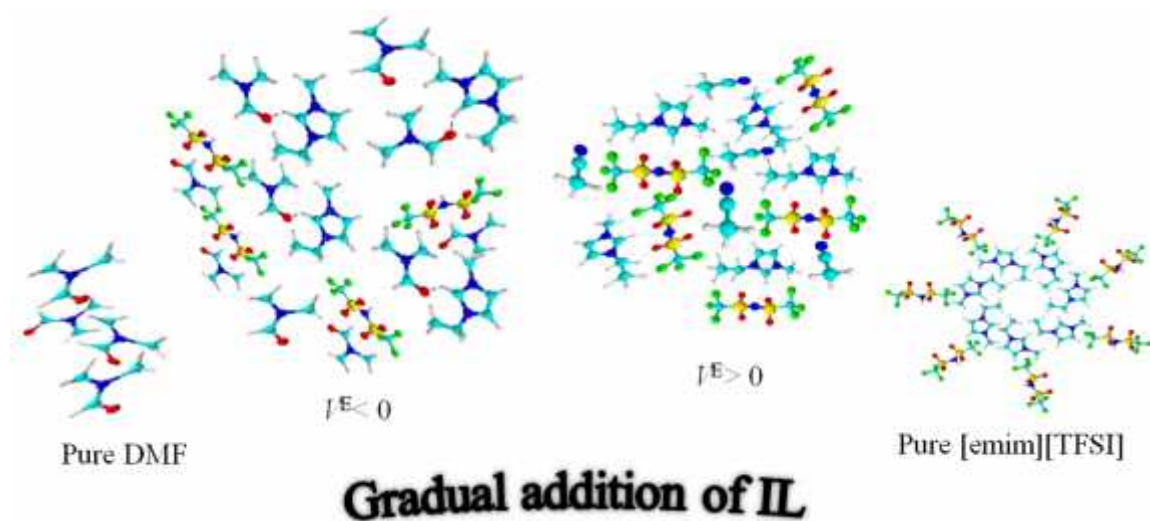


Figure 3.5.3. The V^E for [emim][TFSI]-DMF system as a function of X_{IL} at different temperatures. Solid lines are drawn by using calculated values according to Redlich-Kister equation.

For the binary [emim][TFSI]-DMF system, Figure 3.5.3 shows two opposite effects. These two opposite behavior clearly reveal that an inversion in the sign from negative to positive deviation, means the interaction between [emim][TFSI] and DMF decrease as the concentration of IL increases. The negative excess molar volume reveals that a more efficient packing of attractive interaction occurs when the IL and DMF are mixed. The excess molar volumes give the minimum value at $X_{IL} \sim 0.20$ and a maximum value at $X_{IL} \sim 0.47$ for this system. The minimum value can be due to hydrogen bonds between DMF molecules and IL. DMF is a stable compound with a strong electron-pair donating and accepting ability as mentioned above in introduction (Figure 3.5.3).

Oxygen ion of resonating structure in DMF forms hydrogen bond at C2 position of IL. Formation of hydrogen bond between DMF and C2 H of IL will reduce the hydrogen bond between the cation and anion in the IL, which also contributes to negative excess molar volume. The decrease in magnitude of the negative excess molar volume with an

increase in IL composition can be attributed to the decrease of hydrogen bonding. It can also be understood as a decrease in the concentration of IL, an increase of packing efficiency between IL and DMF contributes to negative deviation. At higher concentrations of IL, maximum value of the V^E is observed due to the dissociation of ions forming the ILs and loss of dipolar interaction of DMF. At higher concentration of IL some extensive self-association through hydrogen bonding or ion-ion interaction might be occurring. The schematic representation of self-association of DMF with ILs is shown in scheme 2.



Scheme 2: Interaction between [emim][TFSI] and DMF.

3.5.4. Viscosity of Binary Mixtures of [emim][TFSI]-DMF and [emim][PF₆]-DMF

Figure 3.5.4.1 represents the variation of viscosities (η) of pure [emim][TFSI], pure DMF and their binary mixtures of [emim][TFSI]-DMF and [emim][PF₆]-DMF with mole fraction of IL. The experimental values of η are presented in Table A3 (Appendix).

The viscosity of pure ILs is much higher than that of DMF. This is due to the fact that the viscosity of an IL is ordinarily influenced by the electrostatic interaction of the cation-anion and other interactions such as hydrogen bonding and the symmetry of the ions. Due to the strong electrostatic forces in the ILs, the viscosity of an IL can be usually 10 to 100 times greater than that of water. As the viscosity is directly affected by the electrostatic interaction, it is affected by the structure of cation and anion present in solution. ILs that are composed of larger ions as well as a delocalized charge should have lower viscosity.

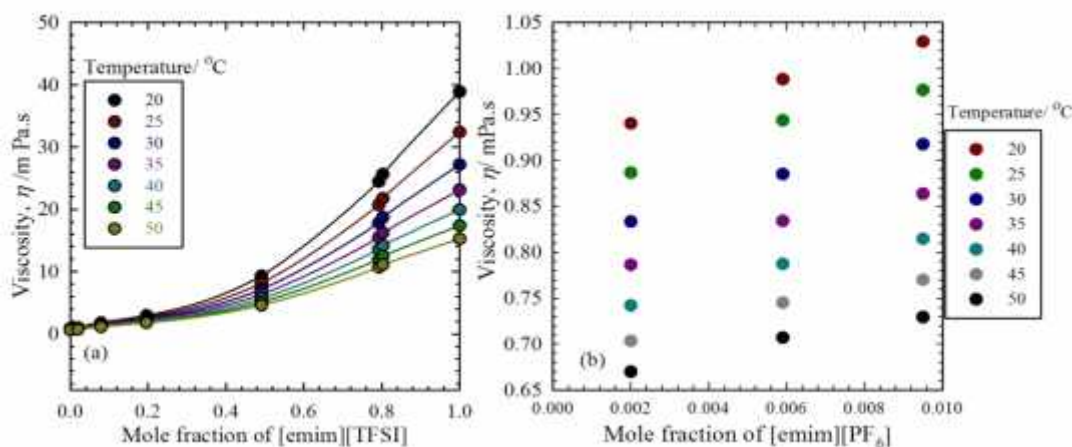


Figure 3.5.4. The of (a) [emim][TFSI] – DMF and (b) [emim][PF₆] binary systems as a function of X_{IL} .

It can be seen in Figure 3.5.4 that the for binary mixtures decreases upon gradual addition of DMF. This was observed for all compositions. This behavior agrees with previous studies of various IL-molecular solvent systems [48]. The decreased more sharply when less DMF was added to the IL. That is, the decrease was particularly strong in dilute solutions of DMF in the IL. This result has been interpreted [49] by the fact that weakening of the strong Coulomb interaction occurred upon mixing with the neutral solvent leading to a higher mobility of the ions. It is established elsewhere that the packing of ions and aggregates in the crystal of many imidazolium-based ILs often show clustering features [50]. In the microscopic structural model for bulk phase IL, clusters of ions ([cation][anion]_n) are formed. The formation of clusters imparts rigidity in the structure of IL. Due to this rigidity the viscosity of pure ILs are very high. So, when DMF is added the hydrogen bonds are formed between the C2 H of cation and oxygen atom in DMF molecule. As a result, the hydrogen bonds between the cations and anions in the clusters gets weakened and the three dimensional network is disrupted. This reduces the rigidity and introduces increased rheological or flow behavior to the IL. This is why the solution gradually becomes less viscous with increasing amount of DMF.

3.5.5. Effect of Temperature on the Viscosity IL-DMF Systems

In general, at elevated temperatures the kinetic energy of the molecules increases and the intermolecular forces decreases. Therefore, the molecular liquids at higher temperature have less resistance to the flow and hence it becomes less viscous. The change of viscosities with temperature are shown in Figure 3.5.5

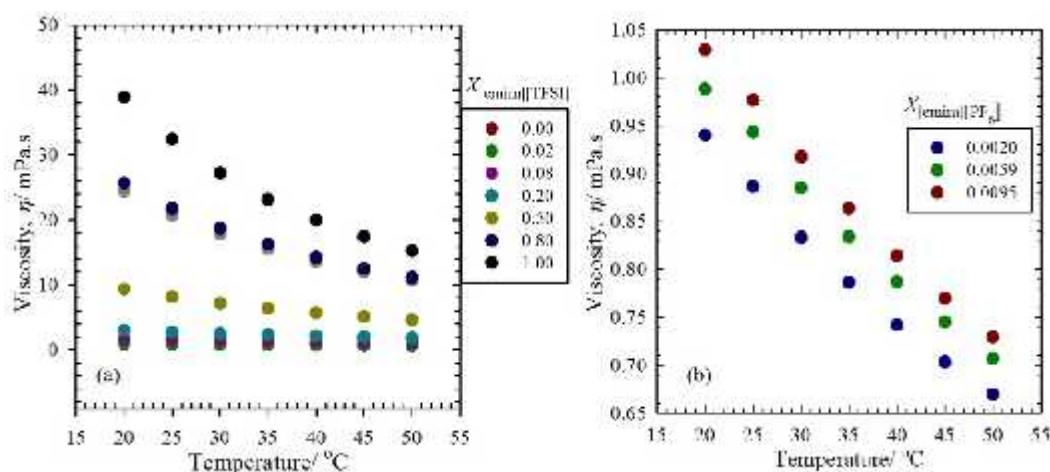


Figure 3.5.5. Viscosity of (a) [emim][TFSI]-DMF and (b) [emim][PF₆]-DMF systems as a function of temperature.

For pure IL there is a sharp decrease in viscosity with increasing temperature, but as mole fraction of DMF increases, the binary mixtures become less sensitive to temperature change. The change in viscosity of pure DMF is very small with increasing temperature compared to that of the pure IL. This can be explained by the considering the strength of interactions that occur in the liquids. The forces that hold molecules together in a liquid are ion-ion interaction, ion-dipole interaction, hydrogen bonding, dipole-dipole interaction, London force etc. Stronger interaction between the species in solution will cause higher sensitivity towards temperature. In pure IL, along with the predominant Coulombic interactions between ion pairs, van der Waals interaction and hydrogen bonds are present which make them more sensitive to temperature change. But in neutral organic solvent, DMF weak forces like, dipole-dipole interaction, London force etc. are present. Having forces considerably weaker than those in the pure IL thus the temperature sensitivity of DMF is the least of all.

3.5.6. Excess Viscosity of IL-DMF Binary Systems

The viscosity of ideal liquid mixtures can be expressed by Bingham's equation which is based on the principle of additivity. The deviation of experimental viscosity from the ideal behavior is the excess viscosity of the solution. The excess viscosity ($\Delta\eta$) with mole fraction of IL were calculated at temperatures from 20 to 50 °C by the following equation and then fitted to Redlich- Kister polynomial expression.

$$\Delta\eta = \eta - (x_1\eta_1 + x_2\eta_2) \quad (3.3)$$

This effect is illustrated in the figure 3.5.6 and the calculated values are presented in Table A4 (Appendix).

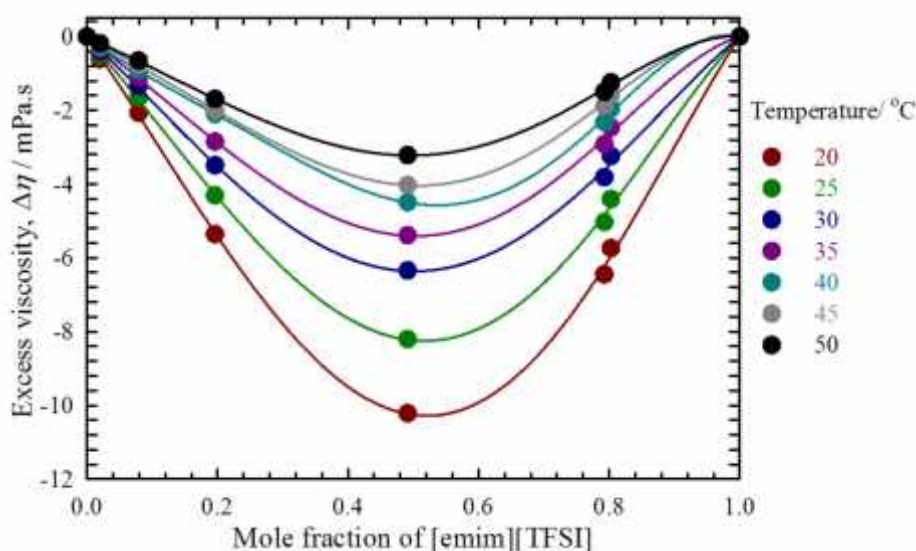
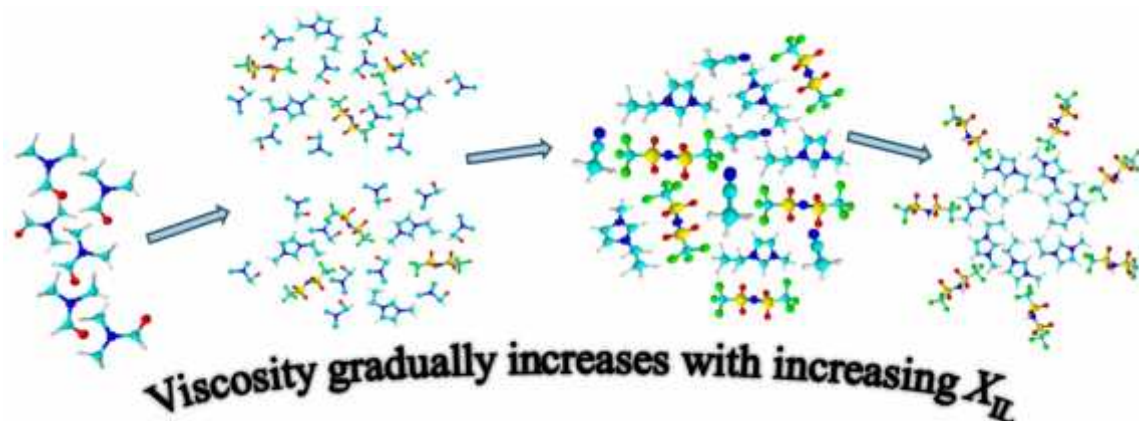


Figure 3.5.6.1. Excess viscosity of [emim][TFSI]-DMF system as a function of X_{IL} . Solid lines are drawn by using calculated values according to Redlich- Kister equation.

The $\Delta\eta$ of all binary mixtures of [emim][TFSI]-DMF was found to be negative in the whole range. As the mole fraction of DMF in the mixture was increased, the viscosity attained more negative value. Negative value indicates that the experimental viscosity is less than the calculated ideal viscosity. Generally negative excess viscosity results from the entrapment of DMF in the matrices of larger species. When DMF is added to pure IL, the hydrogen bonds between [emim]⁺cation and [TFSI]⁻ anion in the quasi three dimensional network gets weakened with the formation of bond between cation of IL and DMF molecules. This leads to higher mobility of the cation and anion and decreased resistance to flow which results in the lower viscosity of solution than the ideal value.

The schematic representation of above explanation of DMF with ILs is shown in scheme 3.



Scheme 3: Interaction between [emim][TFSI] and DMF.

3.5.7. Refractive Index of IL Based Binary Systems

Refractive index of binary mixtures gives information about ionic interactions. For the two binary systems composed of two ILs with DMF the refractive index were recorded and are illustrated as a function of temperature. Figure 3.5.7 represents refractive index of [emim][TFSI]-DMF system as a function of mole fraction of IL.

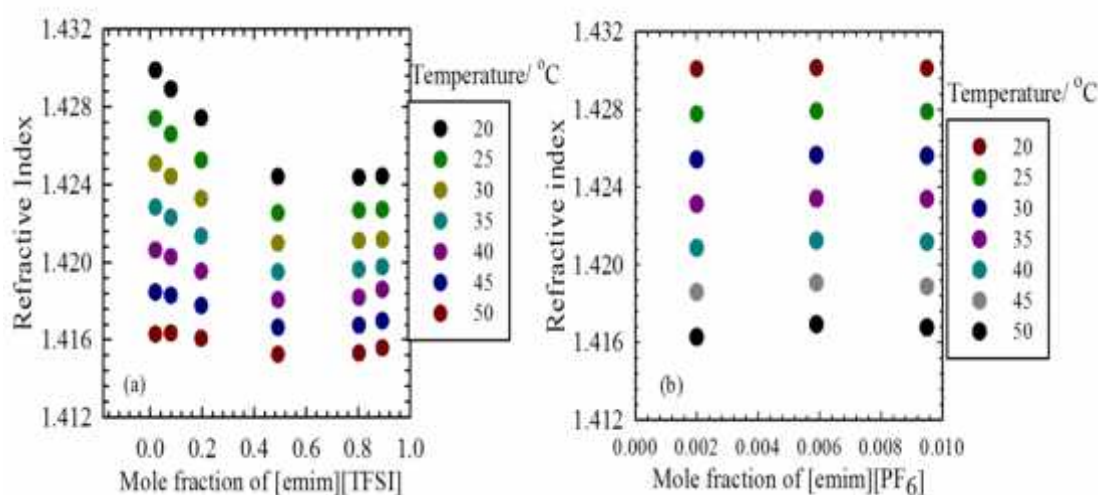


Figure 3.5.7. Refractive index of (a) [emim][TFSI] – DMF and (b) [emim][PF₆] binary systems as a function of X_{IL} .

On entering a transparent material, light bends at the interface due to a decrease in velocity, in a phenomenon known as refraction. The refractive index of a material is a dimensionless number that describes how light propagates through that medium. It is defined as

$$n = \frac{c}{v}$$

where c is the speed of light in vacuum and v is the velocity of light in the medium. The n of binary systems as a function of mole fraction of [emim][TFSI] and [emim][PF₆] in the binary mixtures is shown in Figure 3.5.7. The values of n are tabulated in table A3. At all temperatures, the n of binary mixtures ([emim][TFSI]-DMF) decrease with increasing amount of IL.

The n of binary systems as a function of temperature is shown in Figure 3.5.7.1

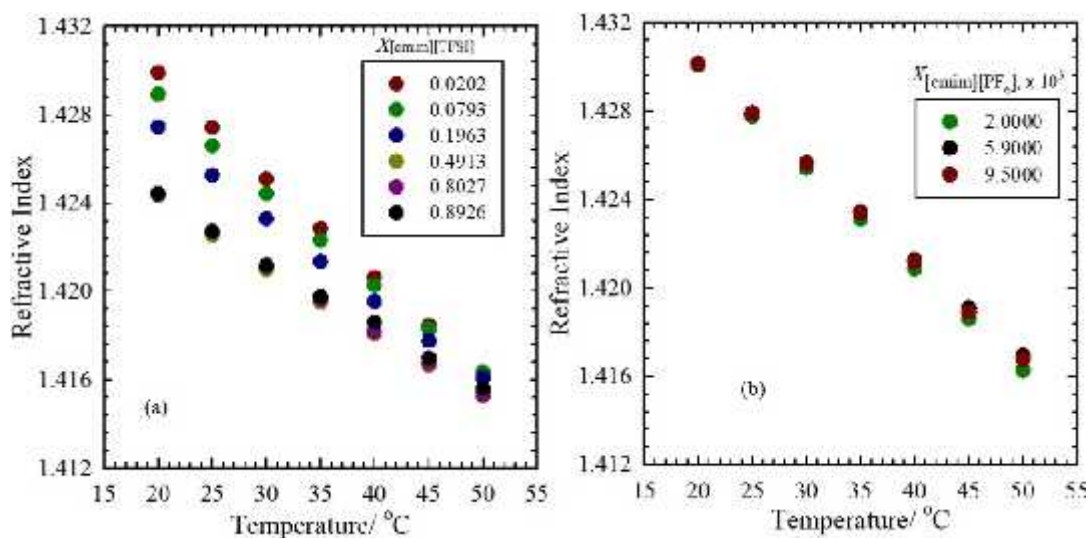


Figure 3.5.7.1. Refractive index of (a) [emim][TFSI]-DMF and (b) [emim][PF₆]-DMF system as a function of temperature.

3.5.8. Excess Refractive Index of IL-DMF Binary Systems

Figure 3.5.8 shows the variation of excess refractive index (n) values for the binary mixtures of IL with DMF at different temperatures ranges. The n of binary systems as a function of mole fraction of [emim][TFSI] are shown in Figure 3.5.8. For the binary

[emim][TFSI]-DMF system, excess refractive indices present a minimum and maximum. The negative n can be due to decrease of free volume than in the ideal solution so photon will be more interact with the molecules or ions constituting the compound; as a result light travels at a lower velocity in the medium and its refractive index will be higher than in an ideal solution. Positive n values give the opposite result.

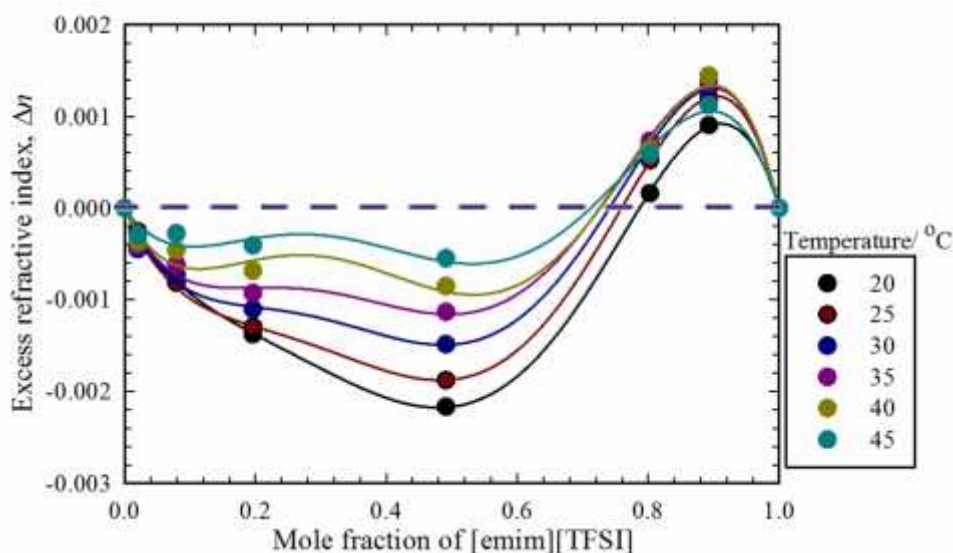


Figure 3.5.8.1. Excess refractive indices for [emim][TFSI]-DMF systems as a function of X_{IL} at different temperature. Solid lines are drawn by using calculated values according to Redlich- Kister equation.

3.6. Conclusions

The density, viscosity and refractive index of the binary mixtures of ILs and DMF are strongly dependent on the amount of DMF present in the system. The decrease of both density and viscosity with addition of DMF in pure IL arises from the disruption of three-dimensional hydrogen bonded network formed by the cations and anions in pure ILs. DMF forms hydrogen bonds with cations and as a consequence cation-anion interaction in ILs becomes weaker. At higher mole fraction of ILs the density decreases sharply but when the mole fraction of DMF is high then the decrease of density with temperature follows a non-linear pattern. The V^E shows positive and negative values at all temperature. Positive values indicate the packing efficiency between [emim][TFSI] and DMF decreases and negative values reveal that the hydrogen bond is formed between

[emim][TFSI] and DMF. The negative values of Δn indicate the entrapment of small molecules into the larger one. It can be inferred from the analyses of density, viscosity and refractive index that [emim][TFSI] interacts strongly with DMF and hydrogen bonding is prominent for IL-DMF binary systems.

References

- [1] M. Freemantle, *An Introduction to Ionic Liquids*, RSC Publishing, Cambridge, 2010.
- [2] S. Baj, A. Chrobok, S. Derfla, *Green Chemistry*, **2006**, 8, 292-295.
- [3] K. R. Seddon, *Journal of Chemical Technology and Biotechnology*, **1997**, 68, 351-356.
- [4] P. Wasserscheid, W. Keim, *Angewandte Chemical International*, **2000**, 39, 3772-3789.
- [5] R. F. Van, R. A. Sheldon, *Chemical Review*, **2007**, 107, 2757-2785.
- [6] E. R. Cooper, C. D. Andrews, P. S. Wheatley, P. B. Webb, P. Wormald, R. E. Morris, *Nature*, **2004**, 430, 1012-1016.
- [7] M. Yoshizawa, A. Narita, H. Ohno, *Australian Journal of Chemistry*, **2004**, 57, 139-144.
- [8] L. C. Branco, J. G. Crespo, C. A. M. Afonso, *Angewandte Chemical International*, **2002**, 41, 2771-2773.
- [9] Dietz, M. L. Sep, *Science and Technology*, **2006**, 41, 2047-2063.
- [10] P. Attri, P. Venkatesu, A. Kumar, *Physical Chemistry Chemical Physics*, 2011, 13, 2788-2796.
- [11] P. Attri, P. Venkatesu, *Physical Chemistry Chemical Physics*, **2011**, 13, 6566-6575.
- [12] K. R. Seddon, *Nature Materials*, **2003**, 2, 363-365.
- [13] V. N. Plechkova, K. R. Seddon, *Chemical Society Reviews*, **2008**, 37, 123-150.
- [14] P. Attri, P. M. Reddy, P. Venkatesu, A. Kumar, T. Hofman, *Journal of Physical Chemistry B*, **2010**, 114, 6126-6133.
- [15] P. Attri, P. Venkatesu, A. Kumar, *Journal of Physical Chemistry B*, **2010**, 114, 13415-13425

- [16] P. J. Scammells, J. L. Scott, R. D. Singer, *Australian Journal of Chemistry*, **2005**, 58, 155-169.
- [17] K. R. Seddon, A. Stark, M. Torres, *Pure and Applied Chemistry*, **2000**, 72, 2275-2287.
- [18] M. Blesic, J. N. C. Lopes, M. F. C. Gomes, L. P. N. Rebelo, *Physical Chemistry Chemical Physics*, **2010**, 12, 9685-9692.
- [19] P. Walden, *Bull. Acad. Imper. Science*, 1914, 1800.
- [20] H. Li Chum, R. V. Koch, L. L. Miller, *Journal of American Chemical Society*, **1975**, 97, 3264.
- [21] J. Fuller, R. T. Carlin, Long HCD, 1994, 299-300.
- [22] J. S. Wilkes, J. M. Zworotko, *Chemical Communications*, **1992**, 104, 965-967.
- [23] A. Noda, K. Hayamizu, M. Watanabe, *Journal of Physical Chemistry B*, 2001, 105, 4603-4616.
- [24] M. A. B. H. Susan, A. Noda, S. Mitsushima, M. Watanabe, *Chemical Communications*, 2003, 938-939.
- [25] H. Tokuda, S. Suzuki, M. A. B. H. Susan, K. Hyamizu, M. Watanabe, *Journal of Physical Chemistry*, **2006**, 110, 19593-19600.
- [26] E. T. Fox, E. Paillard, O. Borodin, W. A. Henderson, *Journal of Physical Chemistry C*, **2013**, 117, 78-84.
- [27] A. Wulf, K. Fumino, R. Ludwig, *Angewandte Chemical International*, **2010**, 49, 449-154.
- [28] E. T. Fox, E. Paillard, O. Borodin, W. A. Henderson, *Journal of Physical Chemistry C*, **2013**, 117, 78-84.
- [29] T. Kavitha, A. Pankaj, P. Venkatesu, R. S. R. Devi, T. Hofman, *Journal of Physical Chemistry B*, **2012**, 116, 4561-4574.
- [30] J. A. Widegren, A. Laesecke, J. W. Magee, *Chemical Communications*, 2005, 1610-1612.
- [31] P. Venkatesu, *Fluid Phase Equilibria*, **2010**, 289, 173-191.
- [32] E. Zagar, M. Zigon, *Polymer*, **2000**, 41, 3513-3521.
- [33] Y. K. Kang, H. S. J. Park, *Molecular Structure*, 2004, 676, 171-176.
- [34] B. García, R. Alcalde, J. M. Leal, J. S. Matos, *Journal of Chemical Society, Faraday Trans*, 1997, 93, 1115-1118.

- [35] P. Venkatesu, M. J. Lee, H. M. Lin, *Journal of Chemical Thermodynamics*, **2005**, 53, 996-1002.
- [36] P. Venkatesu, M. V. P. Rao, *Journal of Chemical and Engineering Data*, **1997**, 42, 90-92.
- [37] P. Venkatesu, M. V. P. Rao, *Journal of Chemical Thermodynamics*, **1998**, 30, 207-213.
- [38] J. A. Riddick, W. B. Bunger, T. K. Sakano, Wiley-Interscience: New York, 1986.
- [39] P. Venkatesu, M. V. P. Rao, D. H. L. Prasad, Y. V. L. Ravikumar, *Thermochimica Acta*, **1999**, 342, 73-78.
- [40] P. Venkatesu, C. G. Sekhar, Rao, T. Hofman, *Thermochimica Acta*, **2006**, 443, 62-71.
- [41] P. Attri, P. M. Reddy, P. Venkatesu, A. Kumar, T. Hofman, *Journal of Physical Chemistry B*, **2010**, 114, 6126-6133.
- [42] P. Attri, P. M. Reddy, P. Venkatesu, *Indian Journal of Chemistry*, **2010**, 49, 736-742.
- [43] P. Bonhote, A. P. Dias, N. Papageorgiou, K. Kalyanasundaram, M. Gratzel, *Inorganic Chemistry*, **1996**, 35, 1168-1178.
- [44] A. Yousefi, S. Javadian, N. Dalir, J. Kakemam, J. Akbari, *Royal Society of Chemistry*, **2015**, 5, 11697-11713.
- [45] P. Attri, P. M. Reddy, P. Venkatesu, A. Kumar, T. Hofman, *Journal of Physical Chemistry B*, **2010**, 114, 6126-6133.
- [46] P. Attri, A. Venkatesu, A. Kumar, *Journal of Physical Chemistry B*, **2010**, 114, 13415-13425.
- [47] R. Mehra, M. Pancholi, *Journal of Physics*, **2006**, 80, 253-263.
- [48] A. Ali, A. K. Nain, *Bulletin of the Chemical Society of Japan*, **2002**, 75, 681-687.
- [49] C. A. Angell, N. Byrne, J. P. Belieres, *Accounts of Chemical Research*, **2007**, 40, 1228-1236.
- [50] P. N. Tshibangu, S. N. Ndwandwe, E. D. Dikio, *International Journal of Electrochemical Science*, **2011**, 6, 2201-2213.
- [51] C. Yang, W. Xu, P. Ma, *Journal of Chemical and Engineering Data*, **2004**, 49, 1794-1801.

Abstract

Two binary systems each consisting of an IL either [emim][PF₆] or [emim][TFSI] with acetonitrile (ACN) have been studied. To understand the molecular interactions between ACN with [emim][TFSI] and [emim][PF₆], n , ρ , η , and conductivity measurement have been performed over the whole composition range. The excess molar volume (V^E), excess viscosity (η^E) and excess refractive index (n^E) were calculated and the results were fitted to Redlich-Kister polynomials equation. The values of V^E and η^E were negative and n^E were positive over the whole composition range for these binary mixtures. The intermolecular interactions and structural effects were analyzed on the basis of the measured and derived properties.

4.1. Introduction

ILs, a unique class of solvent materials composed solely of ions with melting point below 100 °C, are considered to be one of the most attractive materials in the field of modern science and technology. The extraordinary properties [1-2] have made ILs promising for diverse applications [3-10]. To ensure efficient use of ILs in multidisciplinary areas, it is very important to tune the properties of ILs to desirable chemistry in a systematic manner. Binary mixtures of IL and molecular solvents can provide a novel route to achieve controlled tuning of properties of these solvents by variation of composition [11-13]. Research to-date shows that addition of polar solvents to ILs can significantly alter the physico-chemical properties like density, viscosity, refractive index, and conductivity.

On the basis of well-known physical and electrochemical properties, the common non-aqueous electrochemical solvent, ACN is one of the strongest candidate for electrochemical applications. Conductivity of ILs in presence of ACN has been reported to undergo drastic increase. Compared to the intensive investigations on the IL-water mixtures, there have been a few reports on properties of binary systems composed of IL and non-aqueous molecular liquids more specifically ACN. Ma and coworkers [14] measured the densities of binary mixtures of [bmim][PF₆] and [bmim][BF₄] with ACN, benzene and propanol Xu *et al.* [15] studied the excess molar volumes of [bmim][PF₆] with ACN. Based on the simulation studies, Chaban *et al.* [16] reported that binary

mixtures of five imidazolium-based ILs and ACN with a small content of IL enhance conductivity by more than 50 times. Such ability to significantly enhance ionic conductivity by varying exclusively the mole fractions of the mixture components favors the applications of IL and ACN systems as novel non-aqueous electrolytes [17].

The solvent molecules generally interact with anion of the ILs through coordination or other possible intermolecular forces. Anions of the ILs under present study give them hydrophobicity. As ILs comprise entirely of ions, Coulombic interactions must be present in the ILs while the structure and dynamics of pure ACN are driven by dipole-dipole interactions [18]. The presence of ACN is found to decrease the cation-anion Coulombic interaction energies, which is reflected in lowering of viscosities of the IL. Originally, dilution of ILs in molecular solvents is considered as a simple means to reduce their high viscosity for the sake of practical handling. However, not only does it increase the fluidity, but also modifies the overall pattern of intermolecular and inter-ionic interactions as well as the related properties. So, the key issue of the present work is to establish a comprehensive microscopic picture on the structure and dynamics in such systems as a function of mixture composition and nature of the constituents.

4.2. Experimental

4.2.1. Materials

The ILs, [emim][TFSI] and [emim][PF₆] were obtained from Sigma-Aldrich and were used without any further purification. HPLC grade ACN for preparation of binary mixtures was purchased from E. Merck with purity of 99.9%. Water used for purposes like washing glassware was ultrapure water (specific conductivity, = 0.059 $\mu\text{S cm}^{-1}$, BOECO pure, model BOE 8082060, Germany).

4.3. Instruments

Density of binary mixtures was measured with Anton Paar vibrating-tube density meter (DMA 4500 ME), based on oscillating U-tube method. The temperature of the apparatus was controlled automatically within ± 0.01 K by a built-in Peltier device. Refractive index

of binary mixtures was directly measured with Abbemat 300 refractometer having high resolution optical sensor.

4.4. Measurements

4.4.1. Preparation of Binary Mixtures

In general ILs are immiscible with low-dielectric liquids and miscible with medium to high dielectric liquids. Dielectric constant of ACN is 37.71 at 25 °C therefore [emim][TFSI] was completely miscible in ACN. For solid [emim][PF₆] with very low solubility in ACN, binary mixtures of very low mole fraction (up to $X_{IL}=0.009$) of IL could be prepared.

All the binary mixtures of [emim][TFSI]-ACN were prepared gravimetrically in the whole range of composition. After preparation, all samples were sonicated for 20 min to ensure homogeneous mixing.

4.4.2. Measurement of Density, Viscosity, and Refractive Index

The density was measured directly from density meter reading. The viscosity of binary mixtures was measured directly by using small amount of sample (<1.0 mL) into glass capillary which was introduced into a temperature controlled capillary block. The refractive index of binary mixtures was directly obtained by placing the sample on the refractometer cell in the same amount (70 μ L) for each composition.

4.4.3. Conductivity Measurement

For conductivity measurement of the IL and IL-based binary systems, electrochemical impedance spectroscopy (EIS) was used. For this, the potentiostatic impedance spectra at 0.2V were recorded as a function of ac frequency over the range from 100 Hz to 32 MHz with ac potential amplitude of 0.5 mV. From the Nyquist plot that is Z vs $-Z$ plot for each sample, the R_s value was obtained. The cell constant was calculated using standard 0.01 M KCl solution and used to determine value of specific conductivity, from

appropriate calculations. The temperature of the tested solutions was considered to be same as the room temperature.

4.5. Results and discussion

4.5.1. Density of Binary Mixtures of [emim][TFSI]-ACN and [emim][PF₆]-ACN

Density against the change in mole fraction of [emim][TFSI] and [emim][PF₆] in the binary mixtures at different temperatures are illustrated in Figure 4.5.1 and the experimental data are presented in Table A5 (Appendix).

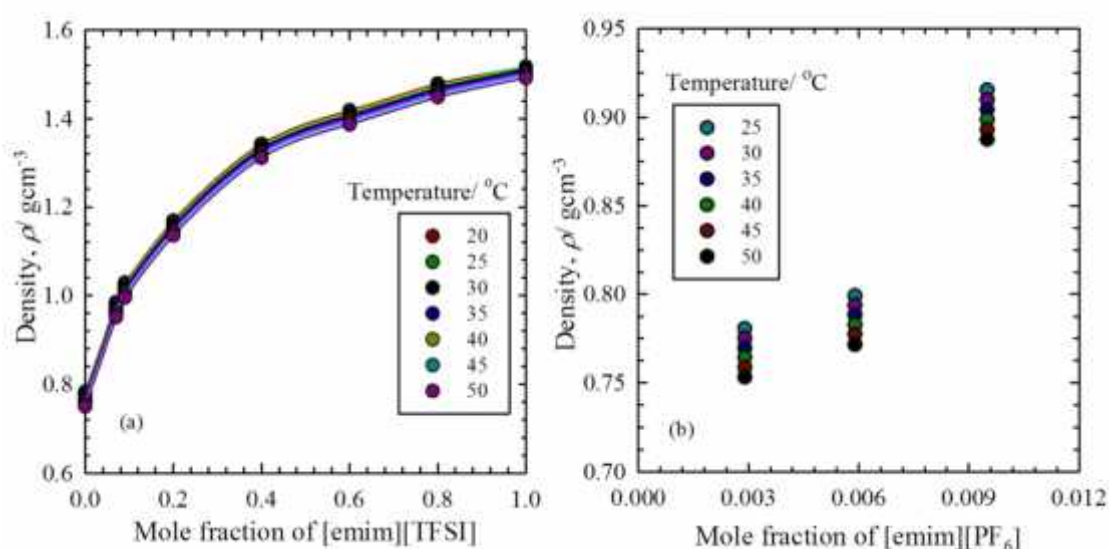


Figure 4.5.1. Density of (a) [emim][TFSI]-ACN and (b) [emim][PF₆]-ACN systems as a function of X_{IL} .

At all temperatures, the density of [emim][TFSI]-ACN and [emim][PF₆]-ACN binary mixtures increase with increasing mole fraction of IL. The decrease in density is more pronounced in the IL rich mixtures than the ACN rich mixtures. This is due to the fact that the hydrogen bond is formed between the fluorine atoms of the [TFSI] anion and the hydrogen atoms of the imidazolium rings. This local quasi network of hydrogen bonds is responsible for the high densities of ILs. Due to larger volume and poor symmetry of the anion, [TFSI], it has been found that anion is structurally favorable to the position near the C2-H group in the imidazolium-based ion-pairs. The most possible point of interaction in the cation for the formation of H-bonding with anion is the C2-H atoms.

When ACN is added to IL, the ACN molecules may either interact with the cation or anion which weakens the existing bonding between the cation and anion. Thus, expansion of volume occurs and lowers in the density.

The density of [emim][PF₆] showed only slight increase with increase in the mole fraction of the IL (Figure 4.5.1(b)). However, the mole fraction range of [emim][PF₆] was limited due to low solubility of [emim][PF₆] in ACN.

4.5.2. Density as Function of Temperature

Density of the [emim][TFSI]-ACN and [emim][PF₆]-ACN binary systems of different compositions as a function of temperature is shown in Figure 4.5.2.

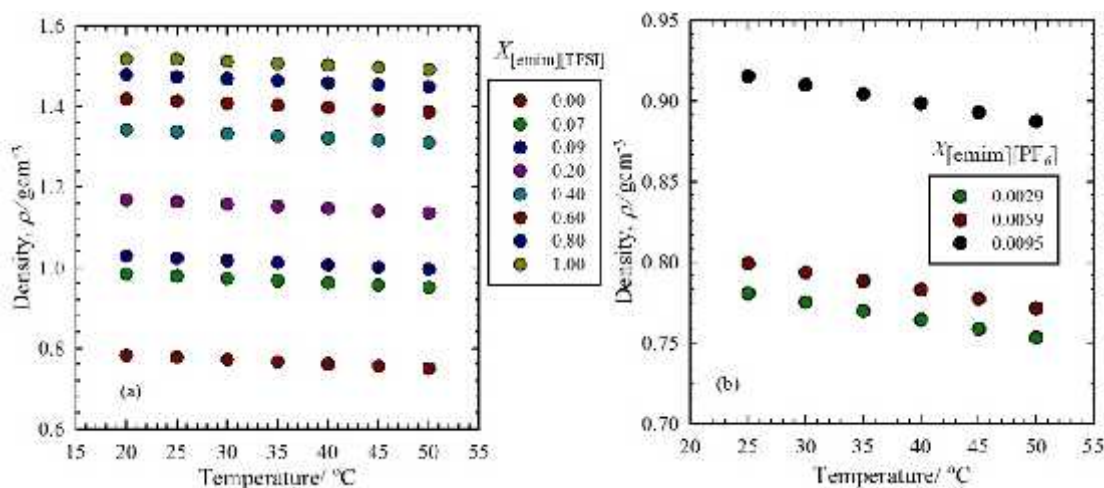


Figure 4.5.2. Density of (a) [emim][TFSI] – ACN and (b)[emim][PF₆]-ACN systems as a function of temperature.

It is evident from Figures 4.5.2(a) that the effect of temperature is more pronounced at higher ACN mole fraction region. The increase in temperature brings about increased thermal motion in molecules. These energetic molecules cause the expansion of volume which may lower density. The densities of the [emim][PF₆]-ACN system was found to be dependent on the temperature as well. The effect of temperature is typical. Increase in temperature reduces the density of the system in a linear fashion. This effect can be observed in Figure 4.5.2 (b).

4.5.3. Excess Molar Volume of IL-ACN Binary Systems

For the binary [emim][TFSI]-ACN system, Figure 4.5.3 shows two opposite effects. The values of V^E for the binary systems under study at different temperatures are listed in Table A5 (Appendix). The V^E is found to be negative when amount of ACN is high, with gradual addition of IL to the system, it becomes positive. The V^E was found to be negative when small amount of IL was added to ACN. The negative value indicates that a more efficient packing and/or attractive interaction occurs when [emim][TFSI] and ACN are mixed. The ACN molecules have strong dipole-dipole interactions with the ions and the ions of [emim][TFSI] are associated through hydrogen bonding. The contribution to negative V^E comes from the fitting of small and planar ACN molecules into the voids created by three-dimensional hydrogen bonded network of IL ions and into the voids present in larger [emim][TFSI] ions. Contributions arising from the fitting of smaller molecules into the voids available in the structure of larger molecules were also considered by others [19-22] for interpreting negative excess molar volume of binary mixtures that contain molecules of different molecular size. Mixing of ACN with IL induces a mutual dissociation of dipole-dipole association in ACN and breaking of H-bonding in IL comprising ions and subsequent formation of new H-bonding between nitrogen atom of -CN group of ACN molecules and hydrogen atom(s) of the IL anion, leading to a contraction in volume, thus resulting into negative V^E values. This trend is observed up to ~ 0.20 mole fraction of [emim][TFSI] in the binary mixtures. With increase in temperature the values become more negative in the region, this is attributed to the breaking of H-bonds between unlike molecules leading to an expansion in volume and hence resulting into an increase in the V^E . Positive excess molar volumes are the result of intermolecular dissociation effect or bond breaking of the pure solvents. In [emim][TFSI]-rich region, the trend refers to the activation of various dispersive and inductive forces as well as the weakening of ion-ion interaction in the IL. When added to pure IL, dipolar ACN molecules interact with the charged head groups of the ions and non polar domains. They orient themselves at the interface between the polar and nonpolar regions of the ILs. So the ion-ion interaction in pure IL is somewhat disrupted and expansion of volume in the binary mixture occurs. This results into positive deviation. However, a significant effect due to the steric hindrance may also contribute in positive deviation.

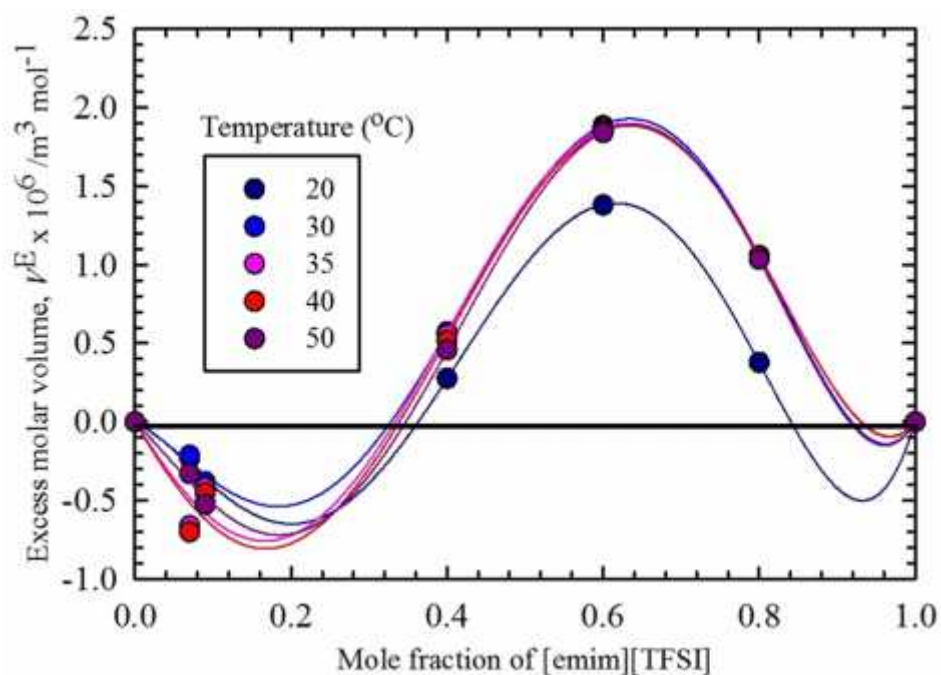


Figure 4.5.3. Excess molar volume V^E for [emim][TFSI]-ACN system as a function X_{IL} at different temperatures. Solid lines are drawn by using calculated values according to Redlich- Kister equation.

The magnitude and sign of V^E values are a reflection of the type of interactions taking place in the mixture, which are the result of different effects containing the loss of the ACN dipole interaction from each other (positive V^E) and the breakdown of the IL ion-pair (positive V^E). The interaction between the ion-pair of ILs increases as compared to ILs and ACN interactions, which leads to positive contribution. The hydrogen bonding between molecules of ACN and ions of IL cover molecular interaction, such as charge-transfer complexes. Thus the hydrogen bonding or physical interaction is very clear in these interactions. There are physical forces/ hydrogen bonding between ACN and [emim][PF₆] ions in binary mixtures. Even though the species are polar, the chemical forces are weaker than physical forces. The positive value of the V^E , over the whole composition range suggests strong hydrogen bonding intermolecular interaction, for the system consisting of a hydrogen bonding as intermolecular interaction, the contraction in the volume on mixing can be considered to occur by the ACN molecule with the smaller free volume making use of the larger free volume of the IL ions.

4.5.4. Viscosity of Binary Mixtures of [emim][TFSI]-ACN and [emim][PF₆]-ACN

The viscosities of pure ACN, pure [emim][TFSI] and binary mixtures of [emim][TFSI]-ACN and [emim][PF₆]-ACN with mole fraction of IL were measured at 5 °C temperature interval from 20 to 50 °C. This effect is illustrated in the Figure 4.5.4 and the experimental values are listed in Table A5 (Appendix).

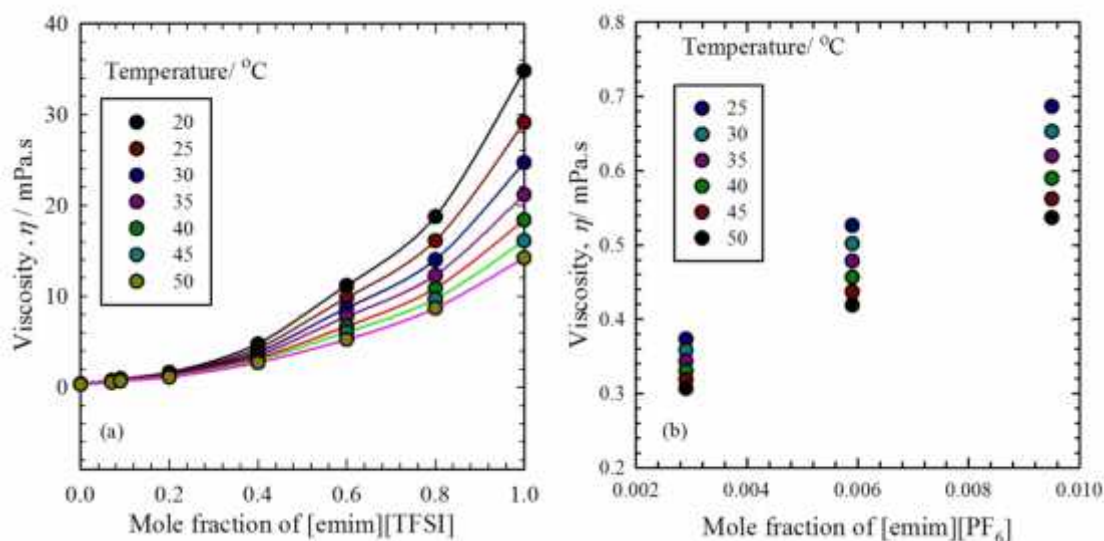


Figure 4.5.4. Viscosity of (a) [emim][TFSI]-ACN and (b) [emim][PF₆]-ACN binary systems as a function of X_{IL} .

4.5.5. Effect of Temperature on the Viscosities of IL-ACN Systems

Experimental viscosity as a function of mole fraction of IL, X_{IL} at different temperatures are presented in Figure 4.5.5. The change of viscosity against temperature for different molar fraction of the [emim][TFSI]-ACN binary mixtures as depicted in Figure 4.5.5. shows interesting profiles. With rise in temperature exponential decrease of η is observed for net [emim][TFSI] and [emim][TFSI]-ACN rich compositions of binary mixtures. This indicates that the impact of temperature on the viscosity of [emim][TFSI]-ACN composition does not remain identical over the entire composition range. The effect of temperature on lowering the viscosity of the binary mixtures is more pronounced for mixtures with high IL content and with increasing amount of ACN in the mixtures it become less sensitive to temperature change. The formation of three dimensional network

at IL-rich region imparts rigidity on the structure of IL, which is absent in pure ACN. With addition of ACN to IL, this three dimensional network structure breaks down into smaller clusters and the rigidity decreases and consequently the mixtures become less sensitive.

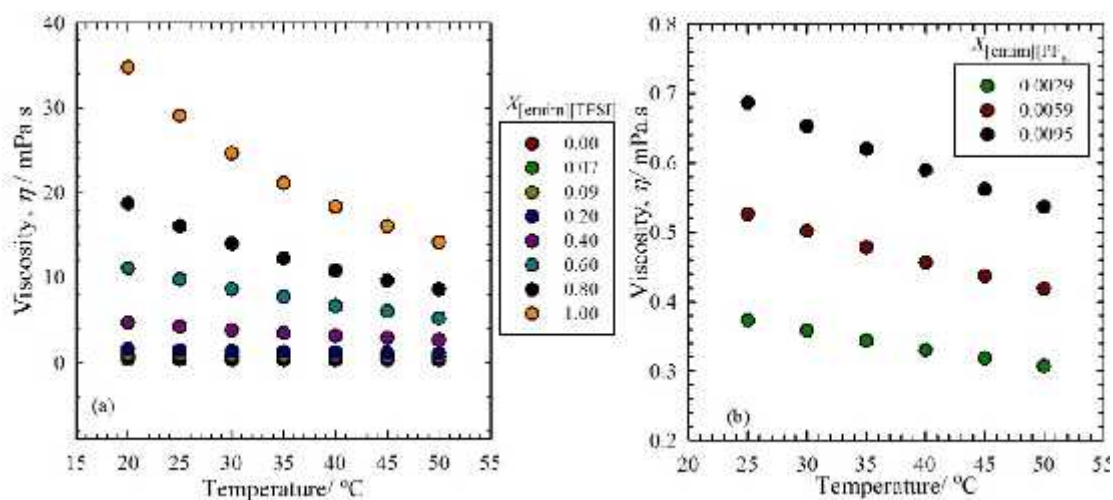


Figure 4.5.5. Viscosity of (a) [emim][TFSI]-ACN and (b) [emim][PF₆]-ACN systems as a function of temperature.

4.5.6. Excess Viscosity of IL-ACN Binary Systems

As the mole fraction of ACN in the mixture increased, the viscosity attained more negative value. Negative value indicates that the experimental viscosity is less than the calculated ideal viscosity. That is, the mixture flows more easily than is expected ideally. Generally weakening of association of molecules is responsible for such observation. The deviations of viscosity may be generally explained by considering the difference in size and shape of the component molecules and the loss of dipolar association. Figure 4.5.6 shows excess viscosity of IL-ACN binary mixtures and the values of η^E for the binary systems under study at different temperatures are listed in Table A6 (Appendix).

From general view, the negative excess viscosity may have resulted from the inclusion of ACN molecules in the matrices of larger species. When ACN is added to pure IL, the hydrogen bonds between the cation and the anion in the quasi three dimensional network

of IL gets weakened with the formation of bond between anion and ACN molecules. This leads to the higher mobility of the cation and the anion and the resistance to flow decreases which results in the lower viscosity of solution than the ideal value. Therefore it appears that the addition of ACN exerts influence on the self association of ILs possibly through hydrogen bond formation.

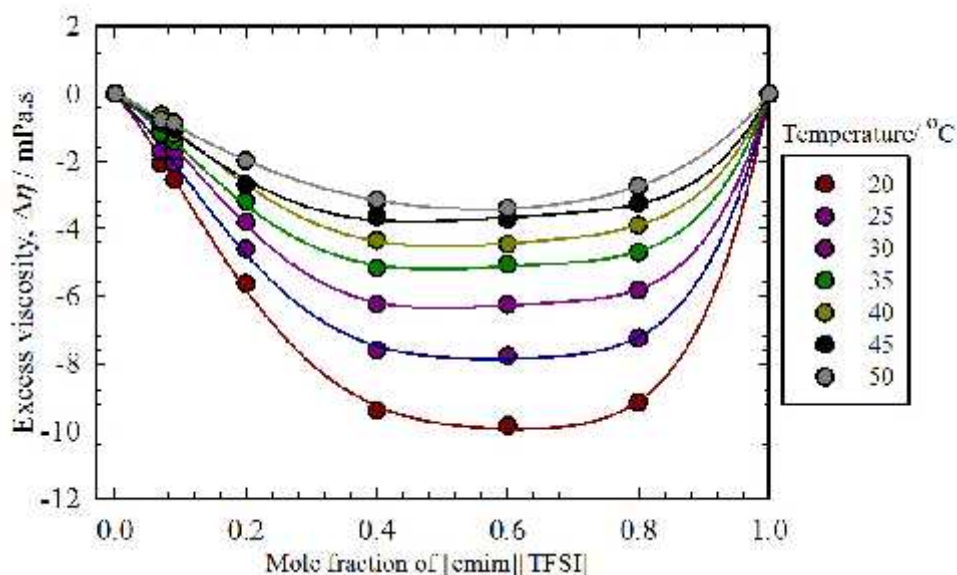


Figure 4.5.6. Excess viscosity of [emim][TFSI]-DMF system as a function of mole fraction of IL. Solid lines are drawn by using calculated values according to Redlich-Kister equation.

4.5.7. Refractive Index of [emim][TFSI]-ACN Binary System

Figure 4.5.7 gives the profile of the change of refractive index with temperature and the values are listed in Table A5 (Appendix) for binary systems of various compositions.

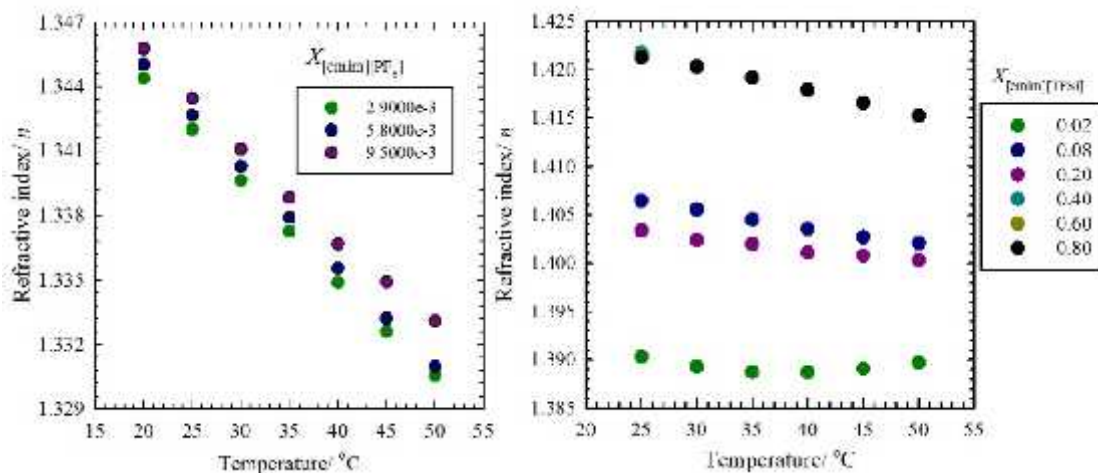


Figure 4.5.7. Refractive index of (a) [emim][TFSI]-ACN and (b) [emim][PF₆]-ACN systems as a function of temperature.

For all composition a decrease is observed with increase in the temperature. It is also observed that, whatever the composition may be, the n value attains an almost constant value at higher temperatures.

4.5.8. Excess Refractive Index of IL-ACN Binary Systems

The excess refractive index (Δn) of binary systems of [emim][TFSI]-ACN as a function of mole fraction of [emim][TFSI] are shown in Figure 4.5.8 and the values are listed in Table A6 (Appendix).

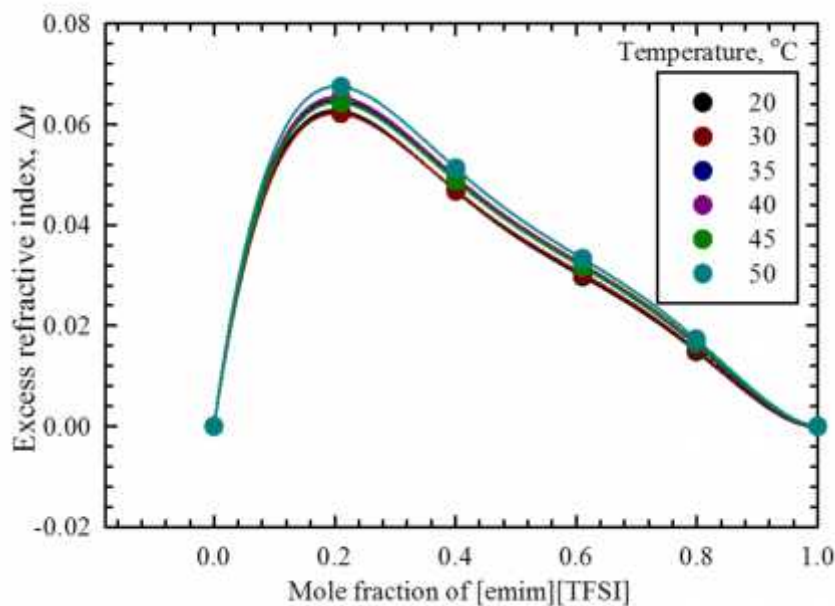


Figure 4.5.8. Excess refractive indices for [emim][TFSI]- DMF systems as a function of mole fraction of IL at different temperatures. Solid lines are drawn by using calculated values according to Redlich- Kister equation.

The curves in Fig. 4.5.8 indicate that values are positive for [emim][TFSI]-ACN mixtures over the entire range of mole fraction of [emim][TFSI] at each temperature.

4.5.9. Conductivity of Binary Mixtures of [emim][TFSI] and ACN

Since the conductivity of any system depends on the number and mobility of the charged species present in the system, it is expected that lowering of viscosities will facilitate the conductivities. The specific conductivities of the pure [emim][TFSI], ACN and binary mixtures were measured at room temperature. The results are shown in Figure 4.5.9. The maximum value of conductivity was observed at $X_{IL} = 0.2105$. The conductivity of pure [emim][TFSI] was found to be 9.07 mScm^{-1} , which increased up to almost 3 times (26.64 mScm^{-1}) than the value for binary mixture with $X_{IL} = 0.2105$.

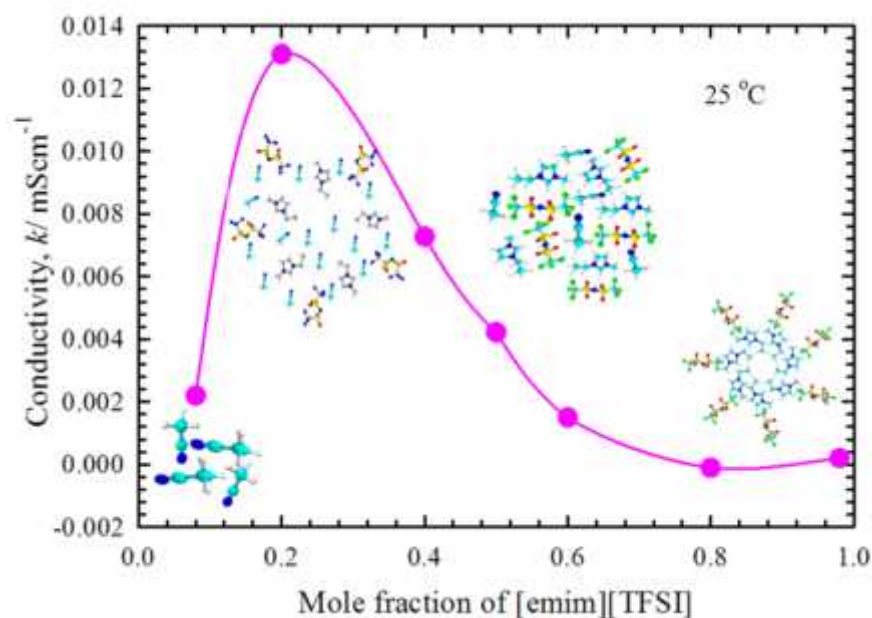


Figure 4.5.9.1. Conductivity of IL-ACN binary system at room temperature.

Since the conductivity of any system depends on the number and mobility of the charged species present in the system, it is expected that lowering of viscosities will facilitate the conductivities. From Figure 4.5.9.1, it is observed that the conductivities of the IL-ACN binary systems have a maximum. The curves obtained can be divided into several parts. The prominent maximum is observed for each binary system at a low mole fraction of IL. The clearly distinguishable patterns of increase and decrease depended on the added mole fraction of IL. At very low IL concentrations, 1:1 contact ion pairs are dominant. At IL mole fraction below or equal to 0.2, the IL behaves as a rather weakly associated conventional electrolyte while at over 0.2 it takes on its IL characteristics, lubricated by the ACN. The κ rises with the increase of the mole fraction of IL at ACN-rich region, reaches a maximum and does not increase further with further increase in mole fraction of it. Two factors are responsible to exhibit such phenomenon, (a) reduction of the mobility of the charge carriers with increasing viscosity and (b) reduction of the number of the charge carriers due to the formation of aggregates. The peak is generally attributed to an increased conductivity due to an increase in the number of charge carriers upon IL addition to the pure solvent. A further increase in the IL concentration results in a decrease in the conductivity due to increased ion-ion interactions (i.e., ionic association) which reduces both the number of effective charge carriers and their mobility (which is also reflected by the increasing viscosity). It is interesting to note that, the maximum conductivity obtained for each binary system is manifold greater than the pure IL. But the proportion is not the same for all systems.

4.6. Conclusions

ILs show unique properties due to their unusual structure and interactions of the ions. Comprising of ions only, they show conductivity which is governed by the size, and symmetry in structure of the ions and their molecular behavior originated from the formation of ion pairs, aggregates, clusters. Asymmetry of anion lowers the conductivity whereas that of smaller cations causes an increase. The effect of anion is more prominent. The density and viscosity are also high due to the formation of rigid clusters other aggregates. Addition of ACN can significantly change properties of IL and properties of IL-ACN binary mixtures are governed by the nature of intermolecular interactions in various compositions and temperatures. The hydrogen bonding between the ions of

[emim][TFSI] are altered by addition of ACN whereas the ions in [emim][PF₆] interact mostly by Coulombic attraction forces. In this work, a scientific knowledge-base has been built up which can be exploited for different IL-based systems to correlate the physico-chemical properties with the structure of the components and compositions. This will be of significant importance to tune the physico-chemical properties of different IL-based systems and to bring dimension in designing novel, cost effective, recyclable, environment-friendly materials for multidisciplinary fields of application.

References

- [1] J. K. Kima, A. Matica, A. Jou-Hyeon, P. Jacobsson, *Journal of Power Sources*, **2010**, 195, 7637-7639.
- [2] M. G. ski, A. Lewandowski, I. Stepniak, *Electrochimica Acta*, **2005**, 51, 5567-5580.
- [3] T. Welton, *Chemical Reviews*, **1999**, 99, 2071-2084.
- [4] C. Lagrost, D. Carrie, M. Vaultier, P. Hapiot, *Journal of Physical Chemistry A*, **2003**, 107, 745-752.
- [5] A. M. Scurto, S. N. V. K. Aki, J. F. Brennecke, *Chemical Communications*, **2003**, 49, 572-573.
- [6] T. Ichikawa, M. Yoshio, A. Hamasaki, T. Mukai, H. Ohno, T. Kato, *Journal of American Chemical Society*, **2007**, 129, 10662-10663.
- [7] J. Fuller, R. T. Carlin, R. A. Osteryoung, *Journal of Electrochemical Society*, **1997**, 144, 3881-3886.
- [8] M. Kosmulski, R. A. Osteryoung, M. Ciszowska, *Journal of Electrochemical Society*, **2000**, 147, 1454-1458.
- [8] N. Papagerorgiou, Y. Athanassov, M. Armand, P. Bonhote, H. Petterson, A. Azam, M. Gratzel, *Journal of Electrochemical Society*, **1996**, 143, 3099-3108.
- [9] U. Schroder, J. D. Wadhawan, R. G. Compton, F. Marken, P. A. Z. Suarez, C. Consorti, S. R. F. De Souza, J. Dupont, *New Journal of Chemistry*, **2000**, 24, 1009-1015.
- [10] D. R. McFarlane, J. Sun, J. Golding, P. Meakin, M. Forsyth, *Electrochimica Acta*, **2000**, 45, 1271-1278.

- [11] A. Diaw, A. Chagnes, B. Carre, P. Willmann, D. Lemordant, *Journal of Power Sources*, **2005**, 146, 682-684.
- [12] C. J. Hogan, J. F. de la Mora, *Physical Chemistry Chemical Physics*, **2009**, 11, 8079-8090.
- [13] M. N. J. Kobrak, *Chemical Physics*, **2006**, 125, 1-11.
- [14] Y. Huo, S. Q. Xia, P. S. Ma, *Journal of Chemical and Engineering Data*, **2007**, 52, 2077-2082.
- [15] Y-j. Xu, J-f. Shen, Q-w. Wang, H. Lin, H. Shiji, 32, 2009, 661-666.
- [16] V. V. Chaban, I. Voroshylova, O. Kalugin, O. Prezdo, *Journal of Physical Chemistry B*, **2012**, 116, 7719-7727.
- [17] A. Jarosik, S. R. Krajewski, A. Lewandowski, P. Radzimski, *Journal of Molecular Liquids*, **2006**, 123, 43-50.
- [18] A. M. Nikitin, Lyubartsev, *Journal of Computational Chemistry*, **2007**, 28, 2020-2026.
- [19] W. Xu, C. A. Angell, *Science*, **2003**, 302, 422-425.
- [20] M. A. B. H. Susan, A. Noda, S. Mitsushima, M. Watanabe, *Chemical Communications*, **2003**, 329, 938-939.
- [21] H. Ohno, M. Yoshizawa, *Solid State Ionics*, **2002**, 154, 303-309.
- [22] M. Yoshizawa, J. P. Belieres, W. Xu, C. A. Angell, *Journal of American Chemical Society*, **2003**, 226.

Abstract

Physico-chemical properties such as density and viscosity of the ternary mixtures of [emim][TFSI] with DMF and ACN have been measured at temperatures ranging from 20-50 °C. These physico-chemical properties have been studied at a fixed X_{DMF} , X_{ACN} or $X_{[\text{emim}][\text{TFSI}]}$ ($= 0.20$) with variation of other two solvents in the ternary mixtures. For all the ternary mixtures, the density values were found to decrease with increasing temperature and mole fraction of different solvents, DMF, ACN and [emim][TFSI]. On the contrary, viscosity values increase and decrease with increasing mole fraction and decreasing temperature. The excess properties such as excess molar volume, excess viscosity and were evaluated from density and viscosity results, respectively. The excess molar volume and excess viscosity of ternary mixtures are negative over the entire mole fraction range. The measured data of the studied ternary mixtures have been correlated with Redlich- Kister equation to calculate ternary adjustable parameters along with standard deviations. The results were interpreted to develop a fundamental understanding of the nature of interactions in IL-molecular solvent ternary mixtures.

5.1. Introduction

Ternary mixtures have attracted considerable attention for the confirmation of their solvating power, the strength of unlike molecular hydrogen-bond interactions, and the molar ratio of stable adducts in the complex system [1-5].

Mixed solvents containing different molecular solvents with ILs are important soft complex materials of biological and pharmaceutical interest. In Chapters 2-4, different physico-chemical properties; density, viscosity, refractive index and conductivity were extensively investigated for binary mixtures of polar solvents, DMF and ACN with hydrophobic ILs, [emim][TFSI] and [emim][PF₆] over the entire concentration range to understand the H-bonding and molecular interaction behavior between unlike molecules.

The ILs, as described in Chapter-1 stand for a class of liquids composed entirely of ions with very low melting points below 100 °C. Because of their unique physical properties [6-9], they have been considered as heat transfer solvents, lubricants for processing biomass, and the working fluid in batteries, capacitors, solar cells and in biocatalysts [10-16]. The design of industrial processes and new products based on ILs or their mixtures with organic solvents are only possible when their thermodynamic properties like excess molar volume, excess viscosity, excess refractive index are adequately known. However, these properties of ILs mixtures with organic molecular liquids are limited, [17-25] which greatly restrict their applications and further development. Thus, there is a need for comprehensive study of thermodynamic and physical properties of IL mixtures.

The diesel extractive desulfurization (EDS) process involves separation of sulfur compounds from fuel using a liquid extracting agent that is not miscible with diesel. According to literature, oxidative desulfurization (ODS) seems to be a good alternative for diesel desulfurization [26-29]. Imidazolium based ILs are used for most of EDS, ODS and ECODS studied [30, 31]. The [emim][TFSI] is one of the investigated IL.

Numerous attempts have been made to explore the molecular level interaction in ternary mixtures of DMF with water [32-35] and different organic solvents and ACN with different organic solvents [36] and IL with ethylene carbonate and lithium bis(trifluoromethanesulfonyl)azanide [37], 2-aminothiazole in DMF-water [38], organic solvents [39] and tetrafluoroborate with monoethanolamine and water [40].

Thermodynamics of ternary mixtures [41-43] of ILs has not received as much attention compared to binary mixtures despite that all thermodynamic properties of ternary mixtures should, in principle, be determinable from the properties of their sub binary mixtures. Sharma *et al.* [39] observed thermodynamic properties; excess molar volume, excess isentropic compressibilities, excess molar enthalpies and excess heat capacities of ternary mixtures containing imidazolium based ionic liquids and organic solvents. The

observed thermodynamic properties of ternary mixtures have been calculated by utilizing the topology of the constituents of mixtures.

In this work, with a view to understanding molecular level interaction of ternary system of DMF with ACN and [emim][TFSI], series of ternary mixtures were prepared. The ternary mixtures consisting of a fixed mole fraction of DMF with ACN and [emim][TFSI], constant mole fraction of ACN with [emim][TFSI] and DMF and finally at a fixed concentration of IL with DMF and ACN over the entire concentration range were investigated in detail through measurements of physico-chemical properties, density, viscosity. The binary mixtures of DMF and ACN chosen in this study appear interesting since they have nearly equal values of the dielectric constant and a similar type of H-bond interactions with highly polar solvents, DMF and ACN with ILs. This study thus aims at exploring the effect of a third solvent on the H-bond interactions and dipolar ordering of the binary mixtures with varying solvents.

5.2. Experimental

5.2.1. Materials

ACN (E. Merck, HPLC grade), DMF (Fisher Scientific, HPLC grade), and [emim][TFSI] (Sigma-Aldrich) were used as received without further purification.

5.3. Instruments

The density and viscosity of the binary mixtures were measured with *Anton Paar* (Model DMA 4500 M) vibrating tube density meter, Lovis 2000ME microviscometer with accuracy of $\pm 10^{-6}$ mPas. For weighing the components for preparing binary liquid mixtures, a digital microbalance UBT-110 from UNILAB, USA was used. The mixtures were sonicated using a LU-2 Ultrasonic cleaner, Labnics Equipments, USA.

5.4 Measurements

5.4.1 Preparation of Ternary Mixtures

All the ternary mixtures; [emim][TFSI] with DMF and ACN were prepared gravimetrically with a precision of ± 0.0001 g in the temperature range of 20-50 °C . All samples were sonicated for 20 min to ensure homogeneous mixing. Due to low solubility of [emim][PF₆], ternary mixtures of [emim][PF₆]-DMF-ACN could not be prepared.

5.5. Results and Discussion

5.5.1. Physico-chemical Properties of Ternary Mixtures of [emim][TFSI] with DMF and ACN

5.5.1.1. Density as a Function of Mole Fraction and Temperature

The density of ternary mixtures [emim][TFSI] with DMF and ACN at a fixed mole fraction of DMF, ACN and [emim][TFSI] (= 0.20) with varying other two solvents with a temperature range at 20-50 °C . The values of experimental densities of ternary mixtures at several temperatures are listed in Tables A7, A9, and A11 (Appendix). The densities data were used to determine excess molar volume, V^E , of ternary mixtures using the following equations

$$V^E = \frac{X_I M_I + X_D M_D + X_A M_A}{\rho} - \left(\frac{X_I M_I}{\rho_I} + \frac{X_D M_D}{\rho_D} + \frac{X_A M_A}{\rho_A} \right) \quad (5.1)$$

The V^E values of the ternary mixtures were fitted to Redlich-Kister equation 5.2

$$X_1^E (X = V^E, \Delta n) = x_1 x_2 [\sum_{n=0}^2 (X_{12}^n)] ((x_1 - x_2)n] + x_2 x_3 [\sum_{n=0}^2 (X_{23}^n)] (x_2 - x_3)n] + x_1 x_3 [\sum_{n=0}^2 (X_{13}^n)] (x_1 - x_3)n] + x_1 x_2 x_3 [\sum_{n=0}^2 (X_{123}^n)] (x_2 - x_3)n x_1^n] \quad (5.2)$$

where $X_{12}(n)$ ($n = 0$ to 2) etc. are the adjustable parameters of the constituent binaries. The X^n parameters for [emim][TFSI] with DMF and ACN were taken from literature [44, 45]. The $X_{123}(n)$ ($X = V^E$ or ρ) ($n = 0$ to 2) and so forth, are parameters characteristic of $(1 + 2 + 3)$ mixture and were determined by fitting the measured data to equation 5.2 by least-square optimization.

The change of density and excess molar volume of ternary mixtures at a fixed X_{DMF} , X_{ACN} and $X_{[emim][TFSI]}$ is 0.20 with variation of other two solvents are discussed below in the following sub-sections.

5.5.1.1.1. At a Fixed Mole Fraction of DMF is 0.20

Figure 5.5.1 shows the change in density of ternary mixtures with respect to mole fraction of [emim][TFSI] and temperature.

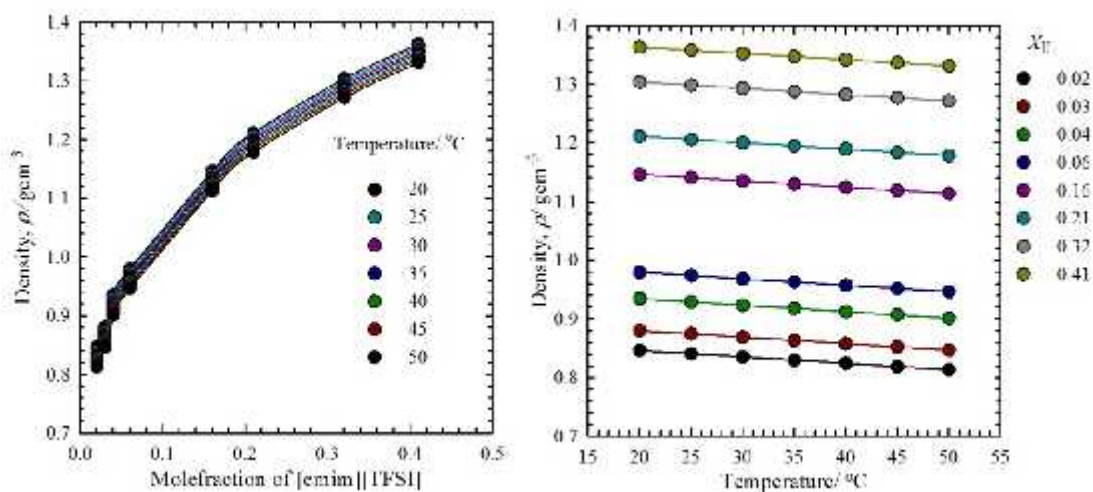


Figure 5.5.1. Density for the [emim][TFSI]-DMF-ACN system as a function of IL mole fraction at different temperature where X_{DMF} is fixed.

At all temperatures the densities of [emim][TFSI] with DMF and ACN ternary mixture increase with the increasing mole fraction of [EMIM][TFSI]. However, the increase is not linear. The increase is more pronounced in IL-rich mixtures than in solvent-rich mixtures. Density of the [emim][TFSI]-ACN-DMF ternary systems of different compositions as a function of temperature is shown in Figure 5.5.1. The excess molar volume values for the studied mixtures are recorded in Table A8 (Appendix).

The excess molar volumes for ternary mixtures are negative over the entire composition range as shown in Figure 5.5.2.

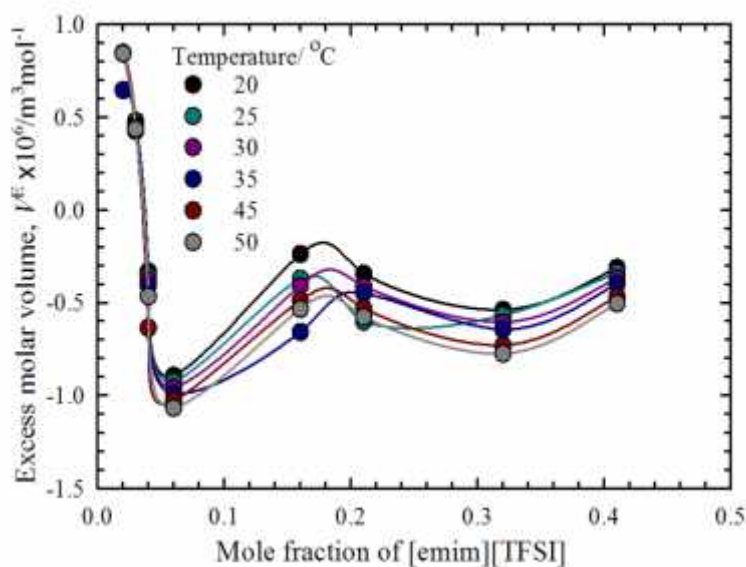


Figure 5.5.2. Excess molar volume for [emim][TFSI]- DMF- ACN system as a function of IL at different temperatures at a fixed X_{DMF} is 0.20.

ILs are complex solvents and are capable of interacting simultaneously with other organic solvents via ionic hydrogen bonding [46] and dipole interactions. The negative excess

molar volume values for the mixtures studied suggest that a more effective packing and/or attractive intermolecular interaction occurred when DMF and ACN are mixed with [emim][TFSI].

5.5.1.1.2. At a Fixed Mole fraction of ACN is 0.20

Density as a function of mole fraction of [emim][TFSI] for ternary mixtures with DMF and ACN, with fixed X_{ACN} at different temperatures are illustrated in the Figure 1.1.2.1. Density of the [emim][TFSI]-ACN-DMF ternary systems of different compositions as a function of temperature of the investigated mixtures are listed in Table A9 (Appendix) and the profiles are shown in Figure 5.5.3. Density increases with increase in the mole fraction of [emim][TFSI] and decreases with increasing temperature.

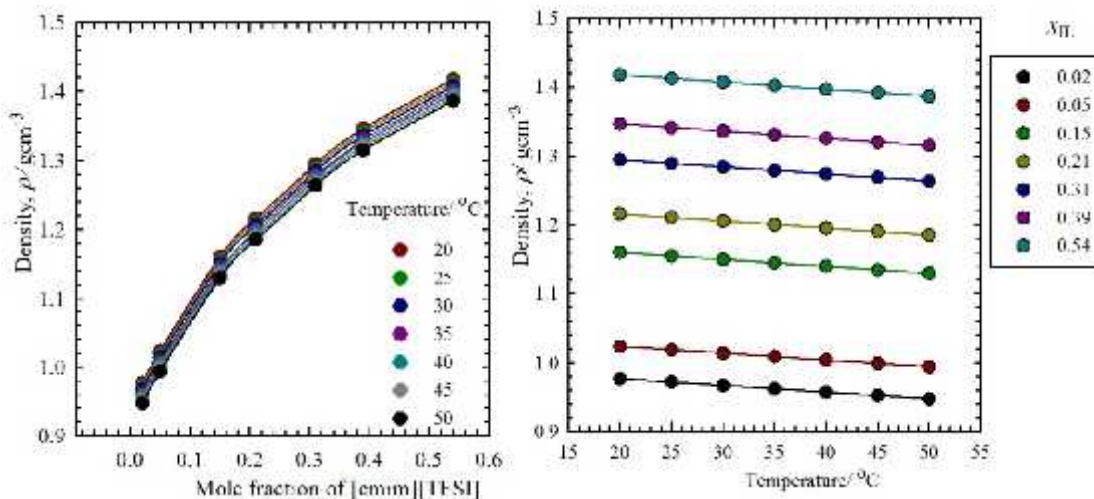


Figure 5.5.3. Density for the [emim][TFSI]- DMF- ACN system as a function of X_{IL} at different temperature where X_{ACN} is fixed.

Excess molar volume was calculated from density data by using equation 5.2 and was fitted to Redlich-Kister equation. For the ternary system [emim][TFSI]-ACN-DMF system, Figure 5.5.4, shows negative result for excess molar volume. The values of excess molar volume are shown in Table A10 (Appendix).

Due to ionic hydrogen bonding and dipole interaction between organic solvents, DMF and ACN and [emim][TFSI] excess molar volume results give negative values where X_{ACN} is fixed at 0.20.

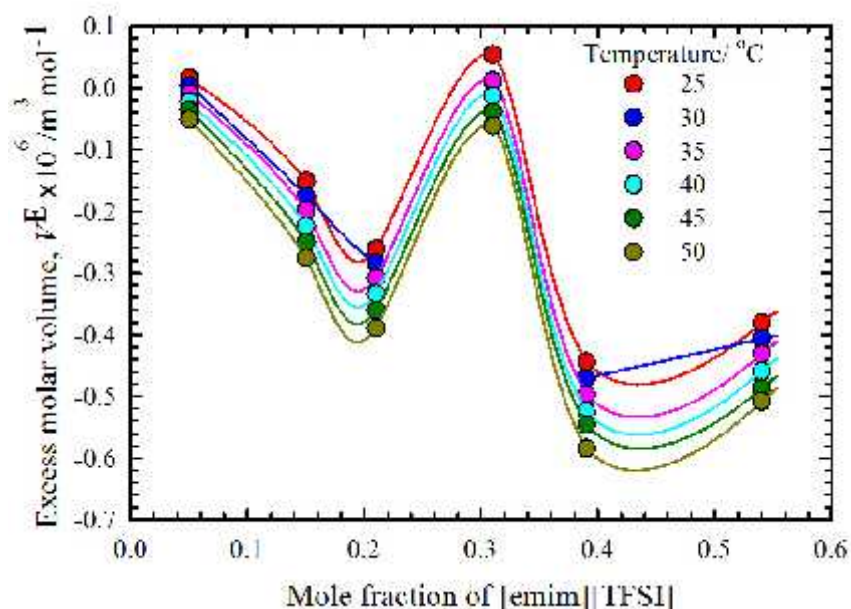


Figure 5.5.4. Excess molar volume for [emim][TFSI]-DMF-ACN system as a function of IL mole fraction at different temperatures at a fixed mole fraction(0.20) of ACN.

5.5.1.1.3. At a Fixed Mole fraction of [emim][TFSI] (0.20)

At a fixed mole fraction (0.20) of [emim][TFSI] in ternary systems the density of the [emim][TFSI]-ACN-DMF system was found to be dependent on the temperature as well. The effect of temperature is typical. Increase in temperature reduces the density of the system in a non-linear fashion. This effect can be observed in Figure 5.5.5. and the experimental values are presented in Table A11 (Appendix).

The variation of density of the [emim][TFSI]-DMF-ACN ternary mixtures (X_{IL} , is fixed at 0.20) with X_{DMF} at different temperatures is shown in Figure 5.5.5. The density vs. mole fraction profiles shows a non-linear increase to indicate significant intermolecular interactions between the components of the ternary system. In order to investigate the deviation of density from ideal behavior, the excess molar volume of the ternary mixtures have been calculated by using equation (5.2).

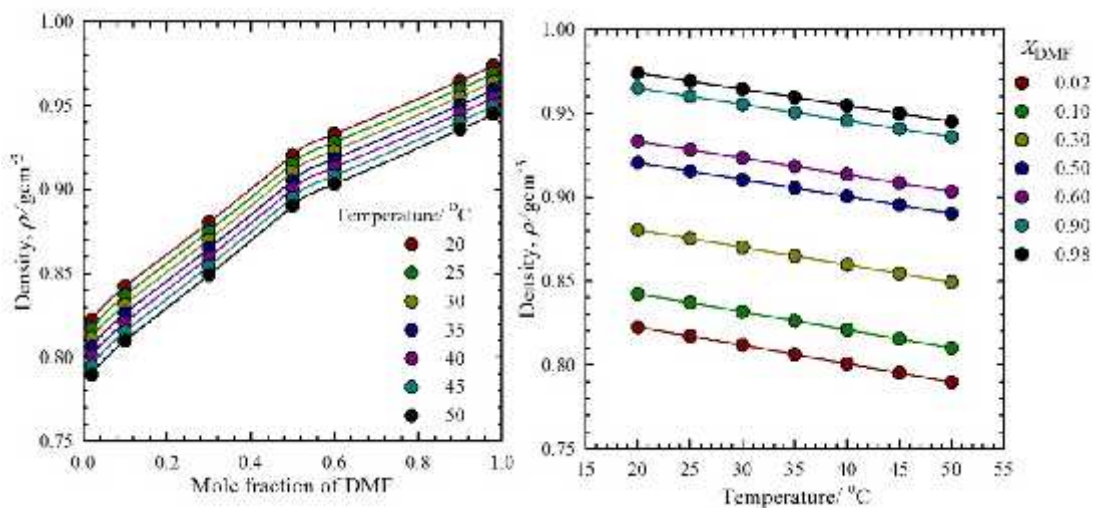


Figure 5.5.5. Density for the [emim][TFSI]-DMF-ACN system as a function of X_{IL} at different temperature where the X_{IL} is fixed at 0.20.

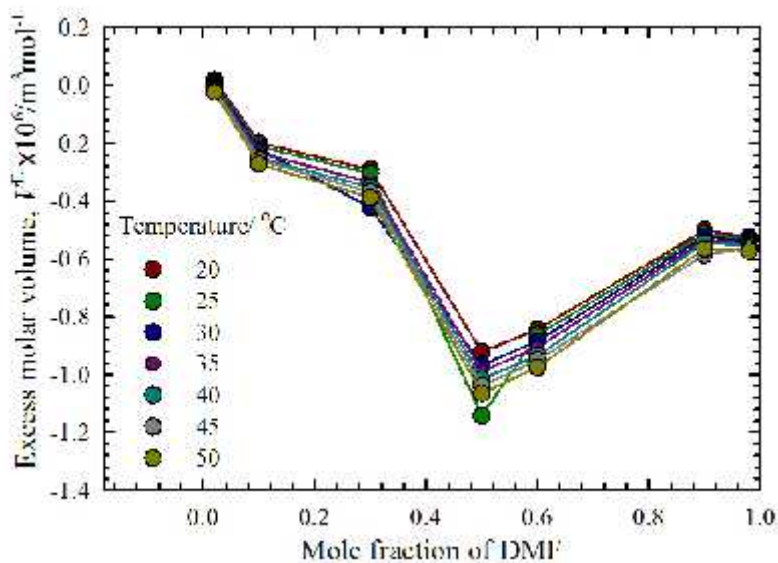


Figure 5.5.6. Excess molar volume for [emim][TFSI]- DMF- ACN system as a function of X_{IL} at different temperatures at a fixed X_{IL} is 0.20.

At constant $X_{[emim][TFSI]}$, the excess molar volume shows negative results over the entire composition range. Figure 5.5.6 shows the change of excess molar volume in ternary mixtures. Negative values of excess molar volume for the ternary mixtures comprising of [emim][TFSI] with DMF and ACN at fixed X_{IL} is 0.02 can be attributed to more effective packing or attractive intermolecular interaction between [emim][TFSI] and DMF and ACN.

5.5.1.2. Viscosity as a Function of Mole Fraction and Temperature

The viscosity of ternary mixtures [emim][TFSI] with DMF and ACN at 20-50 °C of investigated mixtures are reported in Table A13, A14, A15 (Appendix). The viscosity data were utilized to determine viscosity deviation, $\Delta \eta$, for ternary mixtures using the following equations:

$$\Delta \eta = \eta - (X_{IL} \eta_{IL} + X_{DMF} \eta_{DMF} + X_{ACN} \eta_{ACN}) \quad (5.3)$$

where X is the mole fraction of IL, DMF and ACN and η is the viscosity of ternary mixtures. The $\Delta \eta$ values of the ternary mixtures were fitted to Redlich-Kister equation 5.2.

The change of viscosity and excess viscosity of ternary mixtures at a fixed X_{DMF} , X_{ACN} , and $X_{[emim][TFSI]}$ is 0.2 with variation of other two solvents are discussed in the following sub-sections.

5.5.1.2.1. Viscosity of Ternary Mixtures of [emim][TFSI]-DMF-ACN at a Fixed X_{DMF} 0.20

The viscosity of ternary mixtures; [emim][TFSI]-ACN-DMF with mole fraction of [emim][TFSI] were measured at 5 °C temperature intervals from 20 to 50 °C. The effect is illustrated in the Figure 5.5.7.

The strong Coulombic interactions between the ions are weakened upon mixing with the polar solvents, DMF and ACN, which leads to a higher mobility of the ions and a lower viscosity of the mixtures [47]. This indicates that the viscosity of ILs could be therefore tuned for several applications by adding organic solvent or by changing temperature [48]. Due to the wide range of possible molecular interactions between the three components, deviations can occur from ideal behavior. These viscosity deviations are quantified as viscosity deviation or excess viscosity, η^E . Positive values of η^E are indicative of strong interactions, whereas negative values indicate weaker interactions.

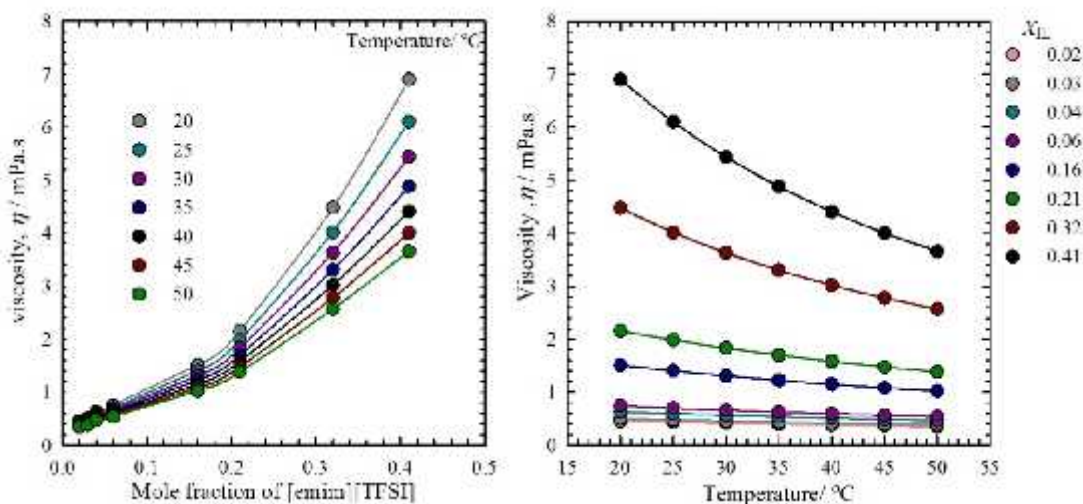


Figure 5.5.7. Viscosity for the [emim][TFSI]-DMF-ACN system as a function of IL mole fraction at different temperatures where the X_{DMF} is fixed at 0.20.

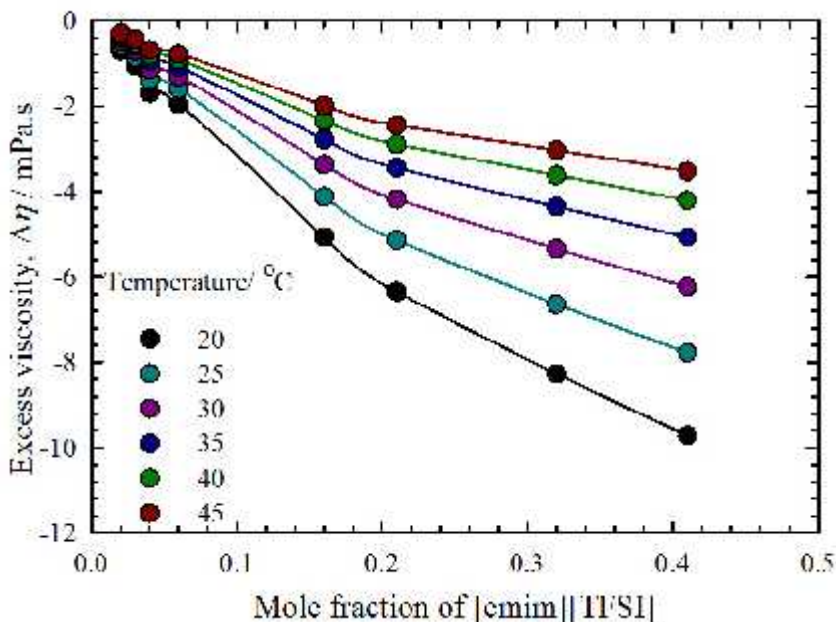


Figure 5.5.8. Excess viscosity for [emim][TFSI]-DMF-ACN system as a function of IL mole fraction at different temperatures at a fixed X_{DMF} is 0.20.

Since [emim][PF₆] is solid, and not completely soluble in all compositions of ACN, the study of viscosity in the whole composition range could not be performed. Therefore, the excess viscosity of [emim][TFSI] is discussed in this section. The excess viscosities of ternary mixture of [emim][TFSI] with DMF and ACN, where the mole fraction of DMF is fixed at 0.20 over the entire composition range are shown in Figure 5.5.8.

The deviation of experimental viscosity from the ideal behavior is the excess viscosity of the solution. The excess viscosity of the ternary mixtures was found to be negative over entire range of composition. Viscosity attained more negative value when the mole fraction of molecular solvents is low. Negative value indicates that the experimental viscosity is less than the calculated ideal viscosity. That is, the mixture flows more easily than is expected ideally. Generally weakening of association of molecules is responsible for such observation. The deviations of viscosity may be generally explained by

considering the difference in size and shape of the component molecules and the loss of dipolar association.

5.5.1.2.2. Viscosity of [emim][TFSI]-DMF-ACN at a Fixed X_{ACN} is 0.20

The ternary systems consisting of [emim][TFSI]-ACN-DMF at a fixed X_{ACN} were also studied under in similar conditions. The results are plotted in Figure 5.5.9. The viscosity increases with increasing mole fraction of IL in the ternary [emim][TFSI]-DMF-ACN systems.

Figure 5.5.10 shows the change in excess viscosity of ternary mixtures with mole fraction of [emim][TFSI]. Excess viscosity gradually decreases with increasing mole fraction of [emim][TFSI].

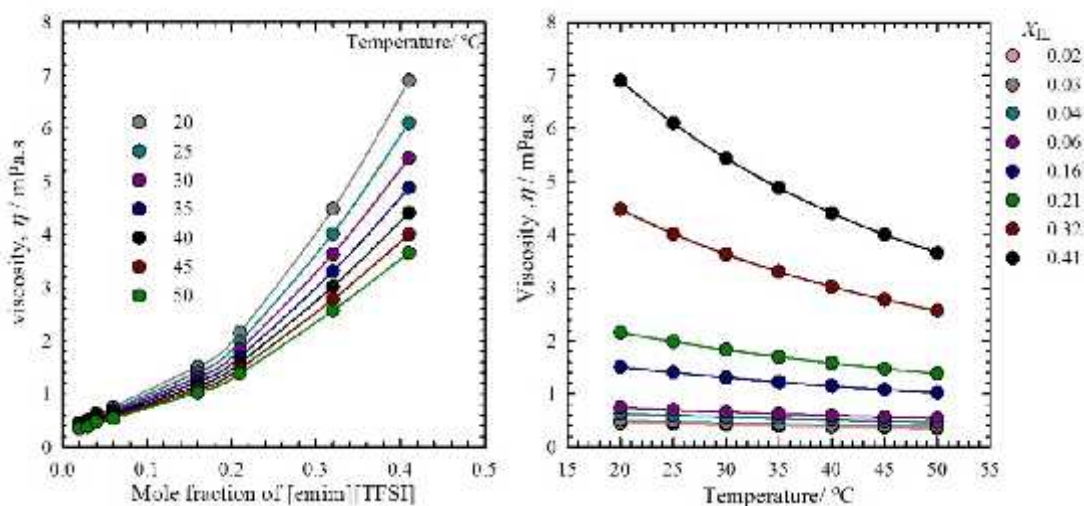


Figure 5.5.9. Viscosity for the [emim][TFSI]-DMF-ACN system as a function of IL mole fraction at different temperature where the X_{ACN} is fixed at a 0.20.

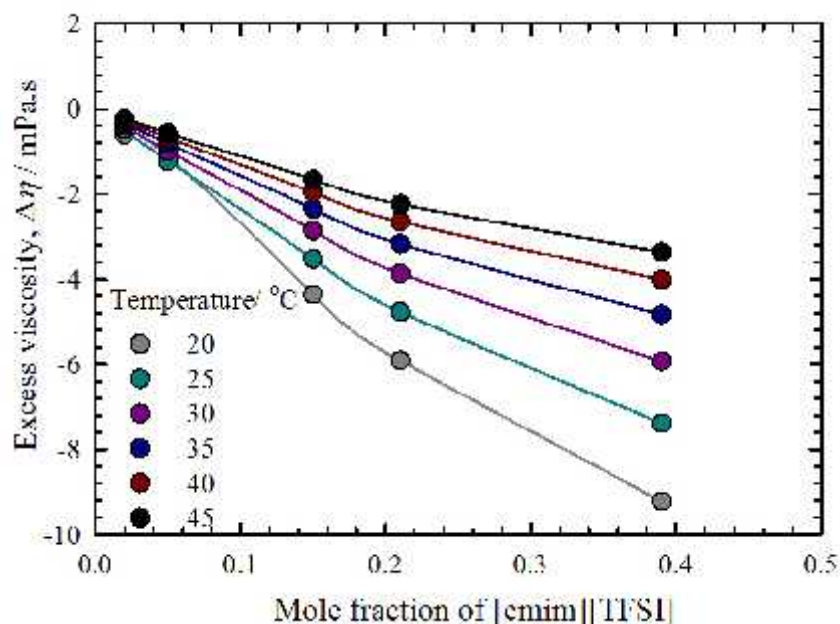


Figure 5.5.10. Excess viscosity for [emim][TFSI]-DMF-ACN system as a function of IL mole fraction at different temperatures at a fixed X_{ACN} is 0.20.

5.5.1.2.3. Viscosity of Ternary Mixtures at a Fixed Mole fraction of IL is 0.20

Figure 5.5.11 shows the viscosity vs. mole fraction of DMF and temperature for ternary mixtures. Viscosity gradually increases with increasing X_{DMF} and with decreasing temperature viscosity gradually increase. The viscosity gradually increases up to $X_{DMF} \sim 0.45$ then it remains almost constant followed by an increase again up to $X_{DMF} \sim 1.0$. Figure 5.5.11 shows the change of excess molar volume in ternary mixtures.

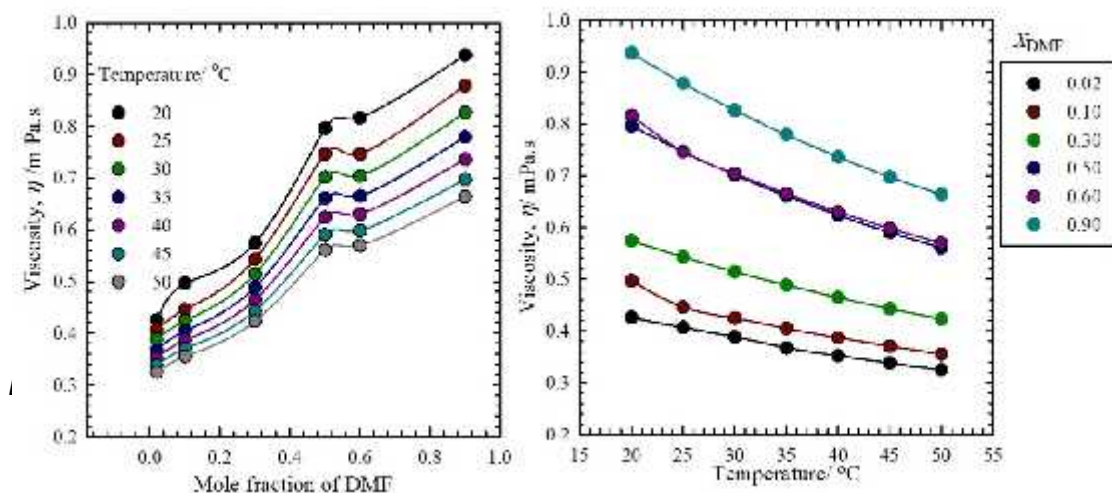


Figure 5.5.11. Viscosity for the [emim][TFSI]-DMF-ACN system as a function of IL mole fraction at different temperature where the X_{IL} is fixed at 0.20.

Figure 5.5.12 indicates that results are negative for [emim][TFSI]-DMF-ACN ternary mixtures over the entire range of X_{DMF} at each temperature. The shows a initial increase with increasing X_{DMF} and then decreases. The maximum increase is observed for the X_{DMF} at 0.45.

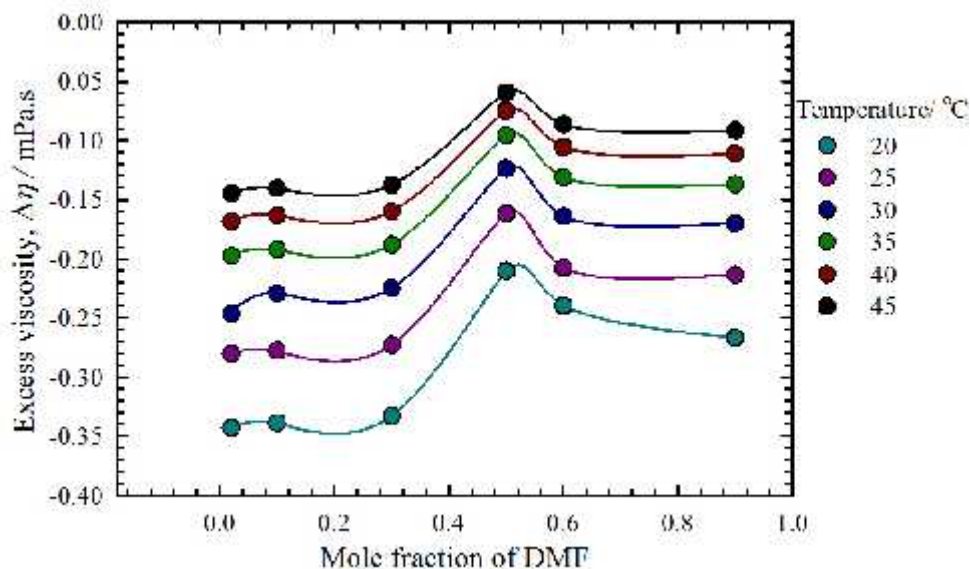


Figure 5.5.12. At fixed mole fraction of IL Excess viscosity for [emim][TFSI]-DMF-ACN system as a function of IL mole fraction at different temperatures at a fixed X_{IL} is 0.20.

5.6. Conclusions

Physico-chemical properties of ternary mixtures comprising DMF, ACN and [emim][TFSI] show different patterns with increasing mole fraction and temperatures. The density, viscosity and refractive index increase with increasing mole fraction of [emim][TFSI] and DMF at fixed DMF, ACN and [emim][TFSI], respectively. On the contrary, density, viscosity and refractive index decrease with increasing temperature. The excess molar volume and excess viscosity results of investigated ternary mixtures are negative over the entire mole fraction range may be indicates ionic hydrogen bonding and dipole interaction between organic solvents, DMF and ACN and [emim][TFSI].

References

- [1] F. Corradini, A. Marchetti, M. Taglizucchi, L. Tassi, *Fluid Phase Equilibria*, **1996**,124, 209-220.
- [2] G. Foca, M. Manfredini, D. Manzini, A. Marchetti, L. Pigani, S. Sighinolfi, L. Tassi, A. Ulrici, *International Journal of Thermophysics*, **2004**, 25, 839-855.
- [3] R. J. Sengwa, Madhvi, S. Sankhla, S. Sharma, *Journal of Solution Chemistry*, **2006**, 35, 1037-1055.
- [4] R. J. Sengwa, Madhvi, S. Sankhla, S. Sharma, *Bulletin- Korean Chemical Society*, **2006**, 27, 718-724.
- [5] R. J. Sengwa, S. Sankhla, N. Shinyashiki, *Physics and Chemistry of Liquids*, **2010**, 48, 89-98.
- [6] N. K. Marsh, A. J. Boxall, R. Lichtenthaler, A Review, *Fluid Phase Equilibria*, **2004**, 219, 93-98.
- [7] D. J. Holbray, K. R. Seddon, *Journal of Chemical Society, Dalton*

- Transactions*, **1999**, 2133-2140.
- [8] C. P. Fredlake, M. J. Crosthwaite, G. D. Hert, K. V. N. S. Aki, F. J., *Journal of Chemical and Engineering Data*, **2004**, 49, 954-964.
- [9] D.R. MacFarlane, K. R. Seddon, *Journal of Chemistry*, **2007**, 60, 3-5.
- [10] C. Ye, W. Liu, Y. Chen, L. Yu, *Chemical Communications*, **2001**, 21, 2244-2245.
- [11] R. A. Sheldon, R. M. Lau, M. J. Sorgedragar, F. Van Rantwijk, K. Seddon, *Green Chemistry*, **2002**, 4, 147-151.
- [12] S. H. Schofer, N. Kaftzik, P. Wasserschied, U. Kragl, *Chemical Communications*, **2001**, 425-426.
- [13] J. S. Wilkes, *Journal of Molecular Catalysis A*, **2004**, 214, 11-17.
- [14] V. R. Koch, L. A. Dominey, C. Nanjundiah, M. J. Ondrechen, *Journal of Electrochemical Society*, **1996**, 143, 798-803.
- [15] H. A. Every, A. Bishop, M. Forsyth, D. R. Macfarlane, *Electrochimica Acta*, **2000**, 45, 1279-1284.
- [16] M. Doyle, S. K. Choi, G. Proulx, *Journal of Electrochemical Society*, **2000**, 147, 34-37.
- [17] Q. Zhou, S. L. Wang, P. H. Chen, *Journal of Chemical and Engineering Data*, **2006**, 51, 905-908.
- [18] Y. Zhong, H. Wang, K. Diao, *Journal of Chemical Thermodynamics*, **2007**, 39, 291-296.
- [19] V. H. Alvarez, M. Aznar, *The Open Thermodynamics Journal*, **2008**, 2, 25-38.
- [20] F. Qi, H. Wang, *Journal of Chemical Thermodynamics*, **2009**, 41, 265-272.
- [21] W. Fan, Q. Zhou, J. Sun, S. Zhang, *Journal of Chemical and Engineering Data*, **2009**, 54, 2307-2311.
- [22] Y. Li, H. Ye, P. Zeng, F. Qi, *Journal of Solution Chemistry*, **2010**, 39, 219-230.
- [23] M. M. Taib, T. Murugesan, *Journal of Chemical and Engineering Data*, **2012**, 57, 120-126.

- [24] G. R. Chaudhary, S. Bansal, S. K. Mehta, A. S. Ahluwalia, *Journal of Chemical Thermodynamics*, **2012**, 50, 63-70.
- [25] Y. Gong, C. Shen, Y. Lu, H. Meng, C. Li, *Journal of Chemical and Engineering Data*, **2012**, 57, 33-39.
- [26] M. Te, C. Fairbridge, Z. Ring, *Applied Catalysis A*, **2001**, 219, 267-280.
- [27] J. M. Campos-Martin, M. C. Capel-Sanchez, J. L. G. Fierro, *Green Chemistry*, **2004**, 6, 557-562.
- [28] D. Xu, W. Zhu, H. Li, J. Zhang, F. Zou, H. Shi, Y. Yan, *Energy Fuels*, **2009**, 23, 5929-5933.
- [29] W. Zhang, K. Xu, Q. Zhang, D. Liu, S. Wu, F. Verpoort, X. M. Song, *Industrial and Engineering Chemistry*, **2010**, 49, 11760-11763.
- [30] D. Zhao, Y. Liao, Z. Zhang, *Clean*, **2007**, 35, 42-48.
- [31] T. P. Pham, C. W. Cho, Y. S. Yun, *Water Research*, **2010**, 44, 352-372.
- [32] T. C. Bai, J. Yao, S. J Hana, *Journal of Chemical Thermodynamics*, **1998**, 30, 1347-1361.
- [33] V. S. Prasad, E. Rajagopal, N. M. Murthy, *Journal of Molecular Liquids*, **2006**, 124, 1-6.
- [34] B. Garcia, R. Alcalde, S. Aparicio, J. M. Leal, J. S. Matos, *Physical Chemistry Chemical Physics*, **2001**, 3, 2866- 2871.
- [35] P. B. Morey, A. B. Naik, *International Letters of Chemistry, Physics and Astronomy*, **2015**, 59, 188-198.
- [36] J. Soleymani, E. Kenndler, W. E. Acree, A. Jouyban, *Journal of Chemical and Engineering Data*, **2014**, 59, 2670-2676.
- [37] A. Hofmann, M. Migeot, L. Arens, T. Hanemann, *International Journal of Molecular*, **2016**, 17, 670-678.
- [38] S. A. Chowdhury, J. L. Scott, and D. R. MacFarlane, *Pure and Applied Chemistry*, **2008**, 80, 1325-1335.
- [39] V. K. Sharma, S. Bhagour, S. Solanki, A. Rohilla, *Journal of Chemical and Engineering Data*, **2013**, 58, 1939-1954.

- [40] M. M. Taib, M. M. Akbar, T. Murugesan, *Journal of Molecular Liquids*, **2014**, 190, 23-29.
- [41] B. Wu, Y. M. Zhang, H. P. Wang, *Journal of Chemical and Engineering Data*, **2009**, 54, 1430-1434.
- [42] N. Deenadayalu, Z. Tywabi, S. Sen, T. Hofman, *Journal of Chemical ics*, **2012**, 49, 24-38.
- [43] A. Marciniak, M. Krolikowski, *Journal of Chemical and Engineering Data*, **2013**, 57, 276-285.
- [44] F. Qi, H. Wang, H. *Journal of Chemical Thermodynamics*, **2009**, 41, 265-272.
- [45] B. Garcla, C. Herrera, J. S. Leal, *Journal of Chemical and Engineering Data*, **1991**, 36, 269-274.
- [46] A. Pal, B. Kumar, *Journal of Molecular Liquids*, **2011**, 163, 128-134.
- [47] Y. Tian, X. Wang, J. Wang, *Journal of Chemical and Engineering Data*, **2008**, 53, 2056-2059.
- [48] T. Y. Wu, H. C. Wang, S. G. Su, S. T. Gung, M.W. Lin, C. B. Lin, *Journal of Chinese Chemical Society*, **2010**, 57, 44-50.

6.1 General Conclusions

Physico-chemical properties of binary and ternary mixtures of *N, N*-dimethylformamide (DMF), acetonitrile (ACN) and two ionic liquids, 1-ethyl 3-methyl imidazolium bis trifluoromethane sulfonyl imide [emim][TFSI] and 1-ethyl 3-methyl imidazolium bis trifluorophosphate [emim][PF₆] change with varying compositions of different solvents. In binary mixtures of DMF-ACN, DMF-[emim][TFSI]/[emim][PF₆], and ACN-[emim][TFSI]/[emim][PF₆], the ρ , η and n increase with increasing mole fraction of the solvent. The IL, [emim][PF₆] is solid at room temperature and the solubility of the IL in DMF and ACN is very low. Therefore binary mixtures of IL-DMF and IL-ACN could be prepared only in a limited composition range. The excess molar volume and excess viscosity evaluated from the density and viscosity results, respectively were found negative for DMF-ACN binary mixtures with increasing mole fraction of DMF at all temperatures ranging from 20-50 °C indicating strong dipole-dipole interaction between unlike molecules, while excess refractive index results were positive over the whole composition range. For [emim][TFSI]-DMF and [emim][TFSI]-ACN binary mixtures, the excess molar volume of these two binary mixtures shows two opposite effects with a minimum and maximum value. The excess molar volumes give the minimum value at $X_{IL} \sim 0.20$ and a maximum value at $X_{IL} \sim 0.47$ for DMF-ACN system while for ACN-IL binary system the minimum and maximum value of excess molar volumes were $X_{IL} \sim 0.20$ and $X_{IL} \sim 0.40$, respectively. The minimum value can be due to hydrogen bonds between DMF/ACN molecules and IL where maximum value is for the dissociation of ions forming the IL and loss of dipolar interaction of DMF/ACN.

Physico-chemical properties of ternary mixtures comprising DMF, ACN and [emim][TFSI] show different patterns with increasing mole fraction and temperatures. The density, viscosity and refractive index increase with mole fraction of [emim][TFSI] and DMF at fixed DMF, ACN and [emim][TFSI], respectively. On the contrary, density, viscosity and refractive index decrease with increasing temperature. The excess molar volume and excess viscosity results of investigated ternary mixtures are negative over the entire mole fraction range may be indicates ionic hydrogen bonding and dipole interaction between DMF and ACN and [emim][TFSI]. This will be of significant importance to tune the physicochemical properties of different IL-based systems and to bring new dimension in designing novel, cost effective, recyclable, environment-friendly materials for multidisciplinary fields of application.

6.2 Prospect

IL possesses the greatest environmentally benign character than other conventional molecular solvents. The mixing of molecular solvents and IL is likely to exhibit promising physico-chemical properties which can be tuned for numerous task specific applications with improved efficiency. Ability to be recycled and reused by means of simple physico-chemical process is the important and beneficial advantage of IL-

molecular solvent binary systems. For all these characteristics binary IL-DMF and IL-ACN system and IL-DMF-ACN systems can be conferred as the best green system to support the clean technology and deal with the growing environmental challenge. This work aims at providing an insight into the microscopic environment of the binary and ternary IL-molecular systems. The work could show the prospect of IL-based binary and ternary systems with polar solvents for tunable physicochemical properties and explore task specificity of hydrophobic ILs with controlled addition of molecular solvents under ambient condition.

Table A1

Experimental density (ρ), viscosity (η), refractive index (n), excess molar volume (V^E), excess viscosity ($\Delta\eta$), and excess refractive index (Δn) of DMF-ACN binary mixtures at several temperatures.

X_{DMF}	ρ/gcm^{-3}	$\eta/\text{mPa.s}$	n	$V^E \times 10^6/\text{m}^3\text{mol}^{-1}$	$\Delta\eta/\text{mPa.s}$	Δn
			20 °C			
0.0000	0.7836	0.3790	1.3445	1.0000	0.0000	0.0000
0.1000	0.8079	0.4200	1.3574	0.9000	-0.0079	0.0044
0.1980	0.8293	0.4521	1.3695	0.8020	-0.0237	0.0081
0.5020	0.8848	0.6003	1.3996	0.4980	-0.0248	0.0120
0.5980	0.9003	0.6476	1.4065	0.4020	-0.0239	0.0107
0.7000	0.9135	0.6986	1.4132	0.3000	-0.0014	0.0087
0.9000	0.9385	0.8201	1.4244	0.1000	0.0009	0.0027
1.0000	0.9495	0.8681	1.4303	0.0000	0.0000	0.0000
			25 °C			
0.0000	0.7782	0.3571	1.3424	0.0000	0.0000	0.0000
0.1000	0.8026	0.4003	1.3555	-0.0747	-0.0028	0.0046
0.1980	0.8241	0.4290	1.3683	-0.1184	-0.0192	0.0089
0.5020	0.8798	0.5685	1.3987	-0.1707	-0.0203	0.0134
0.5980	0.8954	0.6148	1.4054	-0.2273	-0.0175	0.0118
0.7000	0.9087	0.6590	1.4117	-0.1236	0.0004	0.0094
0.9000	0.9337	0.7716	1.4219	-0.0583	0.0003	0.0024
1.0000	0.9447	0.8173	1.4280	0.0000	0.0000	0.0000
			30 °C			
0.0000	0.7728	0.3420	1.3404	0.0000	0.0000	0.0000
0.1000	0.7973	0.3821	1.3540	-0.0784	-0.0027	0.0050
0.1980	0.8189	0.4094	1.3677	-0.1250	-0.0174	0.0103
0.5020	0.8748	0.5400	1.3979	-0.1806	-0.0173	0.0147
0.5980	0.8904	0.5828	1.4044	-0.2367	-0.0153	0.0130
0.7000	0.9038	0.6233	1.4102	-0.1313	0.0016	0.0101
0.9000	0.9289	0.7279	1.4197	-0.0610	0.0002	0.0025
1.0000	0.9399	0.7702	1.4257	0.0000	0.0000	0.0000
			35 °C			
0.0000	0.7673	0.3279	1.3386	0.0000	0.0000	0.0000
0.1000	0.7919	0.3659	1.3535	-0.0821	-0.0020	0.0065
0.1980	0.8136	0.3921	1.3686	-0.1324	-0.0150	0.0132
0.5020	0.8698	0.5141	1.3973	-0.1915	-0.0150	0.0162
0.5980	0.8855	0.5535	1.4035	-0.2478	-0.0135	0.0142
0.7000	0.8988	0.5912	1.4089	-0.1396	0.0023	0.0109
0.9000	0.9241	0.6891	1.4177	-0.0648	0.0014	0.0028
1.0000	0.9351	0.7277	1.4234	0.0000	0.0000	0.0000

40 °C						
0.0000	0.7618	0.3153	1.3345	0.0000	0.0000	0.0025
0.1000	0.7865	0.3508	1.3545	-0.0871	-0.0018	0.0135
0.1980	0.8083	0.3740	1.3712	-0.1408	-0.0151	0.0216
0.5020	0.8647	0.4905	1.3971	-0.2027	-0.0136	0.0204
0.5980	0.8805	0.5267	1.4029	-0.2589	-0.0114	0.0176
0.7000	0.8939	0.5616	1.4078	-0.1483	0.0038	0.0134
0.9000	0.9192	0.6535	1.4158	-0.0673	0.0029	0.0036
1.0000	0.9303	0.6879	1.4211	0.0000	0.0000	0.0000
45 °C						
0.0000	0.7563	0.3035	1.3321	0.0000	0.0000	0.0051
0.1000	0.7811	0.3365	1.3595	-0.0929	-0.0020	0.0161
0.1980	0.8030	0.3587	1.3755	-0.1492	-0.0139	0.0241
0.5020	0.8597	0.4678	1.3971	-0.2142	-0.0119	0.0228
0.5980	0.8755	0.5021	1.4024	-0.2701	-0.0102	0.0200
0.7000	0.8889	0.5393	1.4068	-0.1561	0.0043	0.0158
0.9000	0.9144	0.6213	1.4141	-0.0709	0.0036	0.0059
1.0000	0.9255	0.6526	1.4188	0.0000	0.0000	0.0026

Table A2

Coefficients, A_i , for $V_m^E/\text{cm}^3\text{mol}^{-1}$, $\Delta\eta/\text{mPa.s}$, Δn and standard deviation σ for DMF-ACN binary mixtures from equation 2.2: $V_m^E = x(1-x)\sum_{i=0}^4 A_i(1-2x)^i$

Temperature, °C	A_1	A_2	A_3	A_4	σ
$\Delta\eta$					
20	-0.1020	-0.0834	0.0864	-0.0161	0.0035
25	-0.0813	-0.1010	0.0866	0.0751	0.0034
30	-0.0699	-0.0931	0.0742	0.0653	0.0033
35	-0.0611	-0.0801	0.0766	0.0453	0.0030
40	-0.0529	-0.0866	0.0717	0.0413	0.0031
45	-0.0476	-0.0774	0.0706	0.0198	0.0029
V^E					
20	-0.7227	0.0546	0.1451	-0.3086	0.0284
25	-0.7615	0.0483	0.1415	-0.3247	0.0291
30	-0.8014	0.0432	0.1476	-0.3282	0.0292
35	-0.8466	0.0346	0.1536	-0.3158	0.0296
40	-0.8926	0.0294	0.1585	-0.3362	0.0298
45	-0.9389	0.0149	0.1565	-0.3355	0.0303
Δn					
20	0.0481	0.0117	-0.0082	-0.0043	0.0004
25	0.0538	0.0162	-0.0159	-0.0057	0.0004
30	0.0597	0.0225	-0.0183	-0.0097	0.0005
35	0.0663	0.0344	-0.0104	-0.0137	0.0006
40	0.0597	0.0225	-0.0183	-0.0097	0.0005

Table A3

Experimental ρ , η , n , V^E , $\Delta\eta$ and Δn of [emim][TFSI]-DMF binary mixtures at several temperatures.

X_{DMF}	ρ/gcm^{-3}	$\eta/\text{mPa.s}$	n	$V^E \times 10^6/\text{m}^3\text{mol}^{-1}$	$\Delta\eta/\text{mPa.s}$	Δn
20 °C						
0.0000	0.9495	0.8681	1.4303	0.0000	0.0000	0.0000
0.0202	0.9870	1.0280	1.4299	-0.0310	-0.6120	-0.0003
0.0793	1.0781	1.8176	1.4289	-0.0385	-2.0660	-0.0008
0.1963	1.2083	2.9868	1.4274	-0.0777	-5.3574	-0.0001
0.4913	1.3828	9.3408	1.4244	0.5792	-10.2175	-0.0022
0.7927	1.4805	24.4610	1.4244	0.0929	-6.4484	0.0002
0.8028	1.4839	25.6550	1.4244	0.0373	-5.7373	0.0009
1.0000	1.5235	38.8950	1.4227	0.0000	0.0000	0.0000
25 °C						
0.0000	0.9447	0.8173	1.4279	0.0000	0.0000	0.0000
0.0202	0.9822	0.9642	1.4274	-0.0345	-0.4944	-0.0004
0.0793	1.0732	1.6667	1.4266	-0.0480	-1.6557	-0.0008
0.1963	1.2033	2.7174	1.4253	-0.0886	-4.3104	-0.0001
0.4913	1.3777	8.1386	1.4225	0.5792	-8.2050	-0.0019
0.7927	1.4754	20.738	1.4227	0.0930	-5.0352	0.0005
0.8028	1.4788	21.7690	1.4227	0.0360	-4.4054	0.0012
1.0000	1.5185	32.4070	1.4207	0.0000	0.0000	0.0000
30 °C						
0.0000	0.9399	0.7702	1.4257	0.0000	0.0000	0.0000
0.0202	0.9774	0.9070	1.4251	-0.0397	-0.3994	-0.0004
0.0793	1.0683	1.5292	1.4244	-0.0584	-1.3357	-0.0007
0.1963	1.1983	2.4717	1.4233	-0.1021	-3.4916	-0.0011
0.4913	1.3726	7.1585	1.4210	0.5706	-6.3413	-0.0015
0.7927	1.4703	17.8270	1.4211	0.0897	-3.8109	0.0006
0.8028	1.4737	18.7350	1.4212	0.0312	-3.2384	0.0013
1.0000	1.5134	27.1850	1.4192	0.0000	0.0000	0.0000
35 °C						
0.0000	0.9351	0.7277	1.4234	0.0000	0.0000	0.0000
0.0202	0.9725	0.8540	1.4228	-0.0448	-0.3281	-0.0004
0.0793	1.0634	1.4093	1.4223	-0.0711	-1.0935	-0.0006
0.1963	1.1932	2.2790	1.4213	-0.1142	-2.8495	-0.0009
0.4913	1.3624	6.3413	1.4195	0.5649	-5.3883	-0.0011
0.7927	1.4653	15.4920	1.4196	0.0883	-2.9193	0.0007
0.8028	1.4686	16.2300	1.4198	0.0299	-2.4656	0.0014
1.0000	1.5084	23.1120	1.4178	0.0000	0.0000	0.0000

40 °C						
0.0000	0.9303	0.6879	1.4211	0.0000	0.0000	0.0000
0.0202	0.9677	0.8063	1.4206	-0.0501	-0.2727	-0.0003
0.0793	1.0585	1.3038	1.4203	-0.0833	-0.9117	-0.0004
0.1963	1.1883	2.1009	1.4195	-0.1315	-2.1009	-0.0006
0.4913	1.3624	5.6633	1.4181	0.5589	-4.4929	-0.0008
0.7927	1.4602	13.5820	1.4182	0.0853	-2.3245	0.0006
0.8028	1.4636	14.2000	1.4186	0.0239	-1.9512	0.0014
1.0000	1.5033	19.9520	1.4167	0.0000	0.0000	0.0000
45 °C						
0.0000	0.9255	0.6526	1.4188	0.0000	0.0000	0.0000
0.0202	0.9629	0.7633	1.4185	-0.0554	-0.2292	-0.0003
0.0793	1.0536	1.2116	1.4183	-0.0952	-0.7686	-0.0003
0.1963	1.1832	1.9455	1.4178	-0.1472	-1.9985	-0.0004
0.4913	1.3574	5.0898	1.4166	0.5514	-4.0259	-0.0005
0.7927	1.4552	12.0030	1.4167	0.0816	-1.8753	0.0005
0.8028	1.4586	12.5130	1.4170	0.0188	-1.5779	0.0011
1.0000	1.4983	17.3940	1.4155	0.0000	0.0000	0.0000
50 °C						
0.0000	0.9207	0.6190	1.4165	0.0000	0.0000	-
0.0202	0.9580	0.7244	1.4163	-0.0608	-0.1921	-
0.0793	1.0487	1.1286	1.4163	-0.1090	-0.6524	-
0.1963	1.1782	1.8076	1.4161	0.1571	-1.6922	-
0.4913	1.3523	4.6038	1.4152	0.5432	-3.2171	-
0.7927	1.4502	10.6970	1.4153	0.0771	-1.4979	-
0.8028	1.4536	11.1380	1.4156	0.0128	-1.2430	-
1.0000	1.4933	15.2720	1.4144	0.0000	0.0000	-

Table A4

Coefficients, A_i , for $V^E/\text{cm}^3\text{mol}^{-1}$, $\Delta\eta/\text{mPa.s}$, Δn and standard deviation σ for [emim][TFSI]-DMF binary mixtures from equation 2.2: $V_m^E = x(1-x)\sum_{i=0}^4 A_i(1-2x)^i$

Temperature, °C	A_0	A_1	A_2	A_3	σ
		$\Delta\eta$			
20	-41.0380	4.6411	14.6279	-4.0978	0.1617
25	-32.9532	3.1185	13.2057	-4.1913	0.1489
30	-25.4445	0.2464	9.8502	-1.2679	0.1475
35	-21.6208	0.5888	12.0221	-4.8872	0.1082
40	-18.0995	4.9620	13.6042	-14.1466	0.0746
45	-16.1553	0.9571	12.5931	-7.4108	0.0604
50	-12.8940	-0.3247	9.2692	-4.3862	0.0562
		Δn			
20	-0.0087	-0.0018	0.0134	-0.0172	0.0000
25	-0.0075	-0.0015	0.0137	-0.0216	0.0000
30	-0.0060	-0.0009	0.0129	-0.0225	0.0000
35	-0.0046	-0.0003	0.0118	-0.0227	0.0000
40	-0.0037	0.0024	0.0117	-0.0254	0.0001
45	0.0025	-0.0081	-0.0017	-0.0015	0.0002
50	-0.0024	0.0017	0.0092	-0.0187	0.0001
		V^E			
20	2.3477	-3.1154	-6.5092	6.8365	0.0168
25	2.3534	-3.2033	-6.6488	6.9286	0.0160
30	2.2896	-2.8880	-6.4716	5.9430	0.0237
35	2.3143	-3.3774	-6.8978	7.1047	0.0143
40	2.2967	-3.4920	-7.0634	7.2342	0.0149
45	2.2735	-3.5854	-7.2031	7.3257	0.0155
50	2.3285	0.1072	-5.5921	1.3140	0.0634

Table A5

Experimental ρ , η , n , V^E , $\Delta\eta$ and Δn of X_{ACN} at several temperatures for [emim][TFSI]-ACN binary mixtures.

X_{ACN}	ρ/gcm^{-3}	$\eta/\text{mPa.s}$	n	$V^E \times 10^6/\text{m}^3\text{mol}^{-1}$	$\Delta\eta/\text{mPa.s}$	Δn
20 °C						
0.0000	0.7827	0.3829		0.0000	0.0000	
0.0702	0.9845	0.7347		-0.2302	-2.0563	
0.0993	1.0289	0.9343		-0.4056	-2.5448	
0.2000	1.1689	1.6310		-	-5.6323	
0.4000	1.3427	4.7521		0.2765	-9.3916	
0.6000	1.4183	11.1750		1.3793	-9.8492	
0.8000	1.4790	18.7540		0.3774	-9.1506	
1.0000	1.5171	34.7850		0.0000	0.0000	
25 °C						
0.0000	0.7773	0.3661	1.3424		0.0000	0.0000
0.0702	0.9789	0.6867	1.3904		-1.6908	0.0463
0.0993	1.0234	0.8887	1.4065		-2.0635	0.0596
0.2000	1.1634	1.5143	1.4034		-4.5988	0.0453
0.4000	1.3373	4.2617	1.4218		-7.5984	0.0480
0.6000	1.4131	9.8339	1.4213		-7.7731	0.3004
0.8000	1.4739	16.1100	1.4213		7.2440	0.0163
1.0000	1.5171	29.1010	1.4207		0.0000	0.0000
30 °C						
0.0000	0.7719	0.3507	1.3404	0.0000	0.0000	0.0000
0.0702	0.9734	0.6530	1.3893	-0.2141	-1.0809	0.0472
0.0993	1.0178	0.8403	1.4056	-0.3823	-1.7008	0.0595
0.2000	1.1579	1.4114	1.4024		-3.8068	0.0465
0.4000	1.3320	3.8496	1.4204	0.5720	-6.2360	0.0485
0.6000	1.4078	8.7123	1.4203	1.8848	-6.2408	0.0326
0.8000	1.4687	14.0120	1.4203	1.0579	-5.8085	0.0169
1.0000	1.5120	24.6880	1.4192	0.0000	0.0000	0.0000
35 °C						
0.0000	0.7664	0.3369	1.3386	0.0000	0.0000	0.0000
0.0702	0.9678	0.6200	1.3888	-0.2141	-1.1749	0.0485
0.0993	1.0123	0.7950	1.4045	-0.3823	-1.4164	0.0595
0.2000	1.1524	1.3189	1.4020	-	-3.1836	0.0476
0.4000	1.3266	3.4978	1.4192	0.5720	-5.1703	0.0489
0.6000	1.4026	7.7730	1.4192	1.8848	-5.0608	0.0330
0.8000	1.4636	12.2990	1.4192	1.0579	-4.7004	0.0172
1.0000	1.5070	21.1650	1.4178	0.0000	0.0000	0.0000

			40 °C			
0.0000	0.7609	0.3237	1.3345	0.0000	0.0000	0.0000
0.0702	0.9623	0.5898	1.3887	-0.7000	-0.6253	0.0524
0.0993	1.0067	0.7539	1.4036	-0.4523	-1.1949	0.0625
0.2000	1.1468	1.2377	1.4011	-	-2.6973	0.0501
0.4000	1.3213	3.1947	1.4179	0.5160	-4.3515	0.0500
0.6000	1.3974	6.7033	1.4179	1.8610	-4.4542	0.0340
0.8000	1.4584	10.8750	1.4179	1.0566	-3.8937	0.0172
1.0000	1.5019	18.3800	1.4168	0.0000	0.0000	0.0000
			45 °C			
0.0000	0.7554	0.3120	1.3321	0.0000		0.0000
0.0702	0.9567	0.5621	1.3891	-0.8549		0.0552
0.0993	1.0011	0.7167	1.4027	-1.0159		0.0639
0.2000	1.1414	1.1632	1.4008	-2.6973		0.0520
0.4000	1.3160	2.9863	1.4165	-3.6397		0.0510
0.6000	1.3974	6.0497	1.4166	-3.7333		0.0345
0.8000	1.4584	9.6944	1.4166	-3.2456		0.0178
1.0000	1.5019	16.0970	1.4155	0.0000		0.0000
			50 °C			
0.0000	0.7498	0.3013	1.3294	0.0000	0.0000	0.0000
0.0702	0.9510	0.5368	1.3897	-0.3293	-0.7738	0.0585
0.0993	0.9955	0.6830	1.4021	-0.5252	-0.8699	0.0659
0.2000	1.1358	1.0969	1.4003	-	-1.9857	0.0539
0.4000	1.3106	2.7094	1.4152	0.4575	-3.1546	0.0518
0.6000	1.3870	5.2419	1.4152	1.8416	-3.4034	0.0348
0.8000	1.4483	8.6881	1.4153	1.0360	-2.7386	0.0179
1.0000	1.4919	14.2080	1.4144	0.0000	0.0000	0.0000

Table A6

Coefficients, A_i , for $V_m^E/\text{cm}^3\text{mol}^{-1}$, $\Delta\eta/\text{mPa.s}$, Δn and standard deviation σ for [emim][TFSI]-ACN binary mixtures from equation 2.2: $V_m^E = x(1-x)\sum_{i=0}^4 A_i(1-2x)^i$

Temperature, °C	A_0	A_1	A_2	A_3	σ
	Δn				
20	0.1510	0.1599	0.2536	0.2491	0.1407
30	0.1524	0.1566	0.2479	0.2459	0.0914
35	0.1593	0.1631	0.2587	0.2508	0.0996
40	0.1614	0.1638	0.2615	0.2535	0.1019
45	0.1590	0.1612	0.2581	0.2473	0.1203
50	0.1671	0.1692	0.2709	0.2579	0.0398
	V_m^E				
20	3.9855	-12.3326	-13.4444	19.4131	0.0346
30	5.5507	-14.4320	-10.8592	17.1114	0.0366
35	5.5761	-14.0554	-12.5587	13.2176	0.1404
40	5.4679	-14.2428	-12.6963	13.0094	0.1452
45	5.4679	-14.2428	-12.6963	13.0094	0.1452
50	5.2610	-15.1690	-11.8341	16.8286	0.0394
	$\Delta\eta$				
20	-39.1428	5.8090	-20.8517	31.7749	0.1407
30	-25.4073	-0.1935	-13.5171	28.1307	0.0914
35	-20.7777	-0.3858	-11.5745	20.9770	0.0996
40	-18.0827	-0.0345	-6.9208	17.6827	0.1019
45	-15.1141	-1.5007	-8.4512	14.7356	0.1203
50	-13.5347	2.3493	-3.3135	4.5474	0.0398

Table A7

ρ of [emim][TFSI]-DMF-ACN at several temperatures at a fixed X_{DMF} is 0.20.

$X_{\text{[emim][TFSI]}}$	X_{ACN}	20 °C	25 °C	30 °C	35 °C	40 °C	45 °C	50 °C
0.0200	0.7800	0.4100	0.8408	0.8353	0.8299	0.8244	0.8189	0.8133
0.0300	0.7700	0.8799	0.8745	0.8690	0.8636	0.8580	0.8525	0.8470
0.0400	0.7600	0.9344	0.9290	0.9235	0.9180	0.9125	0.9069	0.9013
0.0600	0.7400	0.9796	0.9741	0.9686	0.9631	0.9576	0.9520	0.9465
0.1600	0.6400	1.1460	1.1405	1.1350	1.1296	1.1242	1.1187	1.1132
0.2100	0.5900	1.2109	1.2055	1.2001	1.1947	1.1893	1.1838	1.1784
0.3200	0.4800	1.3034	1.2980	1.2928	1.2875	1.2821	1.2769	1.2716
0.4100	0.3900	1.3626	1.3573	1.3521	1.3468	1.3416	1.3364	1.3312

Table A8 V^E [emim][TFSI]-DMF-ACN at several temperatures at fixed X_{DMF} is 0.20.

$X_{[emim][TFSI]}$	X_{ACN}	20 °C	25 °C	30 °C	35 °C	45 °C	50 °C
0.0200	0.7800	0.8460	0.8468	0.8470	0.6454	0.8449	0.8425
0.0300	0.7700	0.4806	0.4736	0.4231	0.4560	0.4458	0.4343
0.0400	0.7600	-0.3323	-0.3554	-0.3802	-0.4072	-0.6368	-0.4660
0.0600	0.7400	-0.8946	-0.9247	-0.9570	-0.9916	-1.0291	-1.0677
0.1600	0.6400	-0.2392	-0.3728	-0.4096	-0.6593	-0.4905	-0.5352
0.2100	0.5900	-0.3449	-0.6022	-0.4133	-0.4504	-0.5316	-0.5780
0.3200	0.4800	-0.5390	-0.5677	-0.6058	-0.6457	-0.7300	-0.7757
0.4100	0.3900	-0.3123	-0.3387	-0.3677	-0.3983	-0.4664	-0.5047

Table A9 ρ of [emim][TFSI]-DMF-ACN at several temperatures at a fixed X_{ACN} is 0.20.

$X_{[emim][TFSI]}$	X_{DMF}	20 °C	25 °C	30 °C	35 °C	40 °C	45 °C	50 °C
0.0200	0.7800	0.9769	0.9721	0.9672	0.9624	0.9575	0.9526	0.9477
0.0500	0.7500	1.0237	1.0188	1.0139	1.0090	1.0041	0.9991	0.9942
0.1500	0.6500	1.1601	1.1551	1.1500	1.1450	1.1399	1.1349	1.1298
0.2100	0.5900	1.2159	1.2108	1.2057	1.2006	1.1955	1.1904	1.1853
0.3100	0.4900	1.2947	1.2895	1.2844	1.2792	1.2740	1.2689	1.2638
0.3900	0.4100	1.3465	1.3413	1.3361	1.3309	1.3257	1.3205	1.3153
0.5400	0.2600	1.4179	1.4127	1.4075	1.4023	1.3971	1.3919	1.3866

Table A10 V^E of [emim][TFSI]-DMF-ACN at several temperatures at a fixed X_{ACN} is 0.20.

$X_{[emim][TFSI]}$	$X_{[DMF]}$	25 °C	30 °C	35 °C	40 °C	45 °C	50 °C
0.0200	0.7800	0.0163	0.0043	-0.0086	-0.0222	-0.0355	-0.0510
0.0500	0.7500	-0.1513	-0.1743	-0.1987	-0.2233	-0.2492	-0.2754
0.1500	0.6500	-0.2612	-0.2835	-0.3076	-0.3332	-0.3601	-0.3890
0.2100	0.5900	0.0544	0.0331	0.0118	-0.0121	-0.0385	-0.0613
0.3100	0.4900	-0.4434	-0.4702	-0.4964	-0.5246	-0.5454	-0.5839
0.3900	0.4100	-0.3809	-0.4060	-0.4308	-0.4587	-0.4866	-0.5075
0.5400	0.2600	-0.3809	-0.4060	-0.4308	-0.4587	-0.4866	-0.5075

Table A11 ρ of [emim][TFSI]-DMF-ACN at several temperatures at a fixed X_{IL} is 0.20.

X_{DMF}	X_{ACN}	20 °C	25 °C	30 °C	35 °C	40 °C	45 °C	50 °C
0.0200	0.7800	0.8225	0.8172	0.8117	0.8063	0.8008	0.7953	0.7897
0.1000	0.7000	0.8424	0.8371	0.8317	0.8264	0.8210	0.8155	0.8101
0.3000	0.5000	0.8805	0.8753	0.8702	0.8650	0.8598	0.8545	0.8493
0.5000	0.3000	0.9205	0.9155	0.9105	0.9054	0.9004	0.8953	0.8902
0.6000	0.2000	0.9332	0.9282	0.9233	0.9183	0.9133	0.9083	0.9033
0.9000	0.0000	0.9648	0.9600	0.9552	0.9504	0.9455	0.9407	0.9358
0.9800	0.0000	0.9739	0.9691	0.9643	0.9595	0.9547	0.9498	0.9450

Table A12 V^E of [emim][TFSI]-DMF-ACN at several temperatures at a fixed X_{IL} is 0.20.

X_{DMF}	X_{ACN}	20 °C	25 °C	30 °C	35 °C	40 °C	45 °C	50 °C
0.0200	0.7800	0.0195	0.0122	0.0062	0.0006	-0.0072	-0.5558	-0.0229
0.1000	0.7000	-0.1979	-0.2097	-0.2207	-0.2325	-0.2505	-0.2580	-0.2719
0.3000	0.5000	-0.2912	-0.3055	-0.4219	-0.3362	-0.3529	-0.3689	-0.3880
0.5000	0.3000	-0.9223	-1.1426	-0.9671	-0.9902	-1.0153	-1.0403	-1.0652
0.6000	0.2000	-0.8437	-0.8633	-0.8847	-0.9065	-0.9342	-0.9505	-0.9747
0.9000	0.0000	-0.5014	-0.5130	-0.5233	-0.5339	-0.5442	-0.5855	-0.5649
0.9800	0.0000	-0.5251	-0.5318	-0.5402	-0.5479	-0.5558	-0.5638	-0.5729

Table A13 η of [emim][TFSI]-DMF-ACN at several temperatures at a fixed X_{DMF} is 0.20.

$X_{[emim][TFSI]}$	X_{ACN}	20 °C	25 °C	30 °C	35 °C	40 °C	45 °C	50 °C
0.0200	0.7800	0.4547	0.4343	0.4152	0.3980	0.3818	0.3616	0.3476
0.0300	0.7700	0.5027	0.4778	0.4552	0.4346	0.4154	0.3979	0.3819
0.0400	0.7600	0.6271	0.5932	0.5625	0.5350	0.5096	0.4865	0.4651
0.0600	0.7400	0.7456	0.6949	0.6568	0.6230	0.5922	0.5628	0.5365
0.1600	0.6400	1.5095	1.4024	1.3071	1.2228	1.1471	1.0811	1.0210
0.2100	0.5900	2.1569	1.9836	1.8312	1.6990	1.5809	1.4764	1.3819
0.3200	0.4800	4.4744	4.0159	3.6286	3.3001	3.0188	2.7765	2.5664
0.4100	0.3900	6.8958	6.0990	5.4365	4.8772	4.4046	4.0010	3.6538

Table A14 η of [emim][TFSI] with DMF and ACN at several temperatures at a X_{ACN} is 0.20.

$X_{[emim][TFSI]}$	X_{DMF}	20 °C	25 °C	30 °C	35 °C	40 °C	45 °C	50 °C
0.0200	0.7800	0.9650	0.9052	0.8517	0.8033	0.7612	0.7182	0.6839
0.0500	0.7500	1.1910	1.1099	1.0368	0.9717	0.9131	0.8602	0.8130
0.1500	0.6500	2.1162	1.9424	1.7903	1.6582	1.5402	1.4356	1.3426
0.2100	0.5900	2.8451	2.5885	2.3678	2.1758	2.0082	1.8601	1.7313
0.3100	0.4900	4.3371	4.0480	3.4057	3.3097	3.1429	2.7611	2.5234
0.3900	0.4100	6.3237	5.6095	5.0051	4.5004	4.0724	3.7068	3.3869
0.5400	0.2600	7.8560	6.8571	6.1898	4.9760	4.4274	4.1417	3.9040

Table A15 η of [emim][TFSI]-DMF-ACN at several temperatures at a fixed X_{IL} is 0.20.

X_{DMF}	X_{ACN}	20 °C	25 °C	30 °C	35 °C	40 °C	45 °C	50 °C
0.0200	0.7800	0.4257	0.4065	0.3885	0.3674	0.3521	0.3380	0.3249
0.1000	0.7000	0.4967	0.4459	0.4245	0.4046	0.3869	0.3704	0.3553
0.3000	0.5000	0.5741	0.5429	0.5143	0.4885	0.4645	0.4429	0.4230
0.5000	0.3000	0.7958	0.7461	0.7012	0.6607	0.6238	0.5905	0.5603
0.6000	0.2000	0.8160	0.7461	0.7034	0.6650	0.6300	0.5982	0.5693
0.9000	0.0000	0.9370	0.8784	0.8260	0.7789	0.7361	0.6971	0.6638

Table A16 $\Delta\eta$ [emim][TFSI]-DMF-ACN at several temperatures at a fixed X_{DMF} is 0.20.

$X_{[emim][TFSI]}$	X_{ACN}	20 °C	25 °C	30 °C	35 °C	40 °C	45 °C
0.0200	0.7800	-0.7092	-0.5824	-0.4813	-0.4027	-0.3423	-0.2992
0.0300	0.7700	-1.0502	-0.8630	-0.7131	-0.5972	-0.5082	-0.4368
0.0400	0.7600	-1.6924	-1.3850	-1.1392	-0.9492	-0.8035	-0.6869
0.0600	0.7400	-1.9554	-1.6002	-1.3099	-1.0857	-0.9141	-0.7785
0.1600	0.6400	-5.0695	-4.1186	-3.3636	-2.7828	-2.3402	-1.9856
0.2100	0.5900	-6.3458	-5.1409	-4.1824	-3.4464	-2.8888	-2.4451
0.3200	0.4800	-8.2756	-6.6433	-5.3463	-4.3594	-3.6182	-3.0318
0.4100	0.3900	-9.7211	-7.7790	-6.2355	-5.0725	-4.2071	-3.5266

Table A17 $\Delta\eta$ of [emim][TFSI]-DMF-ACN at several temperatures at a fixed X_{ACN} is 0.20.

$X_{[emim][TFSI]}$	X_{DMF}	20 °C	25 °C	30 °C	35 °C	40 °C	45 °C
0.0200	0.7800	-0.5994	-0.4841	-0.3912	-0.3203	-0.2637	-0.2241
0.0500	0.7500	-1.1222	-1.2225	-0.9943	-0.8194	-0.6860	-0.5808
0.1500	0.6500	-4.3571	-3.5214	-2.8566	-2.3474	-1.9630	-1.6587
0.2100	0.5900	-5.9086	-4.7696	-3.8631	-3.1722	-2.6503	-2.2383
0.3100	0.4900	-	-	-	-	-	-
0.3900	0.4100	-9.2167	-7.3806	-5.9300	-4.8296	-4.0097	-3.3637

Table A18 $\Delta\eta$ of [emim][TFSI]-DMF-ACN at several temperatures at a fixed X_L is 0.20.

X_{DMF}	X_{ACN}	20 °C	25 °C	30 °C	35 °C	40 °C	45 °C
0.0200	0.6000	-0.3431	-0.2805	-0.2463	-0.1975	-0.1682	-0.1449
0.1000	0.7000	-0.3387	-0.2779	-0.2292	-0.1922	-0.1630	-0.1403
0.3000	0.5000	-0.3331	-0.2729	-0.2249	-0.1880	-0.1598	-0.1373
0.5000	0.3000	-0.2103	-0.1617	-0.1236	-0.0955	-0.0748	-0.0592
0.6000	0.2000	-0.2396	-0.2077	-0.1641	-0.1311	-0.1057	-0.0863
0.9000	0.0000	-0.2669	-0.2134	-0.1699	-0.1368	-0.1110	-0.0916

List of Attended Seminar

1. 2st National Conference of Bangladesh Crystallographic Association (BCA), Dhaka, Bangladesh, 05 December, 2015.
2. Seminar on *Air Quality and Its Consequence: Bangladesh Perspective*, organized by Establishing Air Quality Monitoring Centre (CP-2196), Dhaka, Bangladesh, 28 December, 2013.
3. Seminar on *Tendam Mass Spectrometry and its Application for Analysis of Chemical Contaminants in Food Stuff*, Dhaka, Bangladesh, 02 June, 2015.
4. Seminar on *3D Gel Printer and Future Life Innovation*, organized by the Material Chemistry Research Laboratory, Department of Chemistry, University of Dhaka, Dhaka, 30 August, 2015.
5. Seminar on *New Trophological States of Quantum Matter*, organized by Bose Centre for Advanced Study and Research in Natural Sciences, University of Dhaka, Dhaka, 25 November, 2015.
6. Seminar on *New Insight into the Chemistry on Carbon Nanotubes and Graphene Oxide and Boron Oxide Nanotubes*, organized by Department of Microbiology, University of Dhaka, Dhaka, 10 December, 2015.

Abstracts Published as Contribution in the Scientific Meeting

1. **Momana Afrose**, Omar Ahmed and Md. Abu Bin Hasan Susan, *Study of Physicochemical Properties of Imidazolium Based Ionic Liquid in Pure and Mixed Polar Solvents*, 37th Annual Conference of Bangladesh Chemical Society (ACBCS), 37th Annual Conference of Bangladesh Chemical Society (ACBCS), 11 April, 2015, Comilla University, Comilla, Bangladesh (Oral presentation).
2. **Momana Afrose**, Omar Ahmed, Md. Yousuf A. Mollah, and Md. Abu Bin Hasan Susan, *Physicochemical Properties of Binary and Ternary Mixtures of an Imidazolium Based Ionic Liquid with Polar Solvents*, 2nd International Bose conference, 3-4 December, 2015 (Poster presentation).

3. Momana Afrose, Omar Ahmed, Md. Yousuf A. Mollah, and Md. Abu Bin Hasan Susan, *Molecular Interactions in Binary and Ternary Mixtures of an Imidazolium Based Ionic Liquid with Polar Solvents*, 16th Assian Chemical Congress (16 ACC), 16-19 March, 2016 (Oral presentation).

4. Momana Afrose, Omar Ahmed, Md. Abu Bin Hasan Susan, *Physical and Excess Properties of Imidazolium Based Ionic Liquids with N, N-dimethylformamide and Acetonitrile*, 1st Symposium on Chemistry for Global Solidarity, 14 October, 2016 (Oral presentation)

5. Momana Afrose, Omar Ahmed, Md. Abu Bin Hasan Susan, *Molecular Environment of Ternary Mixtures of Imidazolium Based Ionic Liquid with Polar solvents*, Third International Conference Kathmandu Symposia on Advanced Materials (KaSAM-2016), 17-20 October, Pokhara, Nepal (Poster presentation).

List of Workshops Attended

1. Characterization and Application of Novel Functional Materials, 31 August and 01 September, 2013, Department of Chemistry, University of Dhaka, Bangladesh.
2. Black Carbon Emission from Brick Kilns in Bangladesh, 16 November, 2014.